Cosmology of interacting baryons, dark matter and dark energy

Thesis for master of science in Astronomy

Henrik Oppen
Institute of Theoretical Astrophysics
University of Oslo
June 2, 2014

Abstract

This master thesis is about interaction models for baryonic matter, dark matter and dark energy. We will work with the components as perfect fluids, and set up interaction models as exchange in energy. Then the thesis will be divided into three parts. In the first part, I will study the interaction models when the universe is described by the Friedmann-Robertson-Walker metric. I will study analytical solutions and the stability of these. In the second part, I will use observational data from supernovae Ia, baryon acoustic oscillations and the cosmic microwave background to see if I can put some contranits on the strength of the interactions, and thereby see if the interaction models can fit into the universe we live in. In the third part, I will study how the interaction models affects the structure formation in the universe, by adding small inhomogeneities to the metric.

I concluded that there are always possible to find stable solutions when the interactions are active, provided that we put limitations on the strength of the interactions. The observational constraints did not conclude the one way or the other, there were no statistical evidence for the presence of my interactions, but also no statistical evidence that ruled our the interactinon models. The different observational data sets gave me different constraints, with the cosmic microwave background giving me the strongest constraints. In the third part, I made the interaction quite strong, and I saw that the structure formation was affected in various ways depending on the sings of the interaction parameters. These then only became hypothetical universe, but they were quite interesting non the less.

Acknowledgments

I want to thank my two supervisor, David Fonseca Mota as my primary supervisor for giving me the opportunity to work with this master thesis, and Jose Beltran Jimenez as my secondary supervisor for all the help you gave me through the whole year, even though I have not seen you since before I started on the thesis. Thank you both. I will also thank my fellow students at the department who has provided a nice student environment. At last, I feel that I must write a few words about the social student organization at the department of physics. I became a part of this studentorganization over four years ago, and this organization, along with the student democracy organization at the department of physics, have kept me in an amazing environment through all the years until to the end of this thesis, and even though I quit from my positions these days, this student organization and the people that were there with me through the years will always be a part of my life that I will remember along with my time as a student.

Contents

Introduction

Cosmology is the study of the universe as a whole. Questions cosmologists work with are often related to how the universe started and what will happen to it in the future, if it has an end or not. Cosmologists are also interested in what the universe contains and how much, and how the content behaves and affects the evolution of the universe. This is also what this thesis is related to: how different components of the universe may interact.

We will divide the content of the universe into three different components: baryons, dark matter and dark energy. The baryons, or baryonic matter, which is a better term for our case, is matter that is made up of massive particles that we know: quarks and leptons in three generations with antiparticles, and the particles they combine to make. Almost everything of this is protons, neutrons and electrons, which are from the first generation. Some of the more exotic stuff from the two other generations will not be studied here. In fact, the definition of a baryon is a particle made out of three quarks/anti-quarks, but in cosmology, it is common to address matter made up of protons and neutrons as baryons (we usually neglect the electrons because the electron mass is much smaller than the proton/neutron mass), and we will rarely mention protons, neutrons and electrons again. In the best models we have for the universe today, baryonic matter only makes up around 4 % of the whole universe, in terms of the energy.

Dark matter is something that we have a lot of different strong evidences for its existence, but we do not know exactly *what* it is. We just know that it is there, and we know that whatever it is, it should interact very weakly with baryonic matter and photons. This means that we can not see dark matter (one of the reasons for the word *dark*), and it will be collisionless - dark matter particles (if it is made up by particles) may pass straight through you as you read this without you knowing. The only thing we know is that the dark matter is affected by gravity according to the equivalence principle. This is often used as a definition of dark matter: something that is not affected by the electromagnetic force, but is affected by gravity. It was this way that dark matter was first "discovered", through studies of the rotations of galaxies. If they were to rotate the way they are, they should be way more massive than the mass that are in the stars we see in them, and so there must be a lot of mass there that we can not see. A lot of the work

in particle physics today is related to finding particles that can make up the dark matter we "see" in the universe today. There are a lot of theories, but all dark matter is still not accounted for by particles that we know. Today, dark matter makes up around 22 % of the energy in the universe.

Dark energy is one of the greatest mysteries of cosmology. Observations of galaxies that are far away from us show that they in average are moving away from us, and the greater the distance, the faster they move. The observations are based on the Doppler effect, and we use them to compute distances to objects that are very far away. The fact that galaxies moves faster away from us the greater the distance to them are is called Hubble's law. But why do galaxies move faster away from us the further they are from us? The answer is that the universe itself is expanding, and the space between the galaxies grow. The movement we then see is just the galaxies following the expansion of space, and we call it the Hubble flow. A universe that is dominated by matter is expected to expand, but the observations tell us that the expansion is accelerating. This is where the dark energy enters: dark energy is what makes the expansion of the universe accelerate. We know that the dominant force on long distances is the force of gravity (which is not really a force in Einsteins general theory of relativity, which will enter this thesis early), and so there must be something out there in order to counter gravity and actually expand the universe, like a repulsive gravity. This is what we call dark energy. Like the dark matter, no one knows what the dark energy really is, we only know that it is there. Dark matter seems to make up around 74 % of the universe today.

At last, radiation, in terms of photons and neutrinos, are also out there, and they do not fit into the three previous components (neutrinos may be treated as baryonic matter if we treat them as massive, but we will not touch the neutrinos at all). We will not focus on radiation either, but it was the dominating component in the early universe, and it will come into play when it plays an important role.

So for this thesis: interacting baryons, dark matter and dark energy. As the title suggests, we will study a universes where these three components interact with each other. Is our universe such a universe? Maybe, we will look at this at some point. But first, what do we mean by interactions, and how will we be working with interactions in this thesis? The second question is actually spot on here: we know that the components interact through gravity, so each of the components feel the two others. But we will not think like that, we will study more direct interactions, where one of the components in some way may become one of the two others. We will treat the three components as perfect fluids, and we will look at the interactions as exchange in energy. So if we have interactions, the energy of one of the components may decrease, while the energy of one of the other components may increase.

To begin with, I will give a short introduction to cosmology. I will start

with the assumption of a homogeneous and isotropic universe, and then set up a metric tensor that let us compute distances in our universe. Then I will fill our universe with our components, and use a set of well known equations to see how our universe works, including inhomogeneous perturbations in the components that will give us formation of structures. Next, I will look at some useful quantities in astronomy that we will need later. After that, I will set up a specific model for our interactions, and we will be ready to start our thesis.

From that point, the thesis will be divided into three parts. In the first part, I will study what is usually called *the background universe*. This is a universe where we still have the metric that I will introduce in the first chapter. I will see how the interaction models looks like in such a universe, and how the evolution of the different components will be, in terms of analytical solutions and stability analysis.

In the second part, I will use observational data to see if our interaction model actually can be used to describe the universe we live in. I will use observations from supernovae type Ia, baryon acoustic oscillations and the cosmic microwave background to see how strong the interactions can be.

In the third part, I will study how the interaction models will affect the formation of structures in the universe. In this part, I will set up a new metric, which is the old one with small inhomogeneities added. The interesting part will then be the evolution of these inhomogeneities on different time and lengthscales.

In the last pages, I will sum up the thesis, and write some words about the road ahead, since there will be more to do with the interaction models. After that follows two appendixes, where I will write some pages about the general theory of relativity, which is very important when studying cosmology, and I will describe some of the mathematical, numerical and statistical methods that I will use through the thesis.

Chapter 1

Cosmology, astrophysics and observations

We begin with a short introduction to cosmology, where we will use the general theory of relativity to find equations that describes how our universe evolves with a given content, and we will see how inhomogeneities in the universe evolve, which is what gives rise to structure formations. Then we will look at some useful quantities that we will need later on, when we are working with observational data.

1.1 Cosmology

In this section, I will give a short introduction in cosmology, which is the geometry of our universe and its content. The geometry and the content of the universe are related through the Einstein equation, Equation A.15. We start with the geometry, which leads us to the left hand side of the Einstein equation, the Einstein tensor.

1.1.1 The Friedmann-Robertson-Walker metric

To find out more about the geometry of our universe, we need a method of measuring distances. We start with some assumptions. We will first assume that our universe is spatially flat. We could have started without assuming this, worked out the general case and then looked at different cases of curvature, but since different curvatures is not a topic in this thesis, I will start with a spatial flat universe right away.

Our second assumption is the usual assumption that our universe is homogeneous and isotropic at large scales, meaning that it looks the same everywhere, and it looks the same in every direction an observer would look - at large scales. This is obviously not true at small scales, as we know from studies of stars and galaxies, and we will actually come back to this later.

The third assumption is that the universe is expanding. The expansion will come in through a scale factor, which will be introduced below.

From Einsteins general theory of relativity, we use what we call *the metric tensor*, $g_{\mu\nu}$, to measure distances. The definition is made through an infinitesimal line element in the four-dimensional space time. Let dx^μ be an infinitesimal change in position in space-time, where we have used a specific set of basis vectors $\mathbf{e}_\mu$. The line element ds^2 is then defined as

$$ds^2 = g_{\mu\nu} dx^\mu dx^\nu,$$

where Einsteins summing convention is used. The quantity ds^2 is what we call *invariant*, which means that it is independent of our choice of basis. So to measure distances, one needs to know the metric tensor $g_{\mu\nu}$..

We want to study a homogeneous, isotropic, spatially flat universe which is expanding. First we need to specify a basis. For time, we choose what we call *cosmic time*, labeled by t. This is the time measured by an observer that follows the expansion of the universe. We already now need the isotropy of the universe to be able to define such a global time coordinate. For spatial coordinates, we use Cartesian coordinates x, y and z. Now we must place the origin of this coordinate system somewhere, so let us choose the center of the Earth. Time $t = 0$ corresponds to the big bang. The coordinates x, y and z is what we call a *coomoving coordinate*. An observer that follows the expansion of the universe has constant coomoving coordinates. Since the universe is expanding, this means for instance that the radial comoving distance $r = \sqrt{x^2 + y^2 + z^2}$ *does not* correspond to the physical distance between the earth and the observer. Since the vectors in our basis are orthogonal, the metric tensor will only have elements on the diagonal - so $g_{\mu\nu} \propto \delta_{\mu\nu}$.

Next, we must get the expansion of the universe into the metric. Imagine an object in space, with infinitesimal, coomoving spatial distance $dr = \sqrt{dx^2 + dy^2 + dz^2}$ from us. We measure the distance at the same cosmic time, so the time interval dt is zero, and so we have $ds^2 = g_{xx}dx^2 + g_{yy}dy^2 + g_{zz}dz^2$ for the invariant, infinitesimal distance to the object. Now, if the physical distance is supposed to grow with time, we need a scale factor $a(t)$ (which may depend on cosmic time, but not on space, due to homogeneity) to account for the expansion, to make the line element invariant: $ds = a dr$. Squaring and factoring, we get $g_{xx} = g_{yy} = g_{zz} = a^2$. Now we have every component of the metric. Written as a matrix, it reads

$$g = (g_{\mu\nu}) = \begin{pmatrix} -1 & 0 & 0 & 0 \\ 0 & a^2(t) & 0 & 0 \\ 0 & 0 & a^2(t) & 0 \\ 0 & 0 & 0 & a^2(t) \end{pmatrix}.$$

The notation may appear strange, so to be clear: g refers to the whole matrix, while $g_{\mu\nu}$ refers to a specific element of the matrix. But, even though g does

not have indices on it, the form of the matrix *is basis dependent*, and we need to separate it from its' inverse $g^{\mu\nu}$. Also note that we use units so that the speed of light c is equal to one. Written out, the line element then becomes

$$ds^2 = -dt^2 + a^2(t)(dx^2 + dy^2 + dz^2). \tag{1.1}$$

This is called the Friedmann-Robertson-Walker (FRW) line element.

Now that we have the metric, we can find the connection coefficients - which, since we use a coordinate basis, reduce to the Christoffel symbols. In terms of the metric, the Christoffel symbols are given by Equation A.5. When we compute them, we divide the indices into time and spatial indices, so we can compute more of them at once. With our metric tensor, there are only two combinations of indices that give non-zero Christoffel symbols:

$$\Gamma^0_{ij} = \delta_{ij} a \frac{da}{dt} = H g_{ij},$$

$$\Gamma^i_{0j} = \Gamma^i_{j0} = \delta^i_j \frac{1}{a}\frac{da}{dt} = \delta^i_j H,$$

where the Hubble parameter H also has been defined. Now we can find the Ricci tensor, Equation A.9. These are the non-zero components:

$$R_{00} = -\Gamma^i_{0i,0} - \Gamma^i_{j0}\Gamma^j_{0i} = -3\frac{1}{a}\frac{d^2a}{dt^2},$$

$$R_{ij} = \delta_{ij}\left(\frac{1}{a}\frac{d^2a}{dt^2} + 2\left(\frac{da}{dt}\right)^2\right).$$

Contracting gives us the Ricci scalar:

$$\mathcal{R} = g^{\mu\nu}R_{\mu\nu} = 6\left(\frac{1}{a}\frac{d^2a}{dt^2} + \left(\frac{1}{a}\frac{da}{dt}\right)^2\right).$$

Now we can find the Einstein tensor, Equation A.11:

$$E_{00} = R_{00} - \frac{1}{2}g_{00}\mathcal{R} = 3\left(\frac{1}{a}\frac{da}{dt}\right)^2,$$

$$E_{ij} = R_{ij} - \frac{1}{2}g_{ij}\mathcal{R} = -\delta_{ij}\left(2\frac{1}{a}\frac{d^2a}{dt^2} - \left(\frac{da}{dt}\right)^2\right),$$

This is to be compared with the energy-momentum tensor through the Einstein equation. When working with the Einstein equation, it is easier to work with T^μ_ν than with $T_{\mu\nu}$, and so we also need $E^\mu_\nu = g^{\mu\alpha}E_{\alpha\nu}$. Raising one index gives

$$E^0_0 = g^{0\alpha}E_{\alpha 0} = -3\left(\frac{1}{a}\frac{da}{dt}\right)^2,$$

$$E^i_j = g^{i\alpha}E_{\alpha j} = -\delta^i_j\left(2\frac{1}{a}\frac{d^2a}{dt^2} + \left(\frac{1}{a}\frac{da}{dt}\right)^2\right). \tag{1.2}$$

Now we have the Einstein tensor, the left hand side of the Einstein equation. This is to be compared with the energy-momentum tensor, which is the topic for the next section.

1.1.2 Cosmic fluids

Now we turn to the content of the universe. We will divide the content of the universe into four kinds: baryonic matter, dark matter, dark energy and radiation. For each component, we have an energy-momentum tensor. We start with the general energy-momentum tensor, which we compare with the Einstein tensor through the Einstein equation, and leave the different components for later.

We will assume that each of the components behave as perfect fluids. This means that there is no viscosity and no thermal conduction present. While this is not true, it is a very good approximation. The energy-momentum tensor is then given by Equation A.13. With one index upstairs and one downstairs, we have

$$T^\mu_\nu = (\rho + p)u^\mu u_\nu + pg^\mu_\nu.$$

The energy-density ρ is what we will work with onwards, so that will be our parameter to use. The pressure p is related to the energy-density ρ through the equation of state, and depends on the component. We need the four velocity, given by Equation A.2:

$$u^\mu = \frac{dx^\mu}{d\tau}.$$

When particles of each component follow the expansion of the universe, they have constant coomoving coordinates, so $dx^i = 0$. By the four velocity identity, we find $u^0u_0 = -1$, so we choose $u^0 = 1$ and $u_0 = -1$. Now we can compute the energy-momentum tensor. We get

$$T^0_0 = (\rho + p)\cdot(-1) + p = -\rho, \qquad T^i_0 = T^0_j = 0, \qquad T^i_j = \delta^i_j p. \tag{1.3}$$

Now we have the general energy-momentum tensor, we can look at some of the components, which each has its own equation of state. We assume that they all have this same simple form:

$$p = w\rho$$

where $w \in \mathbb{R}$ is the equation of state parameter. Baryonic matter and dark matter are pressureless, so $w = p = 0$. For dark energy, w can be -1 when dark energy is modeled by the cosmological constant, but we will leave w as a parameter in our theoretical work, and set it to -1 when we do numerical

simulations. For radiation, the trace of the energy-momentum tensor is zero. From Equation 1.3, we get

$$\mathrm{Tr}(T^{\mu}_{\nu}) = T^{\mu}_{\mu} = -\rho + 3p = 0 \Rightarrow p = \frac{\rho}{3} \Rightarrow w = \frac{1}{3}. \tag{1.4}$$

Now we can find out how the different components evolve with time, by using the conservation equation for the Energy-momentum tensor, Equation A.14. Writing this equation by the partial derivative and the Christoffel symbols, Equation A.7, we have

$$\nabla_{\mu} T^{\mu}_{\nu} = T^{\mu}_{\nu,\mu} + \Gamma^{\mu}_{\sigma\mu} T^{\sigma}_{\nu} - \Gamma^{\sigma}_{\nu\mu} T^{\mu}_{\sigma}.$$

This equation is valid for $\nu \in \{0, 1, 2, 3\}$. First we look at the case when $\nu = 0$, and inserting the non-zero Christoffel symbols:

$$\nabla_{\mu} T^{\mu}_{0} = T^{\mu}_{0,\mu} + \Gamma^{i}_{0i} T^{0}_{0} - \Gamma^{j}_{0i} T^{i}_{j} = -\frac{\partial \rho}{\partial t} - 3\frac{1}{a}\frac{da}{dt}\rho(1+w) = 0,$$

$$\frac{\partial \rho}{\partial t} + 3H\rho(1+w) = 0. \tag{1.5}$$

This is the continuity equation for a cosmic fluid. We see that the energy-density of the different components will change as the universe expands, if $w \neq -1$. As mentioned, we will set $w = -1$ for dark energy when we do numerical simulations. This is one of the strange things about dark energy: the energy-density is contant in time, even when the universe expands, if modeled by $w = -1$.

Setting ν to a spatial index in the energy-momentum conservation equation just gives $0 = 0$. While this is true, it does not give us anything useful.

1.1.3 Relating geometry and cosmic fluids: The Friedmann equations

Now that we have both sides of the Einstein equation, let us use it and see how a is related to ρ. We start with the time-component, $\mu = \nu = 0$:

$$E^{0}_{0} = 8\pi G T^{0}_{0} \Rightarrow -3\left(\frac{1}{a^2}\frac{da}{dt}\right)^2 = -8\pi G\rho \Rightarrow \left(\frac{1}{a}\frac{da}{dt}\right)^2 = \frac{8\pi G}{3}\rho. \tag{1.6}$$

This is the first Friedmann equation. Next, we look at the space component of the Einstein equation:

$$E^{i}_{i} = 8\pi G T^{i}_{i} \Rightarrow -2\frac{1}{2}\frac{d^2a}{dt^2} - \left(\frac{1}{a}\frac{da}{dt}\right)^2 = 8\pi G\rho$$

Inserting the first Friedmann equation and moving the terms around, we get

$$\frac{1}{a}\frac{d^2a}{dt^2} = -\frac{4\pi G}{3}\rho(1+3w). \tag{1.7}$$

This is the second Friedmann equation. If we now choose what components we want to have in our universe and how much of each, we have $\rho(t)$ by Equation 1.5, which gives us $\rho(t)$. This can then be inserted into the Friedmann equation, which gives us $a(t)$, and we have the evolution of the universe. Note that this equation is not independent of the first Friedmann equation, they are related by the Bianchi identities.

1.1.4 The redshift

Redshift z is a time variable that is very much used in cosmology, and is related to the Doppler shift of distant objects. We start with the definition, using the scale factor $a(t)$, where $a_0 = a(t_0) = 1$ as usual:

$$a(t) = \frac{1}{1+z}. \tag{1.8}$$

We see that big bang ($a = 0$) has infinite redshift. Recombination, an era in the early universe where neural atoms were formed, is around redshift $z = 1100$. When we are going to work with observational data, we will always use redshift as a time variable.

1.1.5 The comoving distance

Now that we have the line element, the next thing we will do is to compute the comoving distance r to an object. To do this, we look at a photon that travels from the object to us. A photon moves along what we call null-geodesics, which means that $ds = 0$ for a photon. ds is related to the infinitesimal spatial distance $dr = \sqrt{dx^2 + dy^2 + dz^2}$ by

$$ds^2 = -c^2dt^2 + a^2(t)dr^2 = 0 \Rightarrow cdt = a(t)dr \Rightarrow r = \int_r^o dr' = \int_t^{t_0} \frac{c}{a} dt'.$$

Notice that we follow the photon in this integration, which is why r and t are the lower integration limits, and 0 and t_0 the upper limits. Now we make some substitutions:

$$\frac{1}{a}\frac{da}{dt} = H \Rightarrow dt = \frac{da}{aH} \qquad a = \frac{1}{1+z}$$
$$\Rightarrow \frac{da}{dz} = -\frac{1}{(1+z)^2} \Rightarrow da = -\frac{dz}{(1+z)^2}.$$

Here, the redshift z has come into the picture. In terms of the redshift, our integral becomes

$$r = -c\int_{t_0}^{t} \frac{dt}{a} = -c\int_1^a \frac{da'}{(a')^2 H} = c\int_0^z \frac{1}{H} dz'. \tag{1.9}$$

Note that when t decreases, z increases. So now we have the comoving distance, if we know the redshift z and the Hubble parameter H as a function of redshift z.

1.1.6 The conformal time

Up to this point, we have used cosmic time t as our time variable. While cosmic time suits very well as a starting point and in a lot of situations later, there is another time variable that will be more useful in some situations. This time variable is called the *conformal time*, labeled η, and is defined as

$$d\eta = \frac{dt}{a}. \tag{1.10}$$

1.2 Perturbation theory and the formation of structures

In this section, I will give a background in Newtonian perturbation theory. Here we will look at general perturbations in a non-relativistic fluid, which will do as a background later when we come to baryon acoustic oscillations, where need to look at a specific case of evolution of perturbations. I am here following the lecture notes of Øystein Elgarøy for the Cosmology I course at the University of Oslo [1]. Then I will write some words about the Boltzmann equation, which we will use when we will use later. Using the Boltzmann equation is more advanced than the Newtonian approach, but the Newtonian approach is not good enough when we are looking at photons,which will enter the picture at some places.

1.2.1 Inhomogeneities

One of the first things we do in cosmology is to assume that the universe is homogeneous and isotropic on large scales. This turns out to be a very good approximation on very large scales, but on smaller scales, we know that this can not be true. In the universe today we can see planets, start, cluster of stars, galaxies, clusters of galaxies and superclusters. This means that the universe is not homogeneous at smaller scales, since if the universe was truly homogeneous at all scales at some time, it would stay homogeneous forever. And from that we can say that the inhomogeneities we see today started out sometime.

This starting point was inflation. Quantum fluctuations in the inflation field set up inhomogeneities in the very early universe, which over time have formed the structures we see today. To study how inhomogeneities evolve, we define what we call the *density contrast*, $\Delta(\mathbf{x}, t)$:

$$\Delta(\mathbf{x}, t) = \frac{\rho(\mathbf{x}, t) - \bar{\rho}(t)}{\bar{\rho}(t)}. \tag{1.11}$$

Here, $\rho(\mathbf{x}, t)$ is the energy density of some component of the universe at position $\mathbf{x}$ and time t, and $\bar{\rho}(t)$ is the space-average energy density at time t

of the same component. Now, if $|\Delta| < 1$, we say that the inhomogeneities are in the linear regime, and we can use linear perturbation theory. If $|\Delta| > 1$, we are in the non-linear regime, and non-linear methods must be used. We will only look at the first case. Also, we will only look at scales that are smaller than the particle horizon, and at velocities smaller than the speed of light. We may then use Newtonian perturbation theory, we do not have to deal with Einsteins general theory of relativity.

1.2.2 Perturbation theory for a non-relativistic fluid

Now we are going to do perturbation theory using fluid mechanics, which is good enough for a purpose later. We start with three equations for a fluid that sets up a gravitational field by its own presence, using the Euler description:

$$\frac{\partial \rho}{\partial t} + \nabla \cdot (\rho \mathbf{v}) = 0,$$
$$\frac{\partial \mathbf{v}}{\partial t} + (\mathbf{v} \cdot \nabla)\mathbf{v} = -\frac{\nabla p}{\rho} - \nabla \phi,$$
$$\nabla^2 \phi = 4\pi G \rho.$$

Here, ρ is the mass density of the fluid, $\mathbf{v}$ is the velocity field, p is the pressure and ϕ is the gravitational potential. The first equation is the continuity equation, expressing conservation of mass. The second equation is the Euler equation, the equation of motion for a particle in the fluid, which we get by applying Newtons second law to a particle in the fluid. The forces on the right hand side are then the pressure forces and gravity. The third equation is Poisson's equation, which relates the gravitational potential at a point to the mass density in the same point.

First of all we see that if we have a uniform, stationary state, that is, ρ and p are constant in space and $\mathbf{v} = 0$, there exist only one solution to the system, and that is $\rho = 0$, completely empty space. Now, we are, as usual, going to look at an expanding universe, and then we know that $\mathbf{v} \neq 0$. Then we can have a solution to start with, which is a matter-dominated, expanding universe. Now we can set up perturbations. We label the background solutions (hereby called the unperturbed solutions) by $\bar{\rho}, \bar{\mathbf{v}}, \bar{p}$ and $\bar{\phi}$. Then we add small perturbations to them, like this:

$$\rho = \bar{\rho} + \delta\rho,$$
$$\mathbf{v} = \bar{\mathbf{v}} + \delta\mathbf{v},$$
$$p = \bar{p} + \delta p,$$
$$\phi = \bar{\phi} + \delta\phi.$$

Now, we assume that the unperturbed pressure is homogeneous, so $\nabla \bar{p} = 0$. We have four unknowns in our three equations, and we need a fourth equation

in order to close the system. We then assume that our perturbations are adiabatic, and so the speed of sound in the medium, c_s, is a simple relation between the pressure and the density perturbations:

$$\delta p = c_s^2 \delta \rho.$$

We will use comoving coordinates $\mathbf{r}$, defined with the scale factor: $\mathbf{x} = a(t)\mathbf{r}$, where $\mathbf{x}$ is are the physical coordinates. Using this, we can rewrite the expression for the velocity field:

$$\mathbf{v} = \bar{\mathbf{v}} + \delta\mathbf{v} = H\mathbf{x} + a(t)\mathbf{u}.$$

Here, $\mathbf{u}$ is called the *peculiar velocity*, and describes the deviation from the Hubble flow. H is, as usual, the Hubble parameter. We also have the comoving version of ∇, labeled ∇_c, and defined as

$$\nabla_c = a\nabla.$$

Now, starting with the equation for ρ and manipulating, using the other equations, we end up with this equation:

$$\frac{d}{dt}\left(\frac{\delta\rho}{\bar{\rho}}\right) = \frac{d\Delta}{dt} = -\nabla \cdot \delta\mathbf{v}. \tag{1.12}$$

For the velocity field $\mathbf{v}$, using the sound speed relation and comoving coordinates, we end up with

$$\frac{d\mathbf{u}}{dt} + \frac{2}{a}\frac{da}{dt} = -\frac{c_s^2}{\bar{\rho}a^2}\nabla_c\delta\rho - \frac{\nabla_c\delta\phi}{a^2}. \tag{1.13}$$

And for the gravitational potential, we get

$$\frac{\nabla_c^2\delta\phi}{a^2} = 4\pi G\delta\rho.$$

Now, we are interested in solving for the density ρ. To get an equation where this is the only involved unknown, we take the divergence of Equation 1.13, and combine with the above equation, which gives

$$\nabla_c \cdot \dot{\mathbf{u}} + 2\frac{\dot{a}}{a}\nabla_c\mathbf{u} = -\frac{c_s^2}{\bar{\rho}a^2}\nabla_c\delta\rho - 4\pi G\delta\rho.$$

Using Equation 1.12 and the relation

$$\frac{d^2\Delta}{dt^2} = -\nabla_c \cdot \dot{\mathbf{u}},$$

we end up with

$$\frac{d^2\Delta}{dt^2} + 2\frac{\dot{a}}{a}\frac{d\Delta}{dt} = \frac{c_s^2}{\bar{\rho}a^2}\nabla_c^2\delta\rho + 4\pi G\delta\rho. \tag{1.14}$$

Now we have a partial differential equation. What we do now is to write Δ as a Fourier series:

$$\Delta(\mathbf{r}, t) = \sum_{\mathbf{k}} \Delta_k(t) e^{i\mathbf{k}_c \cdot \mathbf{r}}.$$

Since this is a linear differential equation, Fourier modes Δ_k for different values of the wavenumber k will evolve independently. Equation 1.14 can now be written as

$$\frac{d^2\Delta_k}{dt^2} + 2\frac{\dot{a}}{a}\frac{d\Delta_k}{dt} = \Delta_k(4\pi G\bar{\rho} - k^2 c_s^2). \tag{1.15}$$

Now we have a set of ordinary differential equations, one for each wavenumber k, instead of a partial differential equation. Each equation then describes the time evolution of a perturbation on a lengthscale $d = 1/k$.

Equation 1.15 has the same form as the equation for a damped oscillation or an exponential growth, depending on the sign of the term on the right hand side. The term $4\pi G\bar{\rho}$ on the right hand side is gravity, which makes perturbations grow. The term $k^2 c_s^2$ is pressure, which make perturbations fall until the pressure is to weak, when gravity will take over again. On the left hand side, the term $\dot{a}/a = H$ is some sort of friction: the expansion of the universe slows the growth of perturbations. Now, if a perturbation grows or not is determined by the sign of the right hand side, or in other words, if gravity is larger than the pressure or not. Since k is a constant, we can look at a limiting k where the term switches sign. This wavenumber is known as the *Jeans wavenumber*:

$$k_J = a(t)\frac{\sqrt{4\pi G\rho_0}}{c_s}. \tag{1.16}$$

So if $k > k_J$, the pressure term is largest, and we will have oscillations. If $k < k_J$, gravity is the largest term, and we will have collapse. Note the factor of $a(t)$ in front - this wavenumber is then the comoving Jeans wavenumber. Without the factor $a(t)$, we get the physical Jeans wavenumber. We will use the comoving version later on.

1.2.3 The Boltzmann equation

The Boltzmann equation, which is the correct approach when we are going to use the general theory of relativity to study the structure formation, tells us how the distribution function f for some component evolves with time. The distribution function tells us how many particles of some type we have near a position $\vec{r}$ moving with momentum close to $\vec{p}$ at a time t. Since we will use a general relativistic formulation, we will use x^μ and p^μ in stead of $\vec{r}, \vec{v}$ and t, but this will come into play afterwords. For now, $f(\vec{r}, \vec{v}, t)$ lives in an extended *phase space* that includes time.

As we know, components of the universe will interact with each other, and so we will introduce a collision term, $C[f]$, which takes all these kinds

of interactions (collisions) into account. With this, we can write down the Boltzmann equation, which looks very simple at first glance:

$$\frac{df}{dt} = C[f]. \tag{1.17}$$

What we will do is to write out the left hand side into several terms and compute each term separately. The collision term must also be computed.

We start with a useful, general way to write out the left-hand side. We first divide the momentum $\vec{p}$ into two parts, one absolute value p and one direction $\hat{p}$. The last one is still a vector (with length one), and the first one is a scalar. We then write the left-hand side of the Boltzmann equation like this:

$$\frac{df}{dt} = \frac{\partial f}{\partial t} + \frac{\partial f}{\partial x^i}\frac{dx^i}{dt} + \frac{\partial f}{\partial p}\frac{dp}{dt} + \frac{\partial f}{\partial \hat{p}^i}\frac{d\hat{p}^i}{dt}. \tag{1.18}$$

The strategy later will be to look at each term separately, working with all terms with ordinary derivatives to write them using the quantities that we will work with.

1.3 Observations

An important part of this report is the use of observations to put constraints on the model. In this section, I will define some quantities that we will use when working with observations.

1.3.1 The distance modulus and the luminosity distance

The magnitude scale is an old scale used in astronomy. The idea is very simple: a light-emitting object is assigned a numerical value based on how bright it looks. We still use a very old system here, giving the brightest star on the night sky the value 1 (so we say that a bright star has magnitude 1), and the faintest star have magnitude 6. Now, the human eyes response to brightness is logarithmic, so a magnitude 2 star, for example, has 10 times the intensity of a magnitude 3 star. This magnitude is labeled m. As we know, the intensity of a star, and therefore its magnitude m, depends on the distance to the star. We therefore introduce what we call the *absolute magnitude* of a star, which we define as the apparent magnitude if the distance to the star is ten parsecs. The absolute magnitude is therefore independent of distance, and can be computed based on the luminosity of the star. So if one can compute the absolute magnitude, and observe the apparent magnitude, one can compute the (luminosity) distance D_L to the star. The distance is given through this equation:

$$\mu = m - M = 2.5 \log\left(\frac{D_L}{10[\text{pc}]}\right), \tag{1.19}$$

where we use logarithm base 10. μ is known as the *distance modulus*.

In our case, we are going to use cosmological principles to compute the theoretical luminosity distance to an object, so we can compare with the observed luminosity distance. If we lived in a flat, static universe with Euclidean geometry, the energy flux we receive from a light-emitting astronomical object would be

$$F = \frac{L}{4\pi r^2},$$

where L is the luminosity of the object. If we know the luminosity of the object, we can solve for the distance r, which we now call the luminosity distance d_L:

$$d_L = \sqrt{\frac{L}{4\pi F}}.$$

An object of known luminosity is called a *standard candle*. An example of a standard (or standardizable) candle is supernova type Ia, which we will work with in this thesis.

Now, we do not live in a static universe, but an expanding universe. Due to the expansion, the photons that leave the star will have their wavelengths stretched by the time they reach us. Written in terms of redshift z and the comoving distance r, the flux we receive is

$$F = \frac{L}{4\pi r^2}\frac{1}{(1+z)^2}.$$

With this expression for the flux, the luminosity distance becomes

$$d_L = r(1+z). \tag{1.20}$$

1.3.2 The angular diameter distance

In the above section, we computed the luminosity distance, which is the distance to an object which we compute based on the energy flux we receive from a source. Now, we are going to look at the angular diameter distance. If we have an object of known size, we can compare this to the angular size of the object which we observe, and thereby we can compute the distance to this object. Let the size of the object be D, and assume that it covers an angle $\Delta\theta$ of the sky. We will assume that the distance d from us to the object is much larger than the diameter D of the object. We then use the small angle approximation, and define the angular diameter distance d_A to the distance d like this:

$$d_A = \frac{D}{\Delta\theta}.$$

Now we use the RW line element, Equation 1.1. The object we observe has comoving distance r and diameter D, and we measure the angular diameter $\Delta\theta$ at cosmic time t. We then get

$$ds^2 = r^2 a^2(t)(\Delta\theta)^2 = D^2,$$

which gives

$$D = a(t)r\Delta\theta \Rightarrow d_A = \frac{D}{\Delta\theta} = a(t)r.$$

Or, with redshift z as the variable,

$$d_A = \frac{r}{1+z}, \tag{1.21}$$

where we, as usual, have set $a(t_0) = 1$. Objects which have a known diameter are known as *standard rulers*. Also, by combining Equation 1.21 with Equation 1.20, we get this simple relation between the luminosity distance and the angular diameter distance of an object at redshift z:

$$\frac{d_L}{d_A} = (1+z)^2.$$

1.3.3 The galaxy correlation function

Now I will introduce the galaxy correlation function, which we will run into at some point. I follow the notes of Øystein Elgarøy for the course in cosmology and extragalactic astronomy at the University of Oslo [2].

The galaxy correlation function is a function that tells how galaxies are distributed in space. As we know, galaxies are not randomly distributed in space, the form structures such as groups, clusters and voids. To define the galaxy correlation function $\xi_g(\mathbf{r})$, where $\mathbf{r}$ is a separation vector, we start by choosing two small volumes ΔV_1 and ΔV_2, and one large volume V. The large volume V contains N galaxies, and we assume that the volume V is so large that the Copernican principle applies to this volume, so that it will contain the same number of galaxies no matter where in the universe the volume V is placed. Then we let $n = N/V$ be the average number of galaxies in a volume V. Now, **if** galaxies were truly distributed randomly in space, n could also represent the number density of galaxies in the volumes ΔV_1 and ΔV_2. The probability of finding a galaxy in the volume ΔV_1 would then be

$$\frac{n\Delta V_1}{N} = \frac{n\Delta V_1}{nV} = \frac{\Delta V_1}{V},$$

and the probability of finding a galaxy in the volume ΔV_1 *and* and another galaxy in the volume ΔV_2 would be

$$\Delta P = \frac{\Delta V_1}{V} \cdot \frac{\Delta V_2}{V}.$$

Now, as mentioned, galaxies are not uniformly distributed in space, and the probability of finding a galaxy in ΔV_1 and another in ΔV_2 then differs from this value. The galaxy correlation function is then defined as a meassure of this deviation from uniform distribution, like this:

$$\Delta P = (1 + \xi_g(\mathbf{r}))\frac{\Delta V_1}{V}\frac{\Delta V_2}{V}. \tag{1.22}$$

Here, the variable $\mathbf{r}$ is the separation, going from the galaxy in the volume ΔV_1 to the point where we evaluate the function. This means that if galaxies cluster, $\xi_g(\mathbf{r})$ would be positive, since the probability of finding two galaxies separated by $\mathbf{r}$ is larger than the corresponding probability in a uniform distribution of galaxies. If galaxies avoids each other, $\xi_g(\mathbf{r})$ will be negative.

If we make the Fourier transform of the galaxy correlation function, we get the *power spectrum* of the galaxy correlation function:

$$P_g(k) = \int_V \xi_g(\mathbf{r}) e^{-i\mathbf{k}\cdot\mathbf{r}} d^3r. \tag{1.23}$$

Here, the variable $\mathbf{k}$ is a wave vector.

Chapter 2

A universe with interacting components

2.1 Introducing interactions

In this thesis, we want to study interactions between baryonic matter, dark matter and dark energy. We will look at interactions simply as an exchange in energy and momentum: if there are interactions present, we will have transfer of energy and/or momentum between the three components. This means that the conservation equation for the energy-momentum tensor of each component is modified by interaction terms on the right hand side. Since these interactions must contain both energy and momentum transfer, they will be rank one tensors Q_ν. We let $Q_\nu(b, \mathrm{DM})$ be the energy-momentum exchange between baryons and dark matter, $Q_\nu(b, \mathrm{DE})$ be the energy exchange between baryons and dark energy, and Q_ν(DM,DE) be the energy exchange between dark matter and dark energy. The energy-momentum conservation equations of the three components can then be set up like this:

$$\begin{aligned} \nabla_\mu T^\mu_\nu(b) &= Q_\nu(b, \mathrm{DM}) + Q_\nu(b, \mathrm{DE}), && (2.1)\\ \nabla_\mu T^\mu_\nu(\mathrm{DM}) &= -Q_\nu(b, \mathrm{DM}) + Q_\nu(\mathrm{DM},\ \mathrm{DE}), && (2.2)\\ \nabla_\mu T^\mu_\nu(\mathrm{DE}) &= -Q_\nu(b, \mathrm{DE}) - Q_\nu(\mathrm{DM},\ \mathrm{DE}). && (2.3) \end{aligned}$$

Note the signs on the right hand side, this makes sure that the total energy-momentum tensor $T^\mu_\nu = T^\mu_\nu(b) + T^\mu_\nu(\mathrm{DM}) + T^\mu_\nu(\mathrm{DE})$ is still conserved, $T^\mu_{\nu;\mu} = 0$, and the Einstein equations are the same as before. (This is actually only true at the background level. If we have interactions that alters the dark energy density, this may also set up non-zero perturbations in the dark energy density, which will enter the Einstein equations as well. More about this in later chapters.)

2.2 Setting up an interaction model

From the conservation equations of the energy momentum tensors, one simple question sets up a huge job: find the Qs. In some sense, it is not possible to compute the Qs directly, so I will set up a specific model for the Qs, and then study that model as a dynamical system of interacting fluids. In my model, the interaction terms will contain dimensionless interaction parameters that directly gives the strength of the interaction. I will use α for the interaction strength between baryons and dark matter, β for baryons and dark energy, and γ for dark matter and dark energy. Linear combinations of the energy-momentum tensors involved will enter, so more or less of some component will give more or less interactions. The expansion rate of the universe $\nabla_\mu u^\mu$ will also enter, this will slow down the interactions. At last we have a four-vector s, which is a combination of the four velocities of the two components - how the components move will of course affect the interactions. There are multiple ways of setting up s, and I will use the average four velocity of the two interacting components x and y (and so s depends on which two components that are interacting):

$$s_\nu(x,y) = \frac{u_\nu(x) + u_\nu(y)}{2}.$$

With these starting points (we leave the four velocity as s), we have these forms of the three interaction terms:

$$\begin{aligned} Q_\nu(b,\mathrm{DM}) &= \alpha\nabla_\mu s^\mu(T_{\sigma\rho}u^\sigma u^\rho(b) + T_{\sigma\rho}u^\sigma u^\rho(\mathrm{DM}))s_\nu, \\ Q_\nu(b,\mathrm{DE}) &= \beta\nabla_\mu s^\mu(T_{\sigma\rho}u^\sigma u^\rho(b) + T_{\sigma\rho}u^\sigma u^\rho(\mathrm{DE}))s_\nu, \\ Q_\nu(\mathrm{DM},\mathrm{DE}) &= \gamma\nabla_\mu s^\mu(T_{\sigma\rho}u^\sigma u^\rho(\mathrm{DM}) + T_{\sigma\rho}u^\sigma u^\rho(\mathrm{DE}))s_\nu. \end{aligned}$$

As mentioned earlier, we are assuming that all the components behave as perfect fluids. Then we can use this relation:

$$T_{\mu\nu}u^\mu u^\nu = \rho,$$

and so the equations simplify:

$$\begin{aligned} Q_\nu(b,\mathrm{DM}) &= \alpha\nabla_\mu s^\mu(b,\mathrm{DM})(\rho_b + \rho_{\mathrm{DM}})s_\nu(b,\mathrm{DM}), \\ Q_\nu(b,\mathrm{DE}) &= \beta\nabla_\mu s^\mu(b,\mathrm{DE})(\rho_b + \rho_{\mathrm{DE}})s_\nu(b,\mathrm{DE}), \\ Q_\nu(\mathrm{DM},\ \mathrm{DE}) &= \gamma\nabla_\mu s^\mu(\mathrm{DM},\ \mathrm{DE})(\rho_{\mathrm{DM}} + \rho_{\mathrm{DE}})s_\nu(\mathrm{DM},\ \mathrm{DE}). \end{aligned}$$

2.3 Interactions for the FRW metric

Our equations are written in covariate form so far. For the first part of the thesis, we will work with the background universe, using the FRW metric, with line element given by Equation 1.1. We then have the four velocities:

$u^0 = 1, u_0 = -1$ and $u^i = u_i = 0$ for all components. From this we see that $Q_i = 0$ for all interactions - there is no momentum exchange in in the background universe. For Q_0, we first find the factor $\nabla_\mu u^\mu$ from Equation A.6:

$$\nabla_\mu u^\mu = u^\mu_{,\mu} + \Gamma^\mu_{\alpha\mu} u^\alpha = \frac{3}{a}\frac{da}{dt} = 3H.$$

Q_0 then reads

$$Q_0(b, \mathrm{DM}) = 3H\alpha(\rho_b + \rho_{\mathrm{DM}}),$$
$$Q_0(b, \mathrm{DE}) = 3H\beta(\rho_b + \rho_{\mathrm{DE}}),$$
$$Q_0(\mathrm{DM}, \mathrm{DE}) = 3H\gamma(\rho_{\mathrm{DM}} + \rho_{\mathrm{DE}}).$$

The left hand side of the conservation equations, Equation 2.3, is given by Equation 1.5. Putting together, the interaction equations with the FRW metric takes this form:

$$\frac{\partial \rho_b}{\partial t} + 3H\rho_b = 3H(\alpha(\rho_b + \rho_{\mathrm{DM}}) + \beta(\rho_b + \rho_{\mathrm{DE}})), \quad (2.4)$$
$$\frac{\partial \rho_{\mathrm{DM}}}{\partial t} + 3H\rho_{\mathrm{DM}} = 3H(-\alpha(\rho_b + \rho_{\mathrm{DM}}) + \gamma(\rho_{\mathrm{DM}} + \rho_{\mathrm{DE}})), \quad (2.5)$$
$$\frac{\partial \rho_{\mathrm{DE}}}{\partial t} + 3H\rho_{\mathrm{DE}}(1+w) = 3H(-\beta(\rho_b + \rho_{\mathrm{DE}}) - \gamma(\rho_{\mathrm{DM}} + \rho_{\mathrm{DE}}). \quad (2.6)$$

2.4 The interaction models in different clothings

The interaction models in Equation 2.6 is only one way of writing the equations for the energy-densities. Through the thesis, we will need a lot of other ways of writing them, and I will present these varieties here.

2.4.1 Equations for the background universe

In the upcoming chapters, we will work with the background equations, finding analytical solutions to the equations and studying the stability of the solutions. It is often useful to write the equations using only dimensionless quantities, so we introduce the density parameters $\Omega_i, i \in \{b, \mathrm{DM}, \mathrm{DE}\}$:

$$\Omega_i = \frac{8\pi G}{3H^2}\rho_i.$$

For the time variable, we will use the number of e-foldings N, so that $dN = Hdt$. There also is another "problem": the equation of state parameter w for the dark energy. From now on, we will assume it is a constant. Then I will redefine the density parameters: $\tilde{\alpha} = \alpha/(-w)$, and the same for β and γ. The e-fold number is also rescaled: $\tilde{N} = -wN$. Now we have this set of

equations:

$$\begin{aligned}
\frac{1}{3}\frac{d\Omega_b}{d\tilde{N}} &= (-\Omega_{\rm DE} + \tilde{\alpha} + \tilde{\beta})\Omega_b + \tilde{\alpha}\Omega_{\rm DM} + \tilde{\beta}\Omega_{\rm DE}, \\
\frac{1}{3}\frac{d\Omega_{\rm DM}}{d\tilde{N}} &= (-\Omega_{\rm DE} - \tilde{\alpha} + \tilde{\gamma})\Omega_{\rm DM} - \tilde{\alpha}\Omega_b + \tilde{\gamma}\Omega_{\rm DE}, \\
\frac{1}{3}\frac{d\Omega_{\rm DE}}{d\tilde{N}} &= (-\Omega_{\rm DE} + 1 - \tilde{\beta} - \tilde{\gamma})\Omega_{\rm DE} - \tilde{\beta}\Omega_b - \tilde{\gamma}\Omega_{\rm DM}.
\end{aligned}$$

Now, since we are looking at a flat universe (by that I mean that the 3-space is flat), we have the Friedman constraint:

$$\Omega_b + \Omega_{\rm DM} + \Omega_{\rm DE} = 1. \tag{2.7}$$

Using this, we can write one of the variables in terms of the two others. We will choose to eliminate Ω_b, so we have $\Omega_b = 1 - \Omega_{\rm DM} - \Omega_{\rm DE}$. This means that we now have three equations with only two variables. But, both Einstein equations have actually been used to make these three equations, and the two Einstein equations are not independent. Therefore, only two of the equations are independent. In the following, we will use the equations for $\Omega_{\rm DM}$ and $\Omega_{\rm DE}$ as our independent equations. Rewriting, we get this system of equations:

$$\frac{1}{3}\frac{d\Omega_{\rm DM}}{d\tilde{N}} = (\tilde{\gamma} - \Omega_{\rm DE})\Omega_{\rm DM} + \tilde{\alpha}(\Omega_{\rm DE} - 1) + \tilde{\gamma}\Omega_{\rm DE}, \tag{2.8}$$

$$\frac{1}{3}\frac{d\Omega_{\rm DE}}{d\tilde{N}} = (1 - \tilde{\gamma} - \Omega_{\rm DE})\Omega_{\rm DE} + \tilde{\beta}(\Omega_{\rm DM} - 1) - \tilde{\gamma}\Omega_{\rm DM}. \tag{2.9}$$

Writing the equations in terms of the density parameters $\Omega(b, \text{DM, DE})$ and the number of e-foldings N is very useful when we are going to study the stability of our system. However, we are also interested in finding the analytical expression of the actual density parameters. The easiest way is then to work with the equations in this form:

$$\frac{d\rho_b}{dN} + 3\rho_b = 3(\alpha(\rho_b + \rho_{\rm DM}) + \beta(\rho_b + \rho_{\rm DE})), \tag{2.10}$$

$$\frac{\rho_{\rm DM}}{dN} + 3\rho_{\rm DM} = 3(-\alpha(\rho_b + \rho_{\rm DM}) + \gamma(\rho_{\rm DE})), \tag{2.11}$$

$$\frac{\rho_{\rm DE}}{dN} + 3(1+w)\rho_{\rm DE} = 3(-\beta(\rho_b + \rho_{\rm DE}) - \gamma(\rho_{\rm DM} + \rho_{\rm DE})). \tag{2.12}$$

Here, we have gone back to the actual energy-densities, but kept the number of e-foldings, so that H does not enter the equations directly.

2.4.2 Comparing with observations

In the second part of this thesis, I will compare the universe models I get with the interaction models with observational data, to see if the interaction

models can actually describe our own universe. In the observational data that I will work with, the redshift z defined in Equation 1.8 is used as a time variable, and we then need to rewrite our equations so we get them in terms of z. Also, when we are working with Baryon acoustic oscillations and the cosmic microwave background, I will need a universe model that goes (almost) all the way back to big bang. There are a lot of physics, like inflation and such, that I will not have time to include, and it will not be included, but it is one thing that must be taken into account: the fact that the early universe is dominated by radiation. We then introduce the density parameter for radiation, Ω_r, and since interaction with radiation is not taken into account in this part, we can just use the radiation equation of state, Equation 1.4, and we simply see that the energy-density of radiation evolves like $\rho_r(z) = \rho_{r0}(1+z)^4$.

When changing variable from t to z in our equations, the substitution goes like this:

$$dt = -\frac{1}{1+z}dz, \tag{2.13}$$

and so our system of equations becomes

$$\begin{aligned}
\frac{d\Omega_b}{dz} &= \frac{-3}{1+z}\left(\left(w\Omega_{\mathrm{DE}} + \alpha + \beta + \frac{\Omega_r}{3}\right)\Omega_b + \alpha\Omega_{\mathrm{DM}} + \beta\Omega_{\mathrm{DE}}\right), \\
\frac{d\Omega_{\mathrm{DM}}}{dz} &= \frac{-3}{1+z}\left(\left(w\Omega_{\mathrm{DE}} - \alpha + \gamma + \frac{\Omega_r}{3}\right)\Omega_{DM} - \alpha\Omega_b + \gamma\Omega_{\mathrm{DE}}\right), \\
\frac{d\Omega_{\mathrm{DE}}}{dz} &= \frac{-3}{1+z}\left(\left(w\Omega_{\mathrm{DE}} - w - \beta - \gamma + \frac{\Omega_r}{3}\right)\Omega_{\mathrm{DE}} - \beta\Omega_b - \gamma\Omega_{\mathrm{DM}}\right).
\end{aligned} \tag{2.14}$$

We also need to find the Hubble parameter as a function of redshift, so we rewrite the second Einstein equation, Equation 1.7. This equation becomes

$$\frac{dH}{dz} = \frac{3H}{2(1+z)}\left(1 + w\Omega_{\mathrm{DE}} + \frac{\Omega_r}{3}\right). \tag{2.15}$$

2.4.3 With both w and N

When I will work with inhomogeneous perturbations in the third part of the thesis, I will actually write my equations using the e-fold number N as the time variable, and I will keep the dark energy equation of state parameter w in my equations. Contribution from redshift will also be included. The interaction equations then takes this form:

$$\begin{aligned}
\frac{d\Omega_b}{dN} &= 3\left(\left(w\Omega_{\mathrm{DE}} + \frac{\Omega_r}{3} + \alpha + \beta\right)\Omega_b + \alpha\Omega_{\mathrm{DM}} + \beta\Omega_{\mathrm{DE}}\right), \\
\frac{d\Omega_{\mathrm{DM}}}{dN} &= 3\left(\left(w\Omega_{\mathrm{DE}} + \frac{\Omega_r}{3} - \alpha + \gamma\right)\Omega_{\mathrm{DM}} - \alpha\Omega_b + \gamma\Omega_{\mathrm{DE}}\right),
\end{aligned}$$

$$\frac{d\Omega_{\mathrm{DE}}}{dN} = 3\left(\left(w\Omega_{\mathrm{DE}} + \frac{\Omega_r}{3} - w - \beta - \gamma\right)\Omega_{\mathrm{DE}} - \beta\Omega_b - \gamma\Omega_{\mathrm{DM}}\right),$$

$$\Omega_r = 1 - \Omega_b - \Omega_{\mathrm{DM}} - \Omega_{\mathrm{DE}}. \tag{2.16}$$

The Hubble parameter H is given by this equation:

$$\frac{dH}{dN} = \frac{3H}{2}\left(1 + w\Omega_{\mathrm{DE}} + \frac{\Omega_r}{3}\right). \tag{2.17}$$

2.5 Fixed points

As mentioned, we are interested in the stability of our dynamical system. To analyze the stability, we will find the critical points. These are the points $(\Omega_{\mathrm{DM}}, \Omega_{\mathrm{DE}})$ where the derivatives are zero. When we have such a point, we can study the stability of that point. The stability tells us how the system behaves close to the critical points.

When we study the critical points, we will work with the equations written in terms of the energy-density parameters, $\Omega(b, \mathrm{DM}, \mathrm{DE})$, Equation 2.9. Finding the fixed points is simple, one sets the derivatives to zero:

$$(\tilde{\gamma} - \Omega_{\mathrm{DE}})\Omega_{\mathrm{DM}} + \tilde{\alpha}(\Omega_{\mathrm{DE}} - 1) + \tilde{\gamma}\Omega_{\mathrm{DE}} = 0, \tag{2.18}$$

$$(1 - \tilde{\gamma} - \Omega_{\mathrm{DE}})\Omega_{DE} + \tilde{\beta}(\Omega_{\mathrm{DM}} - 1) - \tilde{\gamma}\Omega_{\mathrm{DM}} = 0. \tag{2.19}$$

Now that we know how to find the fixed points, we will analyze the stability. We use the stability matrix M defined in Equation B.5. In our case, we have two equations, our quantities are Ω_{DM} and Ω_{DE}, and N is our parameter that does not explicitly enter the equations on the right hand sides. So our matrix M becomes

$$M = \begin{pmatrix} \tilde{\gamma} - \Omega_{\mathrm{DE}} & \tilde{\alpha} + \tilde{\gamma} - \Omega_{\mathrm{DM}} \\ \tilde{\beta} - \tilde{\gamma} & 1 - \tilde{\gamma} - 2\Omega_{\mathrm{DE}} \end{pmatrix}. \tag{2.20}$$

In the theoretical parts of this thesis, the study of the stability of the fixed points will be crucial, as it tells us a lot, no matter how complex the analytical solutions look like.

Chapter 3

One interaction

In this chapter, we will look at models where we only have one interaction. This simply means that we will set two of the interaction parameters from Equation 2.9 to zero. This then gives three different models, one for each interaction.

3.1 Dark matter and dark energy

If we set $\tilde{\alpha} = \tilde{\beta} = 0$, the only interaction present is between dark matter and dark energy. The baryons are then decoupled in this model. In this and the upcoming chapter studying one and two interaction models, I will divide each section in two parts: one with critical point and stability analysis, and one where I find the analytical solutions. For this case, I will start with the critical points and stability.

3.1.1 Critical points and stability analysis

Using Equation 2.19 with $\tilde{\alpha} = \tilde{\beta} = 0$, we get this set of equations for the fixed points:

$$\Omega_{\mathrm{DE}}(1 - \Omega_{\mathrm{DM}} - \Omega_{\mathrm{DE}}) = 0,$$
$$(\tilde{\gamma} - \Omega_{\mathrm{DE}})\Omega_{\mathrm{DM}} + \tilde{\gamma}\Omega_{\mathrm{DE}} = 0.$$

One solution to this set of equations is the trivial solution $\Omega_{\mathrm{DM}} = \Omega_{\mathrm{DE}} = 0$, which by the Friedmann constraint gives $\Omega_b = 1$, a universe totally dominated by baryonic matter. With $\tilde{\alpha} = \tilde{\beta} = 0$ and $\Omega_{\mathrm{DM}} = \Omega_{\mathrm{DE}} = 0$, our stability matrix M from Equation 2.20 now becomes

$$M = \begin{pmatrix} \tilde{\gamma} & \tilde{\gamma} \\ -\tilde{\gamma} & 1 - \tilde{\gamma} \end{pmatrix}.$$

The stability of this critical point is determined by the signs of the eigenvalues of M. We get the eigenvalues by the determinant in Equation B.3, which

gives us the characteristic polynomial:

$$\begin{vmatrix} \tilde{\gamma}-u & \tilde{\gamma} \\ -\tilde{\gamma} & 1-\tilde{\gamma}-u \end{vmatrix} = (\tilde{\gamma}-u)(1-\tilde{\gamma}-u)+\tilde{\gamma}^2 = u^2+u+\tilde{\gamma} = 0.$$

$$\Rightarrow u = \frac{1}{2}(1 \pm \sqrt{1-4\tilde{\gamma}}).$$

From this, we see that if $\tilde{\gamma} > \frac{1}{4}$, the eigenvalues are complex with a positive real part, and we get an unstable spiral. If $\tilde{\gamma} \leq \frac{1}{4}$, the eigenvalues are real. Further we see that if $\tilde{\gamma} > 0$, both eigenvalues are positive, while if $\tilde{\gamma} < 0$, one of the eigenvalues (the one with the minus sign) will be negative, the other will be positive, and we have a saddle point. So:

- $\tilde{\gamma} < 0$: Saddle point.
- $\tilde{\gamma} = 0$: No interaction at all.
- $\tilde{\gamma} \in (0, \frac{1}{4}]$: Unstable point.
- $\tilde{\gamma} > \frac{1}{4}$: Unstable spiral.

For the second solution to the equation set, we can see that we need $(1-\Omega_{\rm DM}-\Omega_{\rm DE}) = \Omega_b = 0$ in the first equation. This gives $\Omega_{\rm DM} = 1-\Omega_{\rm DE}$. Inserting this into the second equation gives

$$(\tilde{\gamma}-\Omega_{\rm DE})(1-\Omega_{\rm DE})+\tilde{\gamma}\Omega_{\rm DE} = 0 \tag{3.1}$$

$$\Rightarrow \Omega_{\rm DE} = \frac{1}{2}\left(1 \pm \sqrt{1-4\tilde{\gamma}}\right). \tag{3.2}$$

Since $\Omega_{\rm DE}$ must be a real number, we see that we must have $\tilde{\gamma} \leq \frac{1}{4}$. Further, since $\Omega_{\rm DE} \leq 1$, we must have $\tilde{\gamma} \geq 0$. So, $\tilde{\gamma} \in [0, \frac{1}{4}]$. This condition is valid for both values of $\Omega_{\rm DE}$ (notice the $\pm$ in the expression for $\Omega_{\rm DE}$).

Now we look at the eigenvalues u of the stability matrix M from Equation 2.20. Again we use Equation B.3, which in this case gives this determinant, which again gives us the characteristic polynomial:

$$0 = \begin{vmatrix} \tilde{\gamma}-\Omega_{\rm DE}-u & \tilde{\gamma}-1+\Omega_{\rm DE} \\ -\tilde{\gamma} & 1-\tilde{\gamma}-2\Omega_{\rm DE}-u \end{vmatrix}$$

$$= (\tilde{\gamma}-\Omega_{\rm DE}-u)(1-\tilde{\gamma}-2\Omega_{\rm DE}-u)+\tilde{\gamma}(\tilde{\gamma}-1+\Omega_{\rm DE})$$

$$= u^2+(3\Omega_{\rm DE}-1)u+2\Omega_{\rm DE}^2-\Omega_{\rm DE} = 0.$$

$$\Rightarrow u = \frac{1}{2}\left(1-3\Omega_{\rm DE} \pm \sqrt{9\Omega_{\rm DE}^2-6\Omega_{\rm DE}+1-8\Omega_{\rm DE}^2+4\Omega_{\rm DE}}\right)$$

$$= \frac{1}{2}\left(1-3\Omega_{\rm DE} \pm \sqrt{\Omega_{\rm DE}^2-2\Omega_{\rm DE}+1}\right).$$

Now we insert for $\Omega_{\rm DE}$. Since we have two values for $\Omega_{\rm DE}$ which each gives two values for u, we get four eigenvalues in total. If we use the plus-sign in the expression for $\Omega_{\rm DE}$, we get these two eigenvalues:

$$u_1 = -\frac{1}{4}\left(1 + 3\sqrt{1-4\tilde{\gamma}} + \sqrt{2(1-2\tilde{\gamma}-\sqrt{1-4\tilde{\gamma}})}\right),$$

$$u_2 = -\frac{1}{4}\left(1 + 3\sqrt{1-4\tilde{\gamma}} - \sqrt{2(1-2\tilde{\gamma}-\sqrt{1-4\tilde{\gamma}})}\right).$$

Since both u_1 and u_2 are negative when $\tilde{\gamma} \in [0, \frac{1}{4}]$, this critical point is stable.

Using the minus-sign in the expression for $\Omega_{\rm DE}$, we get these two eigenvalues:

$$u_1 = -\frac{1}{4}\left(1 - 3\sqrt{1-4\tilde{\gamma}} + \sqrt{2(1-2\tilde{\gamma}+\sqrt{1-4\tilde{\gamma}})}\right),$$

$$u_2 = -\frac{1}{4}\left(1 - 3\sqrt{1-4\tilde{\gamma}} - \sqrt{2(1-2\tilde{\gamma}+\sqrt{1-4\tilde{\gamma}})}\right).$$

Here, if $\tilde{\gamma} < 0$, we have an unstable point, but this is excluded because $\Omega_{\rm DE} \leq 1$, as discussed earlier. When $\tilde{\gamma} \in [0, \frac{1}{4}]$, one of the eigenvalues is positive while the other is negative, so we have a saddle point.

3.1.2 The analytical solution

The next job is to find the analytical solution to our equations. With $\alpha = \beta = 0$, Equation 2.12 looks like this:

$$\rho_b' + 3\rho_b = 0, \tag{3.3}$$

$$\rho_{\rm DM}' + 3\rho_{\rm DM} = 3\gamma(\rho_{\rm DM} + \rho_{\rm DE}), \tag{3.4}$$

$$\rho_{\rm DE}' + 3(1+w)\rho_{\rm DE} = -3\gamma(\rho_{\rm DM} + \rho_{\rm DE}). \tag{3.5}$$

Here, the prime denotes derivative with respect to the e-fold number N. As mentioned, the baryons are decoupled from the other two components in this model, and the right hand side of the equation for the baryon energy density is zero, The baryons will then follow the usual evolution $\rho_b = \rho_{b0}(1+z)^3$. The other two equations are coupeled to each other. We rewrite them using the quantities $\rho_{\rm D} = \rho_{\rm DM} + \rho_{\rm DE}$ (a common energy density for the dark components) and $R = \rho_{\rm DE}/\rho_{\rm D}$, a ratio of how much of the dark components that are in the form of dark energy. If we then add the two equations for the dark components, we get

$$\rho_{\rm D}' + 3\rho_{\rm D} + 3w\rho_{\rm DE} = \rho_{\rm D}' + 3\rho_{\rm D} + 3wR\rho_{\rm D} = 0. \tag{3.6}$$

As we expect, the fact that we can not neglect the pressure of the dark energy brings R into the picture. Solving for R gives

$$R = -\frac{1}{3w}\left(3 + \frac{\rho_{\rm D}'}{\rho_{\rm D}}\right) = -\frac{1}{3w}\left(3 + (\ln\rho_{\rm D})'\right).$$

To proceed, we must assume that the equation of state parameter w for the dark energy is a constant. We take the derivative of Equation 3.6:

$$\rho_{\mathrm{D}}'' + 3\rho_{\mathrm{D}}' + 3w(R'\rho_{\mathrm{D}} + R\rho_{\mathrm{D}}') = 0.$$

We need the derivative of R:

$$R' = \frac{\rho_{\mathrm{DE}}'\rho_{\mathrm{D}} - \rho_{\mathrm{DE}}\rho_{\mathrm{D}}'}{\rho_{\mathrm{D}}^2} = \frac{1}{\rho_{\mathrm{D}}^2}\left(-3\gamma\rho_{\mathrm{D}} - 3(1+w)R\rho_{\mathrm{D}} - R\rho_{\mathrm{D}}\rho_{\mathrm{D}}'\right)$$

$$= -3\gamma - 3(1+w)R - R\frac{\rho_{\mathrm{D}}'}{\rho_{\mathrm{D}}}.$$

Inserting this, we get

$$\rho_{\mathrm{D}}'' + 3\rho_{\mathrm{D}}' - 9w\gamma\rho_{\mathrm{D}} - 9w(1+w)R\rho_{\mathrm{D}} - 3wR\rho_{\mathrm{D}}' - \rho_{\mathrm{D}}'\left(3 + \frac{\rho_{\mathrm{D}}'}{\rho_{\mathrm{D}}}\right) = 0,$$

$$\rho_{\mathrm{D}}'' + 3\rho_{\mathrm{D}}' - 9w\gamma\rho_{\mathrm{D}} + 3(1+w)\left(3\rho_{\mathrm{D}} + \rho_{\mathrm{D}}'\right) + 3\rho_{\mathrm{D}}' + \frac{(\rho_{\mathrm{D}}')^2}{\rho_{\mathrm{D}}} - \rho_{\mathrm{D}}'\left(3 + \frac{\rho_{\mathrm{D}}'}{\rho_{\mathrm{D}}}\right) = 0,$$

$$\rho_{\mathrm{D}}'' + 3(2+w)\rho_{\mathrm{D}}' + 9(1+w-\gamma w)\rho_{\mathrm{D}} = 0.$$

This is an ordinary linear second order homogeneous differential equation with constant coefficients, and the solution is straight forward: we set up the characteristic polynomial,

$$r^2 + 3(2+w)r + 9(1+w-\gamma w),$$

and find the roots of this polynomial:

$$r = \frac{1}{2}\left(-3(2+w) \pm \sqrt{9(2+w)^2 - 36(1+w-\gamma w)}\right)$$

$$= -\frac{3}{2}(2+w) \pm \frac{3}{2}\sqrt{w(w+4\gamma)} = p \pm q,$$

with

$$p = -\frac{3}{2}(2+w) \qquad q = \frac{3}{2}\sqrt{w(w+4\gamma)}.$$

And the solution of the differential equation is

$$\rho_{\mathrm{D}} = \rho_{\mathrm{D}}^{(0)} e^{p(N-N_0)}\cosh(q(N-N_0)). \tag{3.7}$$

Here, $\rho_{\mathrm{D}}^{(0)}$ is the value of ρ_{D} at $N = N_0$. Computing ρ_{D}':

$$\rho_{\mathrm{D}}' = \rho_{\mathrm{D}}^{(0)}\left(pe^{p(N-N_0)}\cosh(q(N-N_0)) + e^{p(N-N_0)}q\sinh(q(N-N_0))\right),$$

we can now compute the ratio R:

$$R = -\frac{1}{3w}\left(3 + \frac{\rho_{\mathrm{D}}'}{\rho_{\mathrm{D}}}\right) = -\frac{1}{3w}\left(3 + p + q\tanh(q(N-N_0))\right). \tag{3.8}$$

Now let us compare the analytical solution to the stability analysis. For simplicity, we set $w = -1$. We know that

$$\lim_{x\to\infty} \tanh x = 1$$

and so we have

$$\lim_{N\to\infty} R = 1 + \frac{p+q}{3} = \frac{1}{2}\left(1 + \sqrt{1-4\gamma}\right), \tag{3.9}$$

which is the stable critical point we found earlier. The ratio R and the ratio $\rho_{\mathrm{D}}/\rho_{\mathrm{D0}}$ are plotted on Figure 3.1, with $\gamma = 0.1$. We see that R approaches a value around 0.88, which is what we get if we set $\gamma = 0.1$ into equation 3.9. This might seem strange since this interaction gives more dark matter and less dark energy when $\gamma > 0$, but at late time, the expansion of the universe have become so large that the abundance of dark matter will be very small, and the interaction will die out.

In [3], different models for interactions between dark matter and dark energy is used, one which is proportional to the Hubble parameter, as our model is. We see that we obtain the same results, that dark matter dominates in early times and dark energy dominates at late times.

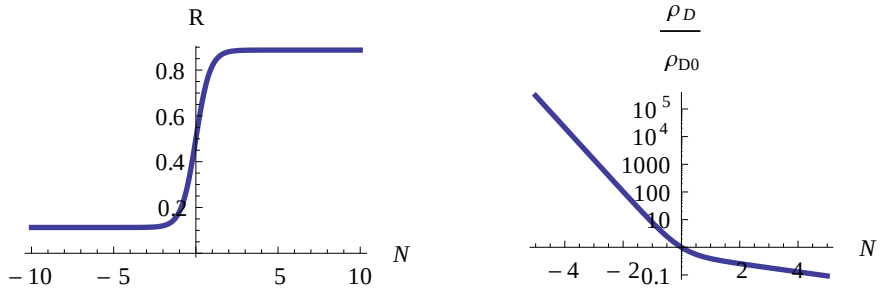

Figure 3.1: The ratio $R(N)$ and the energy-density $\rho_{\mathrm{D}}(N)/\rho_{\mathrm{D0}}(N)$.

3.2 Baryons and dark matter

If we set $\tilde{\beta} = \tilde{\gamma} = 0$, the only interaction present is between baryons and dark matter. The dark energy is then decoupled.

3.2.1 Critical points and stability analysis

In this case, Equation 2.19 for the fixed points becomes

$$\begin{aligned} \tilde{\alpha}(1-\Omega_{\mathrm{DE}}) + \Omega_{\mathrm{DE}}\Omega_{\mathrm{DM}} &= 0, \\ (1-\Omega_{\mathrm{DE}})\Omega_{\mathrm{DE}} &= 0. \end{aligned}$$

From these equations we can see that for a critical point, we must have $\Omega_{\rm DE} \in \{0, 1\}$. If $\Omega_{\rm DE} = 0$, we also get $\tilde{\alpha} = 0$. This gives no interactions at all. So to have a model with an interaction, we must have $\Omega_{\rm DE} = 1$. But this means that $\Omega_b = \Omega_{\rm DM} = 0$, and the dark energy is totally dominating, independent of the strength of the interaction between the other two components, baryons and dark matter.

For the eigenvalues of the stability matrix M, we get a very easy equation for the eigenvalues u:

$$\begin{vmatrix} -1-u & \tilde{\alpha} \\ 0 & -1-u \end{vmatrix} = (-1-u)^2 = 0 \Rightarrow u = -1.$$

This is then a double root, and we can have a term proportional to t in our solution if we have linear independent eigenvectors. Now, since the root is negative, such a solution would die anyway, since

$$\lim_{t\to\infty} te^{-t} = 0.$$

I have plotted a phase map based on Equation 2.19 in Figure 3.2 with $\alpha = 0.1$, and as we see, we indeed have a stable critical point, when both $\Omega_{\rm M}$ and $\Omega_{\rm DE}$ have initial values in the interval [0, 1].

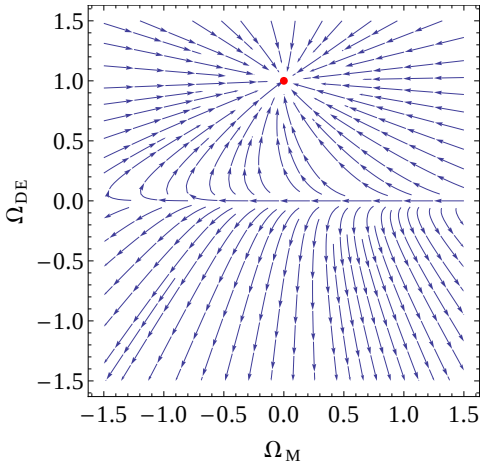

Figure 3.2: A phase map of the interaction model with α being active, α is here set to 0.1.

3.2.2 The analytical solution

Now it is time to look at the analytical solution. Equation 2.12 with $\beta = \gamma = 0$ looks like this (prime denotes derivative with respect to N):

$$\begin{aligned} \rho_b' + 3\rho_b &= 3\alpha(\rho_b + \rho_{\rm DM}), \\ \rho_{\rm DM}' + 3\rho_{\rm DM} &= -3\alpha(\rho_b + \rho_{DM}), \\ \rho_{\rm DE}' + 3(1+w)\rho_{\rm DE} &= 0. \end{aligned}$$

Similar to the previous case, we introduce the combined energy density for matter, $\rho_{\rm M} = \rho_b + \rho_{\rm DM}$, and the ratio $S = \rho_{\rm DM}/\rho_{\rm M}$. Now, since the two components we are working with are pressure less, the equation for the combined matter energy density $\rho_{\rm M}$ will be independent of α, and we will have the usual, decoupled evolution of the matter energy density:

$$\rho_{\rm M} = \rho_{\rm M}^{(0)}(1+z)^3, \tag{3.10}$$

where $\rho_{\rm M}^{(0)}$ is the initial matter energy density. For the ratio S, we get this simple equation with solution:

$$\frac{dS}{dN} = 3\alpha \Rightarrow S = 3\alpha N + S_0, \tag{3.11}$$

where S_0 is the present value of S.

I have plotted these two solutions in Figure 3.3, with $\alpha = 0.1$. As expected, the interaction goes from dark matter to dark energy, and S decreases linearly. Now, remember that the critical point has $\Omega_{\rm DE} = 1$ when $\alpha \neq 0$, so the dark energy is dominating this universe. The initial value for S is $S_0 = 0.8$, which is the value for the ΛCDM model.

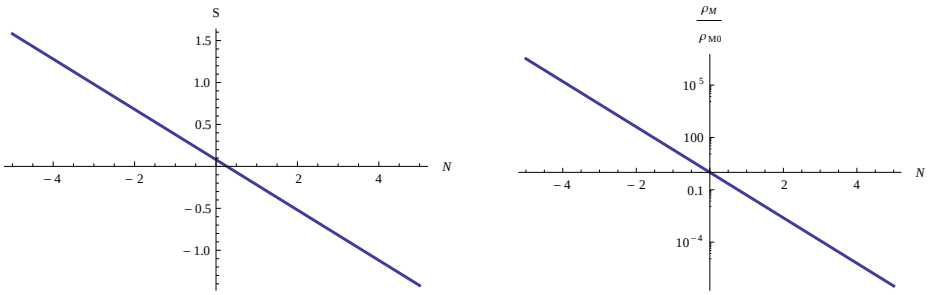

Figure 3.3: The ratio S(N) and the energy-density $\rho_{\rm M}(N)/\rho_{\rm M0}(N)$.

3.3 Baryons and dark energy

In this case, we have $\alpha = \gamma = 0$. Now, since the equations for ρ_b and $\rho_{\rm DM}$ have the exact same form, this case will be the same as the case with interacting dark matter and dark energy, with $\Omega_{\rm DM}$ replaced by Ω_b and β replaced by γ. This regards both the critical points (location and stability) and the analytical solutions. So if we set up $\rho_{b\rm DE} = \rho_b + \rho_{\rm DE}$ and the ratio $U = \rho_{\rm DE}/\rho_{b\rm DE}$, and the two parameters

$$r = -\frac{3}{2}(2+w) \qquad s = \frac{3}{2}\sqrt{w(w+4\beta)}.$$

We have these two solutions:

$$\rho_{b\mathrm{DE}} = \rho_{b\mathrm{DE}}^{(0)} e^{r(N-N_0)} \cosh(s(N-N_0)), \tag{3.12}$$

$$U = -\frac{1}{3w}\left(3 + r + s\tanh(q(N-N_0))\right). \tag{3.13}$$

While the solutions are the same as in the dark matter - dark energy case, the physical meanings will be different, of course. I have plotted the evolutions on Figure 3.4, where β is 0.2. As we see, the ratio U approaches a lower value than R did in Figure 3.1 on page 41, which we expect when we increase γ in Equation 3.9: the limit now is around 0.72 when N goes to infinity.

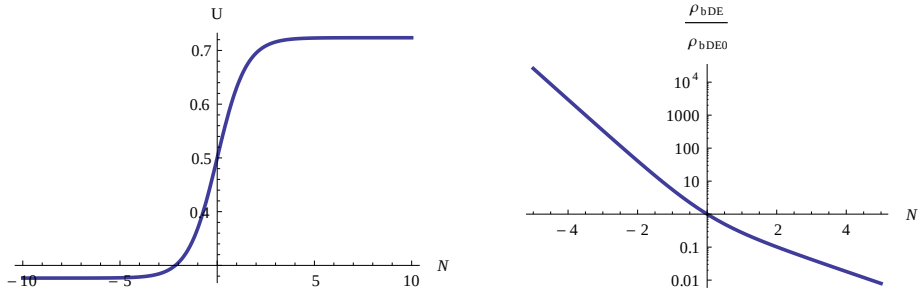

Figure 3.4: The ratio U and the energy-density $\rho_{b\mathrm{DE}}(N)/\rho_{b\mathrm{DE0}}(N)$.

Chapter 4

Two interactions

Now we will look at a model where we have two interactions (or, one interaction turned off). Again, we have three models, one for each interaction turned off. We will study each of the models in two steps: first, we will find the analytical solution. This is pretty straight forward linear algebra, where we will use Mathematica [4] to find eigenvalues and eigenvectors, finding the general solutions for the systems. Now, it can be difficult to understand what will happen just by looking at the analytical solutions, because these will be rather complex, so we will make some plots showing how the two parameters affect the solution in terms of existence of critical points, and what the stability the critical points have. We will also make phase plots for some specific values of the interaction parameters, which will give us the best information of how the solution of the equations are.

4.1 Dark energy - Dark matter and Dark energy - baryons

First, we will study a model where dark energy interacts with both baryons and dark matter, but there is no interaction between baryons and dark matter. This corresponds to setting α to zero. We start with the analytical solution.

4.1.1 Analytical solution

With $\alpha = 0$, our system of equations looks like this:

$$\begin{aligned} \rho_b' + 3\rho_b &= 3\beta(\rho_b + \rho_{\mathrm{DE}}), \\ \rho_{\mathrm{DM}}' + 3\rho_{\mathrm{DM}} &= 3\gamma(\rho_{\mathrm{DM}} + \rho_{\mathrm{DE}}), \\ \rho_{\mathrm{DE}}' + 3(1+w)\rho_{\mathrm{DE}} &= -3(\beta(\rho_b + \rho_{\mathrm{DE}}) + \gamma(\rho_{\mathrm{DM}} + \rho_{\mathrm{DE}})). \end{aligned}$$

where the prime denotes derivative with respect to the e-fold number N. This is a system of linear, first order differential equations with constant

Table 4.1: The coefficients of the characteristic polynomial, in the case where $\alpha = 0$.

Term	Coefficient
Constant	$27(1 - \gamma\beta + w(1 - \gamma - \beta + \gamma\beta))$
u	$27 + 18w - 9(w(\beta + \gamma) - \beta\gamma)$
u^2	$9 + 3w$
u^3	1

coefficients. To solve it, we write it in matrix form: $\boldsymbol{\rho}' = A\boldsymbol{\rho}$, where the matrix A contains all the coefficients. Writing this out, we can see how A looks like:

$$\begin{pmatrix} \rho_b' \\ \rho_{\mathrm{DM}}' \\ \rho_{\mathrm{DE}}' \end{pmatrix} = \begin{pmatrix} 3(\beta-1) & 0 & 3\beta \\ 0 & 3(\gamma-1) & 3\gamma \\ -3\beta & -3\gamma & -3(1+w+\beta+\gamma) \end{pmatrix} \begin{pmatrix} \rho_b \\ \rho_{\mathrm{DM}} \\ \rho_{\mathrm{DE}} \end{pmatrix}.$$

The solution of this set of equations is given by

$$\boldsymbol{\rho} = \sum_{i=1}^{3} c_i \mathbf{v}_i e^{u_i N},$$

where c_i are integration constants (to be determined by initial conditions), u_i are the eigenvalues of the matrix A, and $\mathbf{v}_i$ are the corresponding eigenvectors. So we have an eigenvalue problem, which we solve using linear algebra. First, we need the eigenvalues. We start by computing this determinant:

$$\begin{vmatrix} 3(\beta-1)-u & 0 & 3\beta \\ 0 & 3(\gamma-1)-u & 3\gamma \\ -3\beta & -3\gamma & -3(1+w+\beta+\gamma)-u \end{vmatrix}.$$

This determinant is a cubic polynomial. Then we set the determinant to zero and solve for u. We use Mathematica to compute the polynomial. The coefficients are summarized in Table 4.1. And so we have three eigenvalues, one for each root of this polynomial. Again using Mathematica, I get these three eigenvectors, labeled by i, so $i \in \{1, 2, 3\}$, with u_i the corresponding eigenvalues:

$$\mathbf{v_i} = \begin{pmatrix} \frac{3\gamma^2}{\beta(3\gamma-3-u_i)} - \frac{3(1+w+\beta+\gamma)+u_i}{3\beta} \\ -\frac{3\gamma}{3(\gamma-1)-u_i} \\ 1 \end{pmatrix}.$$

Written out, the three energy densities evolves like this:

$$\rho_b(N) = \sum_{i=1}^{3} c_i \left(\frac{3\gamma^2}{\beta(3\gamma-3-u_i)} - \frac{3(1+w+\beta+\gamma)+u_i}{3\beta} \right) e^{u_i N},$$

$$\rho_{\mathrm{DM}}(N) = \sum_{i=1}^{3} c_i \left(\frac{-3\gamma}{3(\gamma-1)-u_i} \right) e^{u_i N},$$

$$\rho_{\mathrm{DE}}(N) = \sum_{i=1}^{3} c_i e^{u_i N}.$$

4.1.2 Critical points analysis

Now we will look more qualitatively on the analytical solution for the interaction model with $\alpha = 0$, an analysis of the critical points. Equation 2.19 takes this form:

$$\Omega_{\mathrm{DE}}\Omega_{\mathrm{DM}} - \tilde{\gamma}(\Omega_{\mathrm{DE}} + \Omega_{\mathrm{DM}}) = 0, \tag{4.1}$$

$$(1-\Omega_{\mathrm{DE}})\Omega_{\mathrm{DE}} - \tilde{\beta}(1-\Omega_{\mathrm{DM}}) - \tilde{\gamma}(\Omega_{\mathrm{DE}} + \Omega_{\mathrm{DM}}) = 0. \tag{4.2}$$

First, solving for Ω_{DM} gives this expression:

$$\Omega_{\mathrm{DM}} = \frac{\tilde{\gamma}\Omega_{\mathrm{DE}}}{\Omega_{\mathrm{DE}} - \tilde{\gamma}}.$$

Now we get this equation for Ω_{DE} determining the critical points:

$$\Omega_{\mathrm{DE}}^3 - \Omega_{\mathrm{DE}}^2 + (\tilde{\beta} + \tilde{\gamma} - \tilde{\beta}\tilde{\gamma})\Omega_{\mathrm{DE}} - \tilde{\beta}\tilde{\gamma} = 0. \tag{4.3}$$

We will now analyze these equations by region plots and a phase map, shown on Figure 4.1 on the following page. As we know, a cubic polynomial always have 3 complex roots (some of them can appear twice, of course). One of the roots is always real, and in some cases, depending on the coefficients ($\tilde{\beta}$ and $\tilde{\gamma}$ in this case) all three roots can be real. We use Mathematica to make region plots, showing if a root is real or not when we set values for β and γ. A root being real is marked with a dashed contour in the region plots. If the root is real, we make a new area showing where also the Friedman constraint, Equation 2.7 applies. This area is marked with a solid line. Also, when we have a real root, we also compute the eigenvalues of the matrix M in Equation 2.20, and look at the signs of the two eigenvalues. For the stability, only the real part of the eigenvalues are interesting, so I will set the eigenvalues to the real parts of the eigenvalues, so I can easily compare them. If both of the eigenvalues are negative (I check if the product is positive and one of the eigenvalues are negative), we have a stable critical point. These are the blue areas in the region plots. If both eigenvalues are positive (I check if the product is positive and one of the values are positive), we have an unstable critical point. These are the green areas in the region plots. If one eigenvalue is negative and one positive (I check if the product is negative), we have a saddle point. This are the red areas in the region plots. The white areas are when root of the polynomial is complex, and the corresponding

critical point do not exist. The phase map in the figure shows the evolution for the dynamical system. One set of initial conditions corresponds to one trajectory. In this particular phase map, $\beta = 0.2$ and $\gamma = 0.1$. As we can see from the region plots, we then have three critical points, one of each kind of stability, which we can recognize in the phase map. This confirms our stability analysis for this specific case.

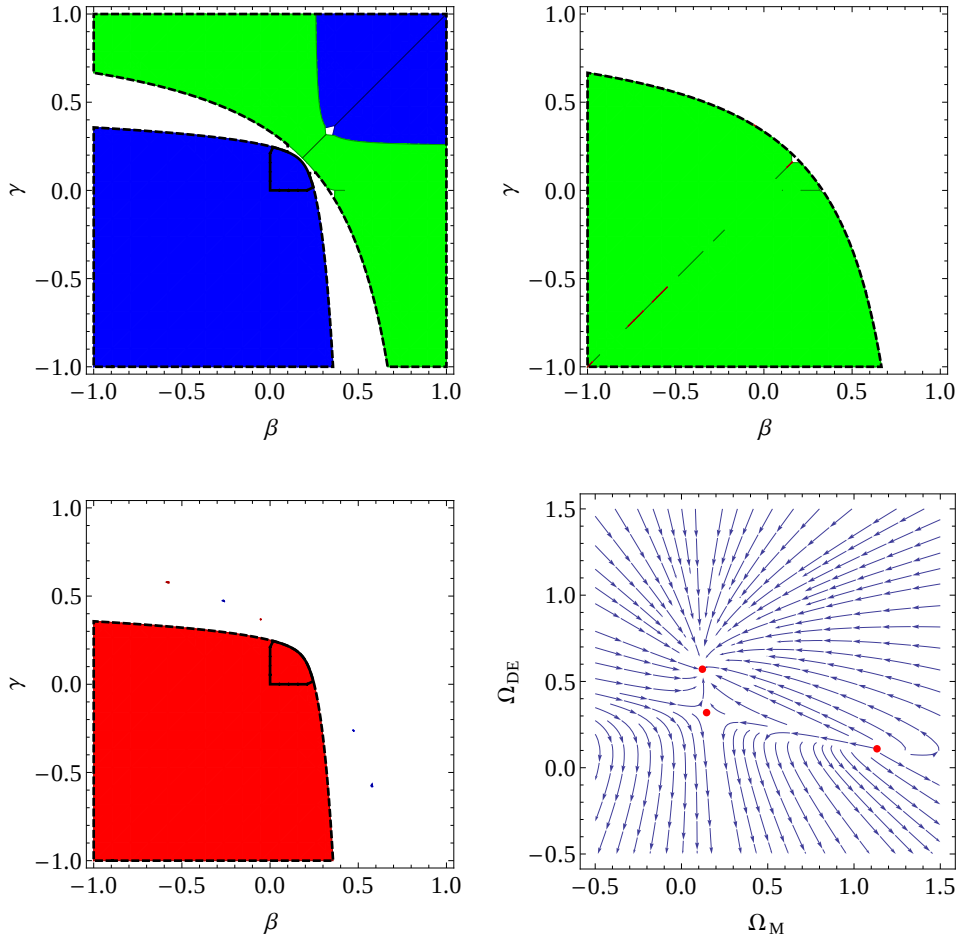

Figure 4.1: Three region plots (one for each root in a cubic polynomial) and a phase map with $\beta = 0.2$ and $\gamma = 0.1$. This is the case with $\alpha = 0$.

4.2 Baryons - dark matter and dark matter - dark energy

Now we go to the case where we have interactions between baryons and dark matter, and dark matter and dark energy. There is no direct interaction

Table 4.2: The coefficients for the characteristic polynomial, in the case $\beta = 0$.

Term	Coefficient
Constant	$27(1 + \alpha\gamma + w(\alpha\gamma - \gamma + 1))$
u	$9(\alpha\gamma - \gamma w + 2w + 3)$
u^2	$9 + 3w$
u^3	1

between baryons and dark energy in this model, so $\beta = 0$. As in the previous case, we will first find the analytical solution using linear algebra, then we will analyze the stability of the solution by having a look at the critical points.

4.2.1 Analytical solution

With $\gamma = 0$, our system of equations looks like this:

$$\rho_b' + 3\rho_b = 3\alpha(\rho_b + \rho_{\mathrm{DM}}), \tag{4.4}$$

$$\rho_{\mathrm{DM}}' + 3\rho_{\mathrm{DM}} = 3(-\alpha(\rho_b + \rho_{\mathrm{DM}}) + \gamma(\rho_{\mathrm{DM}} + \rho_{\mathrm{DE}})), \tag{4.5}$$

$$\rho_{\mathrm{DE}}' + 3(1 + w)\rho_{\mathrm{DE}} = -3\gamma(\rho_{\mathrm{DM}} + \rho_{\mathrm{DE}}), \tag{4.6}$$

where the prime denotes derivative with respect to the e-fold number N. We write this as a matrix equation $\boldsymbol{\rho}' = A\boldsymbol{\rho}$. Written out, it looks like this:

$$\begin{pmatrix} \rho_b' \\ \rho_{\mathrm{DM}}' \\ \rho_{\mathrm{DE}}' \end{pmatrix} = \begin{pmatrix} 3(\alpha - 1) & 3\alpha & 0 \\ -3\alpha & 3(\gamma - \alpha - 1) & 3\gamma \\ 0 & -3\gamma & -3(1 + w + \gamma) \end{pmatrix} \begin{pmatrix} \rho_b \\ \rho_{\mathrm{DM}} \\ \rho_{\mathrm{DE}} \end{pmatrix}.$$

The solution is determined by the eigenvalues u and eigenvectors $\mathbf{v}$ of the matrix A. The eigenvalues are found through the characteristic polynomial, which we find using Mathematica. It is given by this determinant:

$$\begin{vmatrix} 3(\alpha - 1) - u & 3\alpha & 0 \\ -3\alpha & 3(\gamma - \alpha - 1) - u & 3\gamma \\ 0 & -3\gamma & -3(1 + w + \gamma) - u \end{vmatrix}.$$

The coefficients are given in Table 4.3 on page 52. The eigenvalues u_i are now the three roots of the characteristic polynomial. Next we find the eigenvectors, also using Mathematica. Labeling with $i \in \{1, 2, 3\}$, the eigenvectors are

$$\mathbf{v}_i = \begin{pmatrix} \frac{\gamma}{\alpha} - \frac{1}{9\alpha\gamma}\left(3(\gamma - \alpha - 1) - u_i\right)\left(3(\gamma + w + 1) + u_i\right) \\ \frac{-1}{3\gamma}\left(3(\gamma + w + 1) + u_i\right) \\ 1 \end{pmatrix}.$$

And so our analytical solutions are

$$\rho_b(N) = \sum_{i=1}^{3} c_i \left(\frac{\gamma}{\alpha} - \frac{1}{9\alpha\gamma}\left(3(\gamma - \alpha - 1) - u_i\right)\left(3(\gamma + w + 1) + u_i\right)\right) e^{u_i N},$$

$$\rho_{\mathrm{DM}}(N) = \sum_{i=1}^{3} c_i \left(\frac{-1}{3\gamma} \left(3(\gamma + w + 1) + u_i \right) \right) e^{u_i N},$$

$$\rho_{\mathrm{DE}}(N) = \sum_{i=1}^{3} c_i e^{u_i N}.$$

4.2.2 Critical point analysis

Now to the analysis of the critical points. The equations for the critical points, Equation 2.19, now looks like this:

$$(\gamma - \Omega_{\mathrm{DE}})\Omega_{\mathrm{DM}} + \alpha(\Omega_{\mathrm{DE}} - 1) + \gamma\Omega_{\mathrm{DE}} = 0, \tag{4.7}$$

$$(1 - \gamma - \Omega_{\mathrm{DE}})\Omega_{\mathrm{DE}} - \gamma\Omega_{\mathrm{DM}} = 0. \tag{4.8}$$

Solving for Ω_{DM} gives

$$\Omega_{\mathrm{DM}} = \frac{1 - \gamma - \Omega_{\mathrm{DE}}}{\gamma}\Omega_{\mathrm{DE}}.$$

Inserting this, we get this third-degree equation for Ω_{DE}:

$$\Omega_{\mathrm{DE}}^3 - \Omega_{\mathrm{DE}}^2 + \gamma(1 + \alpha)\Omega_{\mathrm{DE}} - \alpha\gamma = 0.$$

This equation has three complex roots. There is always one root that is real, and sometimes, all three roots are real. So we make three region plots, one for each root, and mark with a dashed line where that root is real, when α and γ varies in the interval $[-1, 1]$. We see that for any value for α and γ, one of the roots is real, but it does not have to be the same root always. Further, the Friedman constraint sets up smaller areas, these are marked with a solid line. At last, we look at the eigenvalues of the stability matrix in Equation 2.20. If both eigenvalues have positive real part, we have an unstable critical point. These are the green areas in the region plots. If both the real parts of the eigenvalues are negative, we have a stable critical point. These are the blue areas in the region plots. If the real part of one of the eigenvalues is positive, and the other is negative, we have a saddle point. This is the red area in the region plots. Finlay, we make a phase plot for specific values of α and γ. We set α to 0.05 and γ to 0.2. As expected, we get three critical points, one of each type. The region plots and the phase map are displayed on Figure 4.2 on the facing page.

4.3 Baryons - dark matter and baryons - dark energy

At last, we will study the cased where baryons interact with both dark matter and dark energy, but there is no interaction between the dark components, so $\gamma = 0$. As before, we will first find the analytical solution using linear algebra, then we will analyze the stability by studying the critical points.

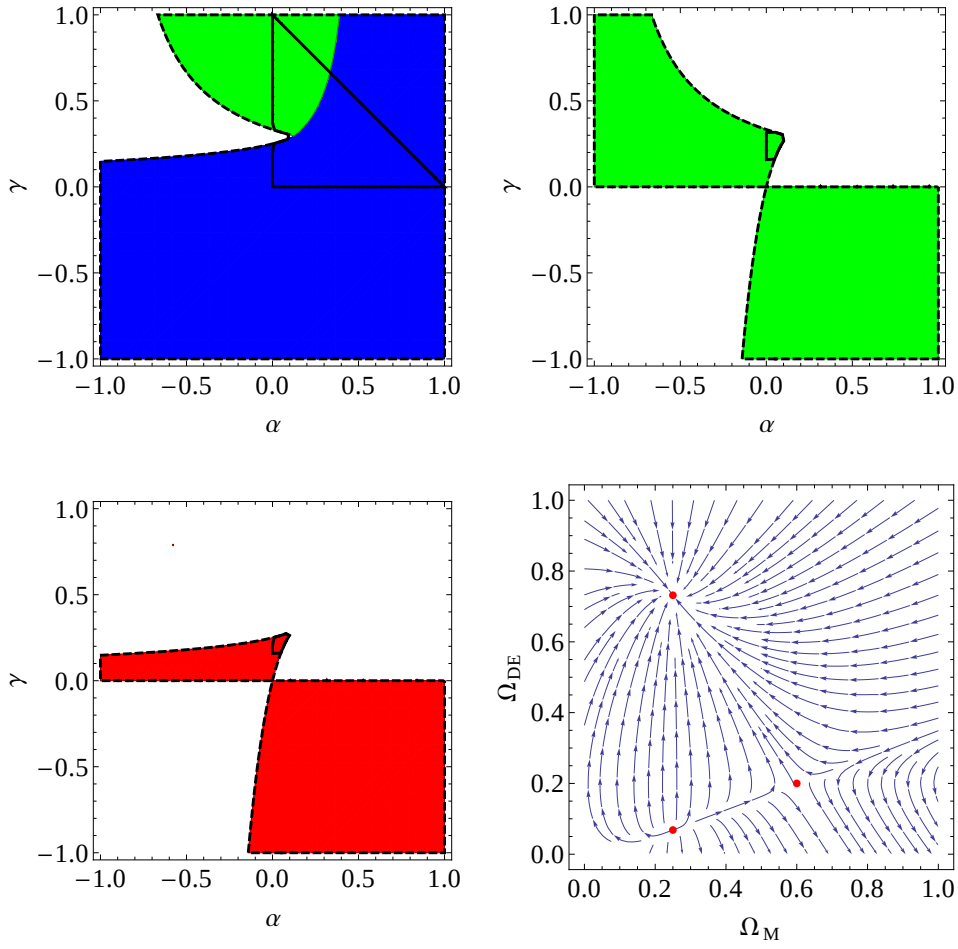

Figure 4.2: Three region plots (one for each root in a cubic polynomial) and a phase map with $\alpha = 0.05$ and $\gamma = 0.2$. This is the case for $\beta = 0$.

Table 4.3: The coefficients of the characteristic polynomial, in the case where $\gamma = 0$.

Term	Coefficient
Constant	$27(w(1-\beta-\alpha\beta)-\alpha\beta-1)$
u	$9(2w-\beta-\alpha\beta+3)$
u^2	$9+3w$
u^3	1

4.3.1 Analytical solution

The set of equations now looks like this:

$$\begin{aligned}
\rho_b' + 3\rho_b &= 3\alpha(\rho_b + \rho_{\mathrm{DM}}) + 3\beta(\rho_b + \rho_{\mathrm{DE}}), \\
\rho_{\mathrm{DM}}' + 3\rho_{\mathrm{DM}} &= -3\alpha(\rho_b + \rho_{\mathrm{DM}}), \\
\rho_{\mathrm{DE}}' + 3(1+w)\rho_{\mathrm{DE}} &= -3\beta(\rho_b + \rho_{\mathrm{DE}}).
\end{aligned}$$

In matrix form, we again have $\boldsymbol{\rho}' = A\boldsymbol{\rho}$. Written out, we can see the layout of the matrix A:

$$\begin{pmatrix} \rho_b' \\ \rho_{\mathrm{DM}}' \\ \rho_{\mathrm{DE}}' \end{pmatrix} = \begin{pmatrix} 3(\alpha+\beta-1) & 3\alpha & 3\beta \\ -3\alpha & -3(\alpha+1) & 0 \\ -3\beta & 0 & -3(\beta+w+1) \end{pmatrix} \begin{pmatrix} \rho_b \\ \rho_{\mathrm{DM}} \\ \rho_{\mathrm{DE}} \end{pmatrix}.$$

As usual, the solutions are determined by the eigenvalues u and eigenvectors $\mathbf{v}$ of A. The eigenvalues u are the roots of the characteristic polynomial, which we get from this determinant:

$$\begin{vmatrix} 3(\alpha+\beta-1)-u & 3\alpha & 3\beta \\ -3\alpha & -3(\alpha+1)-u & 0 \\ -3\beta & 0 & -3(\beta+w+1)-u \end{vmatrix}.$$

This is computed using Mathematica. The polynomial is summarized in Table 4.3. The eigenvectors $\mathbf{v}_i$ are

$$\mathbf{v}_i = \begin{pmatrix} \frac{-1}{3\beta}\left(3(1+\beta+w)+u_i\right) \\ \frac{1}{9\alpha\beta}\left(-9\beta^2 - (3(\beta-\alpha-1)-u_i)(-3(1+\beta+w)-u_i)\right) \\ 1 \end{pmatrix},$$

and so the three solutions are

$$\rho_b(N) = \sum_{i=1}^{3} -c_i \left(\frac{1}{3\beta}\left(3(1+\beta+w)-u_i\right)\right) e^{u_i N},$$

$$\rho_{\mathrm{DM}}(N) = \sum_{i=1}^{3} c_i \frac{\left(-9\beta^2 - (3(\beta-\alpha-1)-u_i)(-3(1+\beta+w)-u_i)\right)}{9\alpha\beta} e^{u_i N},$$

$$\rho_{\mathrm{DE}}(N) = \sum_{i=1}^{3} c_i e^{u_i N}.$$

4.3.2 Critical points analysis

We use Equation 2.19 to analyze the critical points. The equation set looks like this:

$$\Omega_{\mathrm{DE}}\Omega_{\mathrm{DM}} + \alpha\Omega_{\mathrm{DE}} = 0, \tag{4.9}$$

$$(1 - \Omega_{\mathrm{DE}})\Omega_{\mathrm{DE}} + \beta\Omega_{\mathrm{DM}} - \beta = 0. \tag{4.10}$$

Solving for Ω_{DM} gives

$$\Omega_{\mathrm{DM}} = 1 + \frac{\Omega_{\mathrm{DE}} - 1}{\beta}\Omega_{\mathrm{DE}},$$

and we get this third-degree polynomial for Ω_{DE}:

$$\Omega_{\mathrm{DE}}^3 - \Omega_{\mathrm{DE}}^2 + \beta(1 - \alpha)\Omega_{\mathrm{DE}} + \alpha\beta = 0.$$

We now use Mathematica to find the critical points (the roots of this cubic equation), and to analyze them. This is done with three region plots, one for each root, where α and β now are the varying parameters. A root is a critical point if the root is real. This is marked by the dashed lines on the region plots (and so the critical points exists where the area is not white). The Friedman constraint sets up a sub-region, this is marked by the solid lines. Then we can insert the roots into the stability matrix in Equation 2.20 to analyze the stability of the critical points, which is determined by the signs of the eigenvalues of the stability matrix. The blue areas marks a stable critical point, green is an unstable critical point, and red is a saddle point. I have also made a phase map, where I have set $\alpha = -0.05$ and $\beta = 0.2$. We see that we have three critical points, one of each type, as expected from the region plots. The three region plots and the phase map is shown on Figure 4.3 on the following page.

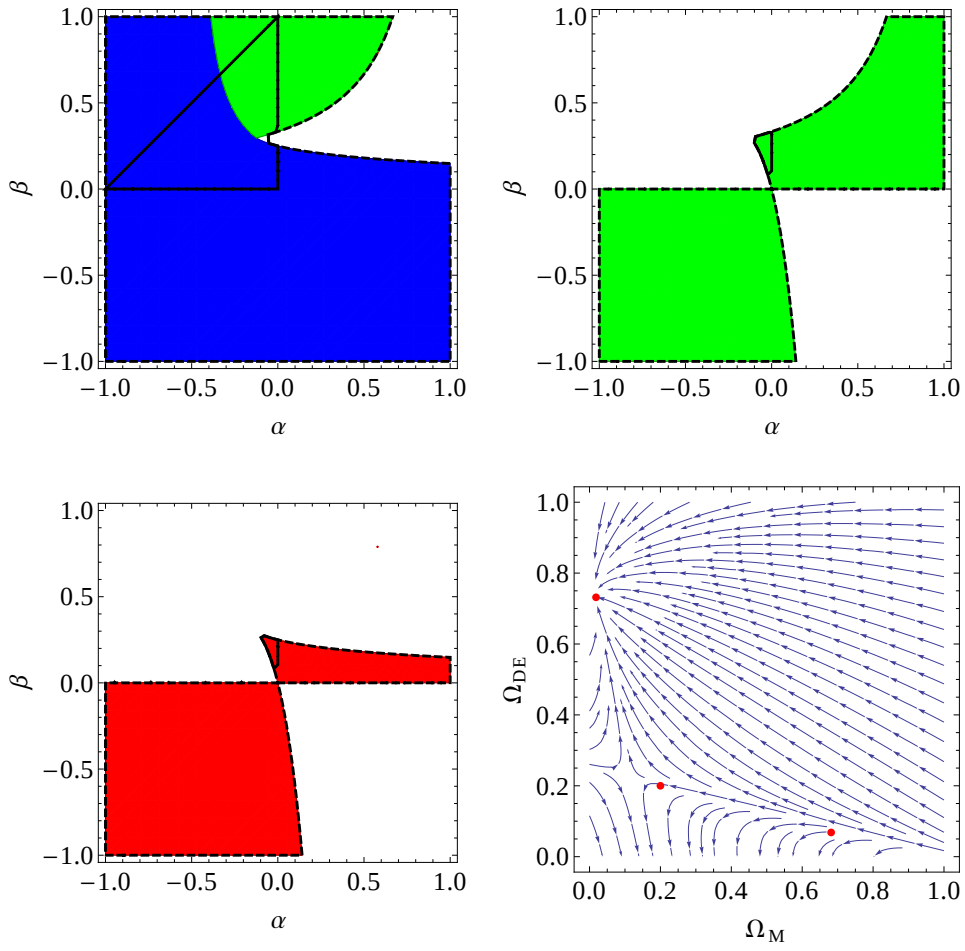

Figure 4.3: Three region plots (one for each root in a cubic polynomial) and a phase map with $\alpha = -0.05$ and $\beta = 0.2$. $\gamma = 0$ in this case.

Chapter 5

Supernovae type Ia

5.1 A white dwarfs rebirth

A supernova is an exploding star, and in such an explosion, the star emits a lot of energy. A typical supernova can have a luminosity greater than a whole galaxy. Supernovae are divided into classes according to the physical mechanisms involved, and we are going to look closer at type Ia supernovae. Type I supernovae are supernovae that do not exhibit hydrogen lines in their spectra. As we know, hydrogen is the most abundant element in the universe, and this suggests that there is something unusual in type I supernovae compared to other types of supernovae. A supernova of type Ia is a type I supernova that have a strong Sn II line in its spectrum. Other type I supernovae shows other, or lack of other, elements in their spectral lines.

Supernovae type Ia occurs in binary star systems, where one of the stars is a white dwarf star. In such a binary star system, the white dwarf may steal mass from its partner, and get heavier. However, due to the white dwarf being made up of degenerate gas, it will actually get smaller when it gets heavier. The degeneracy pressure will then increase to prevent the star from collapsing. There is a limit for when the degeneracy pressure fails to hold the white dwarf stable. In terms of mass, this limit is known as the Chandrasekhar mass, after the Indian physicist Subrahmanyan Chandrasekhar. The limit is around 1.4 solar masses, and when this limit is reached, the white dwarf explodes, and we have a type Ia supernova. Since the physical conditions in the type Ia supernovae are very similar, they will have the same absolute magnitude. By observing their apparent magnitude, we can compute the distance to them. Since supernovae shine so bright, we can see them far across the universe, allowing us to work with models over a large range of distances. The absolute magnitude of a type Ia supernova is around -19.3. Now, there are some factors that may affect the lightcurve (magnitude versus time) of a supernova Ia, extinction and the host galaxy, for example. This means that a supernova Ia is not really a standard candle.

But they are standardizable, which means that by the use of different methods, like SALT2 [5] and MLCS2k2 [6], it is possible to reduce the systematic error that affects the light curves. This is done for our data set, and so we can treat the supernovae Ia as standard candles.

5.2 Observational constraints from supernovae type Ia

I will use the union 2 data set, which consists of 557 type Ia supernovae [7]. In the data set we have name, redshift and distance modulus with uncertainties based on the luminosity distance for the supernovae. What we want to do is to make a model of the universe, based on the FRW metric and the interaction models for the components in the universe. We have already looked at such kind of models, so it only comes down to choosing a set of values for the interaction parameters. Then we can compute the distance modulus based on the luminosity distance for a given redshift. This can then be compared with the measured distance modulus in the data set. We use the χ^2 estimator from Equation B.15 to choose the combination of interaction parameters that fits the model best.

First, it is necessary to our equations in terms of redshift. This is done in Equation 2.14 for the density parameters, and Equation 2.15 for the Hubble parameter. We will neglect contribution from radiation, since we will work with redshifts below 1.5. The equations I want to solve then take this form:

$$\frac{d\Omega_b}{dz} = \frac{-3}{1+z}\left(\left(w\Omega_{\mathrm{DE}} + \alpha + \beta\right)\Omega_b + \alpha\Omega_{\mathrm{DM}} + \beta\Omega_{\mathrm{DE}}\right),$$

$$\frac{d\Omega_{\mathrm{DM}}}{dz} = \frac{-3}{1+z}\left(\left(w\Omega_{\mathrm{DE}} - \alpha + \gamma\right)\Omega_{DM} - \alpha\Omega_b + \gamma\Omega_{\mathrm{DE}}\right),$$

$$\frac{d\Omega_{\mathrm{DE}}}{dz} = \frac{-3}{1+z}\left(\left(w\Omega_{\mathrm{DE}} - w - \beta - \gamma\right)\Omega_{\mathrm{DE}} - \beta\Omega_b - \gamma\Omega_{\mathrm{DM}}\right),$$

$$\frac{dH}{dz} = \frac{3H}{2(1+z)}\left(1 + w\Omega_{\mathrm{DE}}\right).$$

Now, these equations have varying coefficients, so we choose to solve them numerically. We also need initial conditions for the equations. I have chosen to set $\Omega_{b,0}$ to 0.046, which is the best fit value for a ΛCDM universe model with no interactions. When I work with only one active interaction, I let $\Omega_{\mathrm{DM},0}$ be a free parameter, and when I work with two active interactions, I set $\Omega_{\mathrm{DM},0}$ to 0.224, which is the best fit value in the ΛCDM model. $\Omega_{\mathrm{DE},0}$ is then $1 - \Omega_{b,0} - \Omega_{\mathrm{DM},0}$ in all cases, since we neglect contribution from radiation, and we assume that our universe is spatially flat ($\Omega_k = 0$). Now, H_0 should also be a free parameter, but it is actually impossible to determine H_0 based on supernovae type Ia data. We will divide our equations by H_0,

and work with $E = H/H_0$, which then has initial condition $E(z = 0) = 1$ by definition. We will come back to H_0 later.

Now that we have initial conditions, we are ready to solve the equations. Since we are going to constrain values of the interaction parameters, we will run through some combinations of them, solving the equations to get a universe model for each combination. Using the universe model, we can compute the distance modulus to an object at redshift z, using linear interpolation (Equation B.13) to interpolate to the redshift given in the data set, based on our set grid of redshifts. To find which combination of parameters that is the best, we compute the χ^2 estimator, Equation B.15, for each combination of interaction parameters. The combination giving the smallest value for χ^2 is the best value. We will also study the 1, 2 and 3σ confidence regions, which are determined by the value of χ^2 being within a certain distance from the best fit value. These distances are defined in Table B.1 on page 164.

In our case, the χ^2 estimator is given by

$$\chi^2 = \sum_{i=1}^{N} \frac{(\mu(z_i) - \mu_i)^2}{\sigma_i^2},$$

where $\mu(z_i)$ is the distance modulus to an object of redshift z_i, based on our universe model, and μ_i is the measured distance modulus to the object of redshift z_i, which is given in the data set. N is the number of supernovae we have in our data set (557).

Note that this expression for the χ^2 estimator assumes that all the data are uncorrelated. This is actually not true, the data are correlated. In order to account for this, we would have to set up a 557×557 matrix with all the correlations. With this, the computations will take much longer, and therefore, we will not take the correlations into account. This will make our confidence regions a bit smaller than they should be, but the order of magnitude of the constraints will be correct. See the data paper [7] for details.

Since we use the energy flux from the object to determine the distance, we are using the luminosity distance. The distance modulus according to our model is then

$$\mu(z_i) = 5 \log D_L - 5 \log H_0 + \mu_0 \qquad D_L = H_0 d_L \qquad d_L = \int_0^z \frac{1}{H(z')} dz'. \tag{5.1}$$

Our goal is to minimize χ^2, and we can only do this through $\mu(z_i)$. In our program, we solve an equation which gives us $H(z)$, but we go not get H_0 and μ_0, since we have a degeneracy between them. We are also not interested in these quantities, so for each univsere model (in our case given by the interaction parameters, and $\Omega_{DM,0}$ when we work with only one interaction), we can just choose the values for these parameters that minimizes χ^2. Now, we can not solve for each of these parameters, so we put them together to

$\tilde{M} = 5\log H_0 + \mu_0$, and solve for the whole combination $\tilde{M}$. In terms of $\tilde{M}$, we get this expression for χ^2:

$$\chi^2 = \sum_{i=1}^{N} \frac{(5\log d_L(z_i) - \mu_i + \tilde{M})^2}{\sigma_i^2}. \tag{5.2}$$

Finding the value of $\tilde{M}$ that minimized this corresponds to differentiating χ^2 with respect to $\tilde{M}$, and setting this to zero. Doing this, I get

$$\frac{\partial\chi^2}{\partial\tilde{M}} = 0 \Leftrightarrow \tilde{M} = \frac{-1}{2\Sigma}\sum_{i=1}^{N}\frac{10\log(d_L(z_i)) - 2\mu_i}{\sigma_i^2},$$

where

$$\Sigma = \sum_{i=1}^{N}\frac{1}{\sigma_i^2}.$$

Now we have everything we need. We use a C++ program to compute the χ^2 estimator in a 20 by 20 grid. When I do one active interaction, the grid consists of the active interaction parameter varying between -0.2 and 0.2, and $\Omega_{\mathrm{DM},0}$ varying between 0.15 and 0.35. When I do two interactions, the grid consists of the interaction parameters, both varying between -0.2 an 0.2. $\Omega_{\mathrm{DM},0}$ is fixed to 0.224 in this case. Ω_{b0} is fixed to 0.046 in both cases. In the program, we solve differential equations using the Runge Kutta 4 method, Equation B.12, we use linear interpolation for interpolating, using Equation B.13, and I use the trapezoidal rule, Equation B.14 for evaluating the integral for the luminosity distance in Equation 5.1.

5.3 Results

5.3.1 One interaction

In this case, we set two of the interaction parameters to zero. $\Omega_{\mathrm{DM},0}$ is then as a free parameter. We use matlab to make contour plots of the χ^2 estimator. On Figure 5.1 on the facing page, we have the contour plot for the case where α is non-zero, on Figure 5.2, β is non-zero, and the contour plot for the case when γ is non-zero is displayed on Figure 5.3 on page 60. As we can see, we do not get any constraints on α, but we do get some constraints on β and γ. We also get constraints on $\Omega_{\mathrm{DM},0}$.

5.3.2 Two interactions

In this case, we set only one of the interaction parameters to zero, ans we set $\Omega_{\mathrm{DM},0}$ to 0.224, the best-fit value in the ΛCDM model. Again, we run our program, computing the χ^2 estimator for all the combinations of interaction parameters in our interval. Then we use matlab to make contour plots.

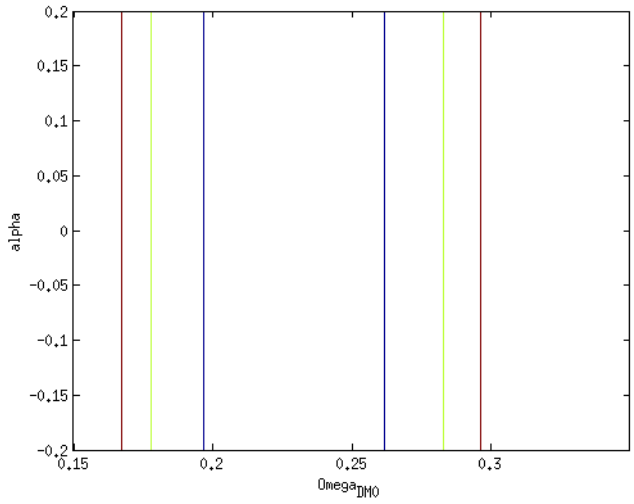

Figure 5.1: The 1, 2 and 3σ confidence regions for the χ^2 estimator, α and $\Omega_{\mathrm{DM},0}$ being the free parameters.

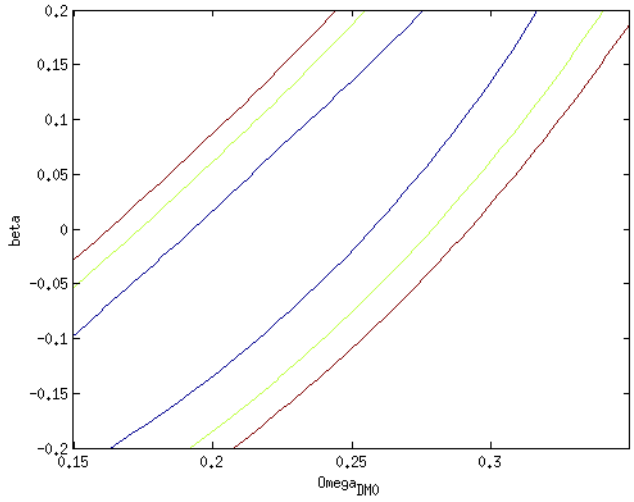

Figure 5.2: The 1, 2 and 3σ confidence regions for the χ^2 estimator, β and $\Omega_{\mathrm{DM},0}$ being the free parameters.

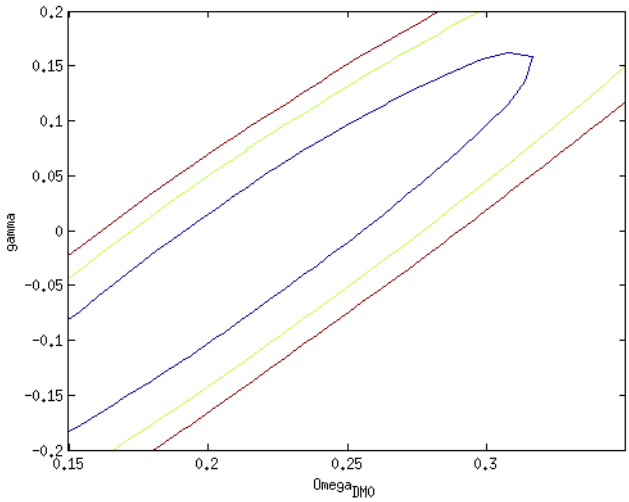

Figure 5.3: The 1, 2 and 3σ confidence regions for the χ^2 estimator, γ and $\Omega_{\mathrm{DM},0}$ being the free parameters.

When α and β are the active interaction parameters, and γ is zero, I get the plot on Figure 5.4. Having α and γ as the two active parameters gives the plot on Figure 5.4, and on Figure 5.6 is the contourplot for the case with β and γ being active parameters. In this case, we get almost no constraints on α, but some constraints on β and γ.

5.4 Discussion

5.4.1 One interaction

When one of the interaction parameters is active, we have left $\Omega_{\mathrm{DM},0}$ as a free parameter. From the model where α is active, we see that $\Omega_{\mathrm{DM},0}$ should be greater than 0.15 and less than 0.3, all three σ regions are inside this interval. The best value seems to be around 0.22, the ΛCDM value. For the two other cases (β and γ being active), the constraints on $\Omega_{\mathrm{DM},0}$ are weaker, and a higher value of the interaction parameter shifts the value of Ω_{DM} towards higher values. This is logical - larger β or γ will give less dark energy, and then there is room for more dark matter. This is also related to the fact that we do not get any constraints on α: since baryonic matter and dark matter affect the expansion of the universe in the same way, we can not use observational data based on a standard candle from redshifts after recombination to constrain α, and so α does not affect Ω_{DM}.

Comparing to the ΛCDM model, we see that this point (the point where the interaction parameter is zero and $\Omega_{\mathrm{DM}} = 0.226$) is inside the 1σ region. This means that we do not have any statistical evidence that the interactions

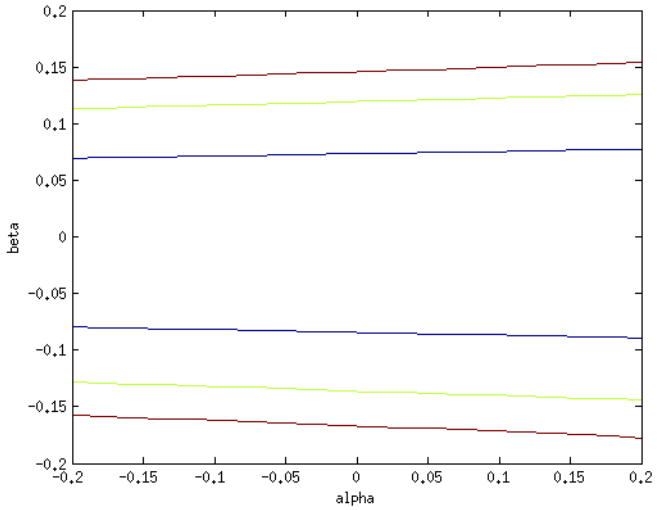

Figure 5.4: The 1, 2 and 3σ confidence regions for the χ^2 estimator, α and β being free parameters.

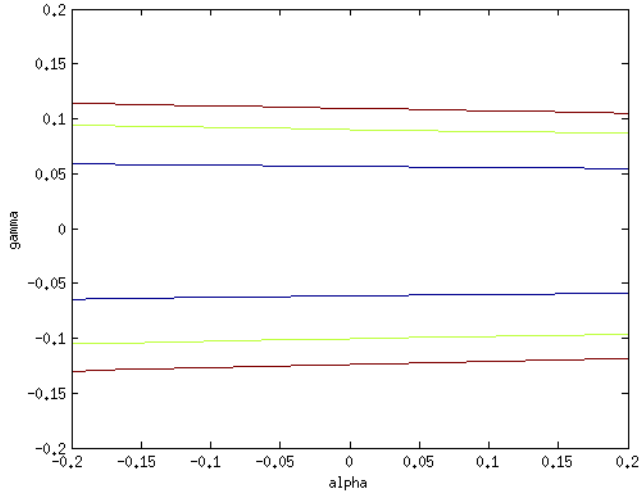

Figure 5.5: The 1, 2 and 3σ confidence regions for the χ^2 estimator, α and γ being free parameters.

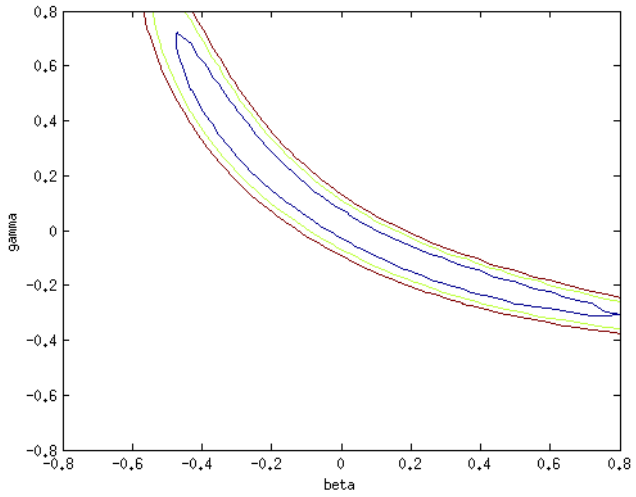

Figure 5.6: The 1, 2 and 3σ confidence regions for the χ^2 estimator, β and γ being free parameters.

are present, maybe they are all zero. On the other hand, since the area of the 1σ region is non-zero, there is also a possibility that the interactions are present, we can not exclude them totally.

5.4.2 Two interactions

Starting with α, we do get some weak constraints on it this time. As mentioned earlier, baryonic matter and dark matter affects the expansion of the universe in the same way, but when two interactions are active, we must also remember that the abundance of baryonic and dark matter is affected by α, which affects how much energy that can go to dark energy. So there is an indirect effect on the expansion of the universe when α is active together with one of the other interaction parameters.

For β and γ, however, we do get stronger constraints: β should have a magnitude less than 0.2, and γ should have a magnitude less than 0.15. When both β and γ are active, we see that one of them can be large if the other is small, so in total, the energy-density of dark energy is balanced. Again, we see that the ΛCDM model is within the 1σ region in all cases, and so there is no statistical evidence for the presence of interactions.

Overall, Supernovae Ia data gives quite weak constraints on the interaction parameters and $\Omega_{\mathrm{DM},0}$, since we can get both β and γ to have a magnitude of 0.15 in some of the 1σ regions, and that are actually quite strong interactions, having huge impacts on the universe.

Chapter 6

Baryon acoustic oscillations

6.1 Baryonic matter structure formations

Baryon acoustic oscillations are small oscillations that are seen in the galaxy correlation function, and comes from the evolution of perturbations of the baryonic matter density with wavenumber larger than the Jeans wavenumber (corresponding to smaller lengthscales) in the early universe. We start with the Fourier transformed differential equation for the evolution of density perturbations, Equation 1.15. Then we will follow a set of lecture notes of Øystein Elgarøy for the course in Comology and Extragalactic Cosmology at the University of Oslo [8]. As mentioned, the wavenumber k we work with now is larger than the Jeans wavenumber k_J defined in Equation 1.16. We will be working with the times when the universe were matter dominated, so the density perturbations $\delta\rho$ have two components: baryonic matter $\delta\rho_b$ and dark matter $\delta\rho_{\mathrm{DM}}$. Dark matter is pressureless and does not interact with photons, so it will only contribute with gravitational potentials for the baryons to fall into. We also assume that this is the only source of gravitational potentials, since the unperturbed density of dark matter is much larger than the unperturbed density of baryonic matter. Baryonic matter, however, is coupeled with the photons at the times we are studying, and will therefore have non-zero pressure.

We will start with Equation 1.15, which in our case takes this form:

$$\frac{d^2\delta\rho_b}{dt^2} + 2H\frac{d\delta\rho_b}{dt} = 4\pi G\bar{\rho}_{\mathrm{DM}}\delta\rho_{\mathrm{DM}} - \frac{k^2c_s^2}{a^2}\delta\rho_b. \tag{6.1}$$

Now, we know that the dark matter perturbation $\delta\rho_{\mathrm{DM}}$ satisfies this equation:

$$\frac{d^2\delta\rho_{\mathrm{DM}}}{dt^2} + 2H\frac{d\delta\rho_{\mathrm{DM}}}{dt} = 4\pi G\bar{\rho}_{\mathrm{DM}}\delta\rho_{\mathrm{DM}}.$$

Inserting this into Equation 6.1, we get

$$\frac{d^2\delta\rho_b}{dt^2} + 2H\frac{d\delta\rho_b}{dt} = \frac{d^2\delta\rho_{\mathrm{DM}}}{dt^2} + 2H\frac{d\delta\rho_{\mathrm{DM}}}{dt} - \frac{k^2c_s^2}{a^2}\delta\rho_b.$$

Now we change to conformal time η, defined as $dt = a(t)d\eta$. Our differential operator then takes this form:

$$\frac{d}{dt} = \frac{1}{a}\frac{d}{d\eta} \qquad \frac{d^2}{dt^2} = -\frac{a'}{a^3}\frac{d}{d\eta} + \frac{1}{a^2}\frac{d^2}{d\eta^2},$$

where I have introduced the notation $a' = da/d\eta$ to save some writing. In a matter dominated universe, we have $a \propto t^{2/3}$, which by integration gives $\eta \propto a^{1/2}$, or $a \propto \eta^2$. We can actually choose units and constants to make this an equality, so we set $a = \eta^2$ in the following. Also, note that

$$\frac{da}{dt} = \frac{a'}{a^2} \Rightarrow H = \frac{1}{a}\frac{da}{dt} = \frac{a'}{a^3}.$$

The equation for $\delta\rho_b$ now becomes

$$a(\delta\rho_b)'' + a'(\delta\rho_b)' = a(\delta\rho_{\mathrm{DM}})'' + a'(\delta\rho_{\mathrm{DM}})' - k^2c_s^2a\delta\rho_b,$$

where we have multiplied with a^3. Using the product rule for differentiation, we have

$$(a(\delta\rho_b)')' = (a(\delta\rho_{\mathrm{DM}})')' - k^2c_s^2a\delta\rho_b.$$

Since the dark matter is pressure less, we know how it evolves: $\delta\rho_{\mathrm{DM}} \propto a \propto \eta^2$, and we can also here choose constants and units to make this an equality. Doing so gives $(a(\delta\rho_{\mathrm{DM}})')' = 6a$. We also have

$$\frac{d}{d\eta}\left(a\frac{d\delta\rho_b}{d\eta}\right) = 2\eta(\delta\rho_b)' + \eta^2(\delta\rho_b)'',$$

and our equation is

$$\eta^2\frac{d\delta\rho_b}{d\eta^2} - 2\eta\frac{d\delta\rho_b}{d\eta} = a(6 - k^2c_s^2\delta\rho_b). \tag{6.2}$$

To go on, we need the sound speed. We must then divide into two regimes, before and after recombination. We start with before recombination. The baryons are then tightly coupeled to the photons, and then the sound speed is constant, and approximated by $c_s \approx c/\sqrt{3}$. We then see that

$$\delta\rho_b = \frac{6}{k^2c_s^2}$$

makes the right hand side of Equation 6.2 zero. Since it is independent of η, it also makes the left hand side zero, and hence it is a particular solution of the equation. To find the general solution, we must find the general solution to the homogeneous equation

$$\eta^2\frac{d^2\delta\rho_b}{d\eta^2} - 2\eta\frac{d\delta\rho_b}{d\eta} + k^2c_s^2\eta^2\delta\rho_b = 0,$$

and then add the particular solution we found above. To solve this equation, we construct

$$p(\eta) = e^{-\int \frac{1}{\eta} d\eta} = e^{-\ln \eta} = \frac{1}{\eta},$$

and then we substitute $v = \delta\rho_b/p$. We then get

$$(\delta\rho_b)' = \frac{v'}{\eta} - \frac{v}{\eta^2} \qquad (\delta\rho_b)'' = \frac{v''}{\eta} - \frac{2v}{\eta^2} + \frac{2v}{\eta^3},$$

and we have

$$v'' + k^2 c_s^2 v = 0,$$

with general solution $v = A\sin(kc_s\eta) + B\cos(kc_s\eta)$, where A and B are integration constants. We must set $B = 0$ to avoid $\delta\rho_b$ going towards infinity at $\eta = 0$. We then set $A = 1/(kc_s)$, and fit it afterwards. Returning to $\delta\rho_b$, our general solution to Equation 6.2 reads

$$\delta\rho_b(\eta) = \frac{6}{k^2 c_s^2} + \frac{\sin(kc_s\eta)}{kc_s\eta} = \frac{6}{\omega^2} + \frac{\sin(\omega\eta)}{\omega\eta}, \tag{6.3}$$

where, since we will study oscillation, I have introduced the frequency $\omega = kc_s$. The constant term $6/\omega^2$ does not vary with time, and can be absorbed in the background density.

Now for the time after recombination. The baryons are then decoupled from the photons, and the sound speed drops. A good assumption is that it drops instantaneously to zero. After recombination, the baryonic density perturbation evolves according to

$$\delta\rho_b(\eta) = C\eta^2 + \frac{D}{\eta}, \eta > \eta_*,$$

where C and D are integration constants, and η_* is the conformal time at recombination. Now, for $\eta = \eta_*$, our two solutions should be equal (or in other words, $\delta\rho_b$ should be continuous at $\eta = \eta_*$). This gives

$$\delta\rho_{b,0}\frac{\sin(\omega\eta_*)}{\omega\eta_*} = C\eta_*^2 + \frac{D}{\eta_*},$$

where $\delta\rho_{b,0}$ is an integration constant. Also, $(\delta\rho_b)'$ should be continuous at $\eta = \eta_*$. This gives

$$\delta\rho_{b,0}\frac{\omega\cos(\omega\eta_*)\omega\eta_* - \omega\sin(\omega\eta_*)}{\omega^2\eta_*^2} = 2A\eta_* - \frac{B}{\eta_*^2}$$

$$\Rightarrow A = \frac{\delta\rho_{b,0}}{3}\frac{\cos(\omega\eta_*)}{\eta_*^2},$$

and so we see that the amplitude of the perturbation after recombination depends on the phase of the oscillating wave at recombination. Since $C \propto$

$\cos(\omega\eta_*)$ and $\delta\rho_b(\eta < \eta_*) \propto \sin(\omega\eta)$, C takes its largest value when $\delta\rho_b = 0$. For the wavenumber k, we then get

$$k = \frac{n\pi}{c_s\eta_*}, \quad n \in \mathbb{N}.$$

The quantity in the denominator is known as the *sound horizon* at recombination, and is given by

$$c_s\eta_* = c_s \int_0^{t_*} \frac{dt}{a(t)}. \tag{6.4}$$

This determines the maximal amplitude of the density perturbations after recombination. The sound horizon at recombination is then a characteristic scale length, or a standard ruler, which is imprinted in the baryonic density perturbations. This is the effect we call *baryon acoustic oscillations* (BAO).

6.2 Observations of BAO

6.2.1 Observational quantities

Now we know what makes baryon acoustic oscillations, and the next question is, how do we make observations of them? Well, for a starting point, we imagine a volume of the universe. In the line of sight direction, we use redshift z as the distance variable. In the transverse direction, we just select an area of the sky (a solid angle). We then map out all the galaxies in this volume, measure their redshifts and the distances between them. Now we can compute the galaxy correlation function, defined in Equation 1.22. In the galaxy correlation function, there will be a peak corresponding to baryon acoustic oscillations (which then will be oscillations in the power spectrum of the galaxy correlation function). We can then read of the quantity $d_z = r_s(z_*)/D_V(z_d)$ from the galaxy correlation function. Here, z_d is our observed redshift, which is the average redshift of the galaxies in the volume we have worked with. The quantity $r_s(z_*)$ is the comoving sound horizon at recombination, which has redshift z_* (more precisely, this redshift is the redshift of the baryon drag epoch, but we will use the redshift at recombination as an approximation, which we set to $z_* = 1089$). We get it by rewriting Equation 6.4 in terms of redshift z. Including the redshift dependence in the sound speed $c_s(z)$, we get this expression for the comoving sound horizon:

$$r_s(z_*) = -\frac{c}{H_0} \int_{z_*}^{\infty} \frac{c_s(z)}{E(z)} dz, \tag{6.5}$$

where $E(z) = H(z)/H_0$. The quantity D_V is a spherically averaged distance measure (due to the shape of the volume we work with, and that we use redshift as distance measure along the line of sight), and is given by

$$D_V(z_d) = \left((1+z)^2 D_A^2(z_d) \frac{cz_d}{H(z_d)} \right)^{\frac{1}{3}}. \tag{6.6}$$

Where $D_A(z_d)$ is the angular diameter distance to an object of redshift z_d, given by Equation 1.21. At last, the sound speed $c_s(z)$ is given by

$$c_s(z) = \left(3\left(1 + \frac{\bar{R}_b}{1+z}\right)\right)^{-\frac{1}{2}}, \tag{6.7}$$

where $\bar{R}_b$ is the baryon-to-photon-energy-density-ratio, given by

$$\bar{R}_b = \frac{3\rho_b}{4\rho_r} = 31500\Omega_b h^2 \left(\frac{T_{\text{CMB}}}{2.7[\text{K}]}\right)^{-4}. \tag{6.8}$$

For more details on the geometry and method for connecting geometry with BAO data, see [9].

6.2.2 The BAO data

We have BAO data from three different surveys. In this section, I will write some lines about each of the data, report the data points with errors, and report the correlations between them. A summary of the data is given in Table 6.1 on the following page, and the inverse covariance matrix for the data, which we need when we compare the data to our interaction models, is given in Table 6.2 on the next page.

The 6-degree Field Galaxy Survey

We have one data point from the 6-degree Field Galaxy Survey (6dFGS). This data set were obtained using the 6-degree Field multi-fibre instrument at the U.K. Schmidt Telescope between 2001 and 2006. The data set consists of redshifts and peculiar velocity of 75 117 galaxies distributed over almost the entire southern sky, an area around 17000 square-degrees. The sample covered an effective volume of 0.08 h^{-3} Gpc^3, and the effective redshift was $z = 0.106$. Our quantity $d_z = d_{0.106}$ was measured to 0.336 ± 0.015. We assume no correlation between this data point and the others. The error enters with the coefficient 4444 into the diagonal in the inverse covariance matrix. See [10] for more details.

The Solan Digital Sky Survey Luminous Red Galaxy sample

The Solan Digital Sky Survey (SDSS) used a 2.5m telescope to obtain imaging data in five passbands. From the photometric component of SDSS, the Luminous Red Galaxy (LRG) sample were selected. These galaxies are associated with massive dark matter halos, and are therefore good tracers of matter. We use the DR7-full sample, which corresponds to all LRGs in the redshift interval from 0.16 to 0.44, and absolute magnitude interval from -23.2 to -21.2. The sample is from an effective volume of $1.2h^{-3}$ Gpc^3, and consists of 89 791 LRGs. The galaxies are split into two nodes, one with

Table 6.1: The baryon acoustic oscillations data set

Sample	Redshift z	$d_z = r_s/D_V(z)$	d_z error
6dFGS	0.106	0.336	0.015
SDSS	0.2	0.1905	0.0061
SDSS	0.35	0.1097	0.0036
WiggleZ	0.44	0.0916	0.0071
WiggleZ	0.60	0.0726	0.0034
WiggleZ	0.73	0.0592	0.0032

Table 6.2: The coefficients of the inverse covariance matrix for the BAO data.

4444	0	0	0	0	0
0	30318	−17312	0	0	0
0	−17312	87046	0	0	0
0	0	0	23857	−22747	10586
0	0	0	−22747	128729	−59907
0	0	0	10586	−59907	125536

redshift $z = 0.2$, where we have $d_{0.2}$ is 0.1905 ± 0.0061, and one with redshift $z = 0.35$, with $d_{0.35} = 0.1097 \pm 0.0036$. The errors enters with coefficients 30318 and 87046 on the diagonal of the inverse covariance matrix. These two data points are correlated, with coefficient -17312, which then enters into the inverse covariance matrix as well. These data are from the article [10] about the SDSS data set, where more details can be found.

The WiggleZ Dark Energy Survey

The WiggleZ Dark Energy Survey consists of a sample of 158 741 bright emission line galaxies in the redshift range from 0.2 to 1.0. The survey was carried out at the Anglo-Australian Telescope between 2006 and 2011, using the AAOmega spectrograph. In this data set, three overlapping redshift intervals were used: $(0.2, 0.6), (0.4, 0.8)$ and $(0.6, 1.0)$. The reported redshift data is then the weighted mean redshift of the galaxy pairs in the reparation interval $(100, 110)H^{-1}$ Mpc. The three redshift data points are 0.44, 0.60 and 0.73, and the corresponding d_z data points are $d_{0.44} = 0.0916 \pm 0.0071$, $d_{0.60} = 0.0726 \pm 0.0034$, and $d_{0.73} = 0.0592 \pm 0.0032$. The errors enters with coefficients 23857, 128729 and 125536 on the diagonal of the inverse covariance matrix. For the correlation between the data points, we get the coefficients -22747, 10586 and -59907 into the covariance matrix as well, see Table 6.2. See the article [11] about the WiggleZ data set for more details.

6.3 Observational constraints from BAO

Now it is time to use the data to constrain my interaction models. We start by setting values for the interaction parameters. We expect smaller confidence regions here compared to the supernovae Ia case, so I use values for the interaction parameters between -1.5 and 1.5. As for the supernovae Ia case, I will let $\Omega_{\text{DM},0}$ be a free parameter when we are doing one interaction, and fix $\Omega_{\text{DM},0}$ to 0.224 when we are doing two interactions. I set up initial conditions, and solve my differential equations. Now, as we see from Equation 6.5, I need in principle to know the value of the Hubble at Big Bang. While I can not go all the way back to big bang, I can set a cutoff value at redshift $z = 10^6$, which I find after trial and error. As we know, z grows faster at early times than at late times, so I will use a logarithmic grid in z. I also need to include contribution from radiation, which dominates the universe at early times.. The set of differential equations I will solve are then given in Equation 2.14 and Equation 2.15. I use the Runge Kutta 4 method, Equation B.12, to solve the equations numerically. Next, we compute the quantity d_z based on the data redshift and our universe model, using the comoving distance is defined in Equation 1.9, and the comoving sound horizon at recombination, $r_s(z_*)$, defined in Equation 6.5, where $z_* = 1089$ is the redshift of recombination. We use the trapezoidal formula, Equation B.14, as our numerical approximation to the integral, and we use the linear interpolation formula from Equation B.13 to interpolate between our preset redshift grid and the redshifts in our integration grid. Then we use Equation 6.6 to find the spherically averaged distance $D_V(z)$, and by dividing $r_s(z_*)$ by $D_V(z)$, we get d_z. Here, z refers to the redshifts in our data set. When this is done for all the points in our data set (six in total), we compute the χ^2 estimator. Now, our data are correlated through the correlation matrix, and so the expression for the χ^2 estimator is a little bit more complicated. What we do is to set up a vector $\mathbf{X}$, where each entry is the computed value for d_z minus the value for d_z given in the data: $X_i = r_s/D_V(z_i) - d_z$. With C being our covariance matrix, whose inverse is given in Table 6.2, we can use the expression in Equation B.16 for the χ^2 estimator:

$$\chi^2 = \mathbf{X}C^{-1}\mathbf{X}^T = \sum_{i,j} X_i C_{ij}^{-1} X_j,$$

where we have a double sum, one over i and one over j. When we have the χ^2 estimator, we can plot the 1, 2 and 3σ confidence regions, which are given in Table B.1 on page 164.

As we see from Equation 6.8, the value we compute for d_z depends on the energy-density of the baryons ρ_b, and so our results are sensitive to Ω_{b0} as well. We therefore marginalize over Ω_{b0} in our program, letting it vary between 0.035 and 0.092, which together with the fact that $\Omega_{b0}h^2 = 0.023$ is a observational value we will use, means that h varies between 0.5 and 0.8.

6.4 Results

6.4.1 One interaction

Running the program and using a matlab script, I get contour plots. When α is the varying interaction parameter, and β and γ are zero, I get the contour plot in Figure 6.1. When β is active, I get the contour plot displayed in Figure 6.2 on the next page, and in Figure 6.3 on the facing page, one can see the contour plot I get when γ is the active interaction parameter.

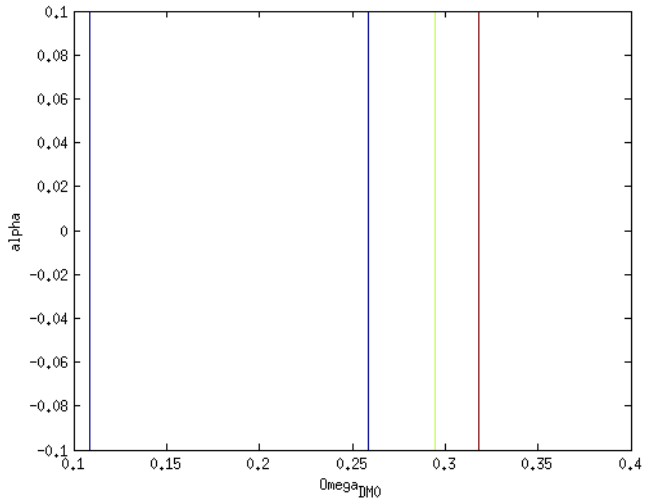

Figure 6.1: Contour plot when α is the non-zero interaction parameter.

6.4.2 Two interactions

When we now open up for two interactions to be present, I would have to make three-dimensional contour plots if $\Omega_{\mathrm{DM},0}$ (or $\Omega_{\mathrm{M},0}$) were free parameters. Therefore, I have chosen to fix both $\Omega_{b,0}$ and $\Omega_{\mathrm{DM},0}$ to 0.046 and 0.224, which is the best values for these parameters in the ΛCDM model. So now I make contour plots where I have two interaction parameters as free variables. When α and β are active, and γ is zero, I get the contour plot on Figure 6.4. If I let α and γ vary, I get the countours on Figure 6.5, and if β and γ are active, I get the contours on Figure 6.6.

6.5 Discussion

6.5.1 One interaction

For all the contour plots, we can see that the ΛCDM model, with all the interaction parameters equal to zero, is inside the 1σ contour. This means

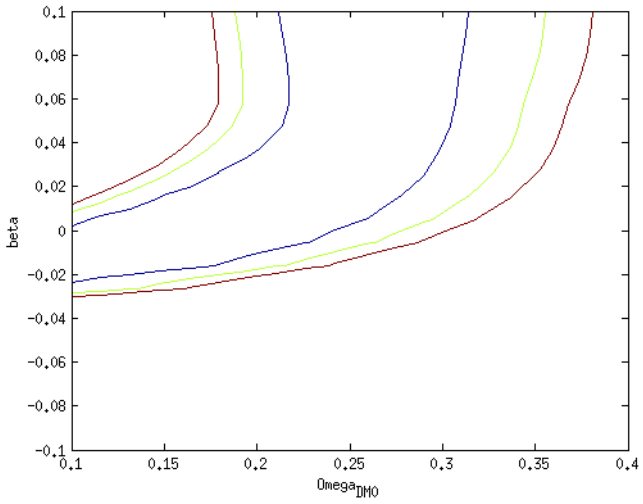

Figure 6.2: Contour plot when β is the non-zero interaction parameter.

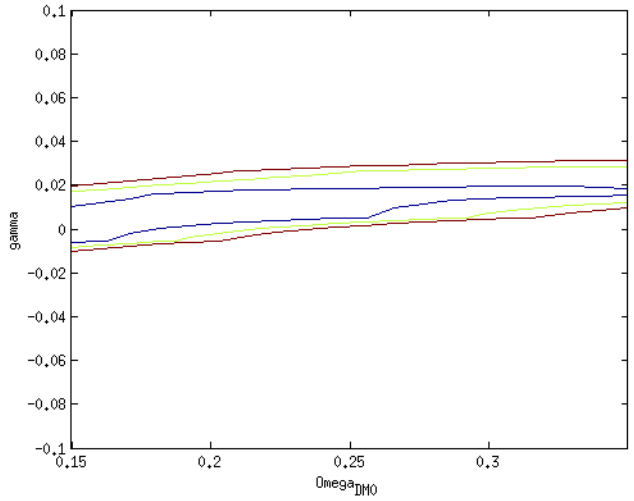

Figure 6.3: Contour plot when γ is the non-zero interaction parameter.

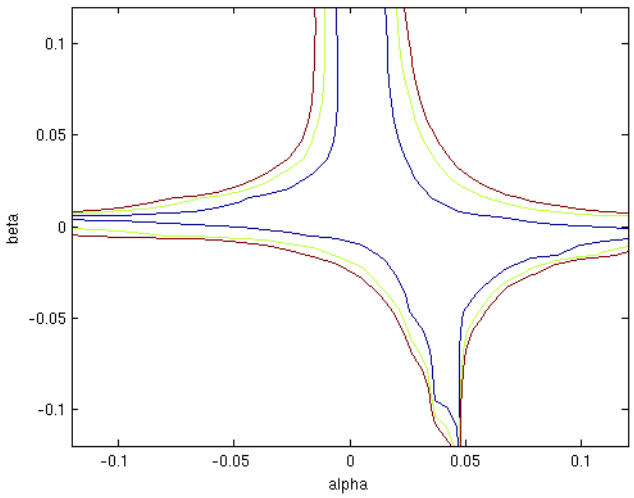

Figure 6.4: Contours when α and β are active interaction parameters.

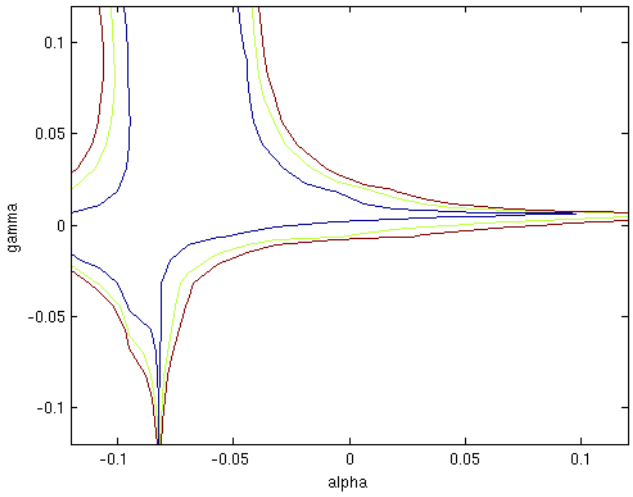

Figure 6.5: Contours when α and γ are active interaction parameters.

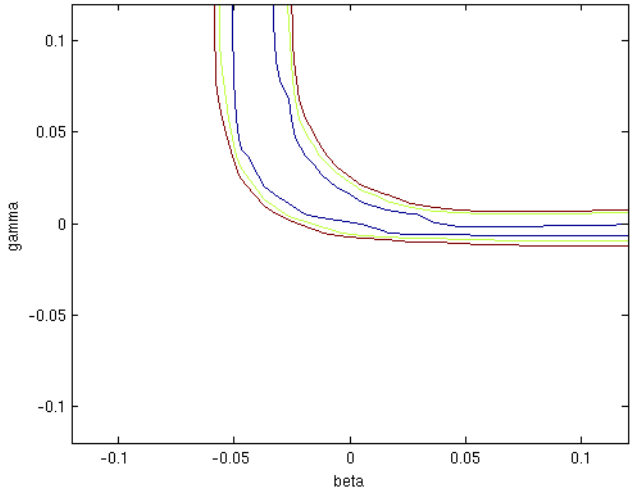

Figure 6.6: Contours when β and γ are active interaction parameters.

that there is no statistical evidence for interactions between any of the three components. On the other hand, the non-zero values are not excluded, and our interaction models are still possible.

For the case with α being the active interaction parameter, we study interactions between baryonic matter and dark matter. We get no constraints on α when we work with BAO. This is because the expansion rate of the universe after recombination is not affected differently by baryonic matter or dark matter, and so we can not use observations based on BAO to find constraints on α, we would have to use observations related to the time before recombination - for example Big Bang Nucleosynthesis.

When β is the active interaction parameter, we have interaction between baryonic matter and dark energy. We get broad contours if $\Omega_{\mathrm{DM},0}$ were to be larger than 0.24. This is because baryons are not very relevant to the expansion rate at the time related to our redshifts in our BAO data set.

At last, when γ is the active interaction parameters, we have interactions between the two dark components: dark matter and dark energy. We get way smaller contours than for the other two cases here. This is because the dark components are the two most important components of the universe at the BAO times.

6.5.2 Two interactions

As in the one-interaction case, we can see from all three contour plots that the ΛCDM model is within the 1σ contour, and so also here we have no statistical evidence for the interactions being present. Also as in the one-interaction case, we can not exclude the interactions either.

We can also see that if one of the interaction parameters is zero, we get the same result as in the one-interaction case, which is a nice consistency check.

We see that if α is active together with β or γ, we get constraints on α. This is because α affects the abundance of the energy in the baryonic and dark matter, which affects how much can then go to the dark energy through the other active interaction. So even though baryonic and dark matter affects the expansion of the universe in the same way, there is still an indirectly effect on α.

The strongest constraints is obtained for the parameter γ, representing the interaction between the two dark components. As in the one interaction case, this is due to the fact that the dark components are dominating over the baryonic matter component at the times where we have our BAO data.

In the end, we also here get weak constraints on the interaction parameters - $\beta = -0.04$ and $\gamma = 0.05$ is inside the 1σ region, for example, and that represents quite strong interactions, making the universe very different from the ΛCDM model. But the BAO constraints are stronger than the supernovae Ia constraints from the last chapter. There may be multiple reasons for this, one being the marginalization that I did over Ω_{b0}, where I could have used a higher resolution or a lower shifted invertall.

Chapter 7

The cosmic microwave background

7.1 Prediction and discovery of CMB: proof of a universe with a finite age

In the middle of the 20th century, the idea of a universe with a finite age, starting with a big bang, was not as strong as it is today. One of the problems astronomers worked on was the abundance of elements in the universe. In order to form helium from hydrogen, a hot, dense universe is required. If the universe is expanding, the universe could have been in such a dense state a long time ago. The problem became present when astronomers tried to compute the age of the universe: approximately 1 billion years. In 1928, the age of the Earth had been measured to be several billion years using radioactivity. And so the Earth were to be older than the universe according to this idea. Then the steady state model seemed to be better: a universe that is homogeneous and isotropic also in time - it has no beginning, no end, and is infinitely old. Of course, if it was to expand (which they knew it did due to Hubble's law), matter must be spontaneously created through the ages to maintain the average density. Calculations showed that the creation rate would be around a few hydrogen atoms per cubic meter every ten billion years. Such a small rate would be impossible to measure. This of course violates the law of conservation of mass-energy, and this question were left unanswered in this model.

Another problem with the steady state model is the abundance of helium in the universe today, which already back then was established to be around one quarter of all the baryonic matter. There was not enough helium created in stars to make up all this, but the big bang model could account for this abundance. So the only problem for the big bang model now was to find a proof of such a big bang. A proof of the big bang has yet to be found, but we have very good theories today of what happend just a fraction of a second

after the big bang.

Anyway, in the big bang model, the early universe should be hot and dense - so hot and dense that the mean free path of the photon was so short that the universe would be very close to thermal equilibrium. The radiation field in this universe should have a blackbody spectrum, and should fill the whole universe. The expansion of the universe would cool this down, and in 1948, predictions showed that the temperature of this radiation field should be around 5 Kelvin today.

The first discovery of the cosmic microwave background was made by two radio astronomers, Arno Penzias and Robert Wilson, at the Bell Laboratories in Holmdel, New Jersey. They were working with a huge horn reflector antenna, that was used to communicate with a satellite. They discovered that no matter how much they cleaned the antenna (including removing some pigeons that had nested inside the horn), there was a persistent hiss in the signal that they could not get rid of. This hiss seemed to be coming continuously from all directions of the sky. This fitted the idea of a blackbody radiation filling the whole universe. In 1965, this was confirmed by observations: the detected radiation had a Planck spectrum with a peak around a wavelength of 1.06 mm, in the microwave region of the electromagnetic spectrum.

And so we have this afterglow of the big bang, filling the whole universe, as a black body radiation field with a temperature of 2.725 ± 0.002 K, according to COBE [12]. Maps of the CMB shows that we have anisotropies in the CMB temperature, red areas being hotter than the mean temperature and blue areas being cooler. If one does a deep analyze of the CMB, one can find an asymmetry in the map. This asymmetry is one of the unsolved mysteries in cosmology today. On Figure 7.1 on the next page is such a map from 2008, made using the five year WMAP data. On Figure 7.2 on the facing page is a map from 2013, which is made using data from the Planck satellite, and has much higher resolution than the map from WMAP.

For more details about the physics and background on CMB, see [13].

7.2 CMB - related quantities

In our data set, we are given three quantities, labeled z_*, l_A and R. The first is the redshift of the CMB. We will use a fitting formula for z_*, given in [14]:

$$z_* = 1048 \cdot (1 + 0.00124(\Omega_{b,0}h^2)^{-0738})(1 + g_1((\Omega_{b,0} + \Omega_{\mathrm{DM},0})h^2)^{g_2}), \quad (7.1)$$

where g_1 and g_2 are given by

$$g_1 = \frac{0.0783(\Omega_{b,0}h^2)^{-0.238}}{1 + 39.5(\Omega_{b,0}h^2)^{0.763}},$$

$$g_2 = \frac{0.56}{1 + 21.1(\Omega_{b,0}h^2)^{1.81}}.$$

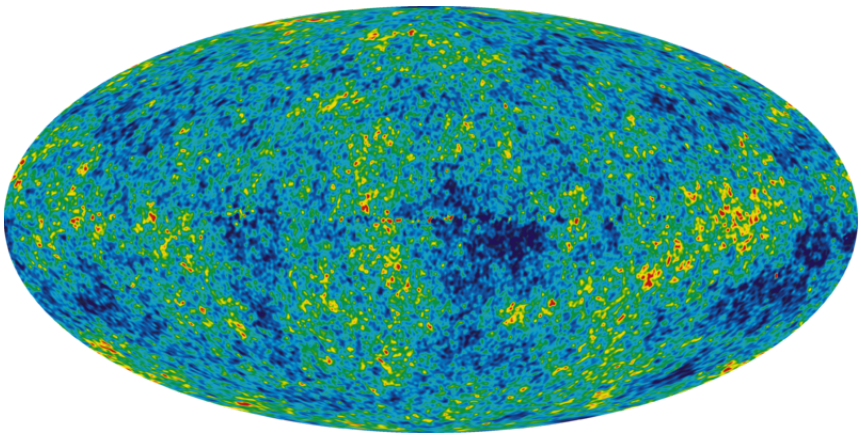

Figure 7.1: A map of the cosmic microwave background, made using the data from WMAP.

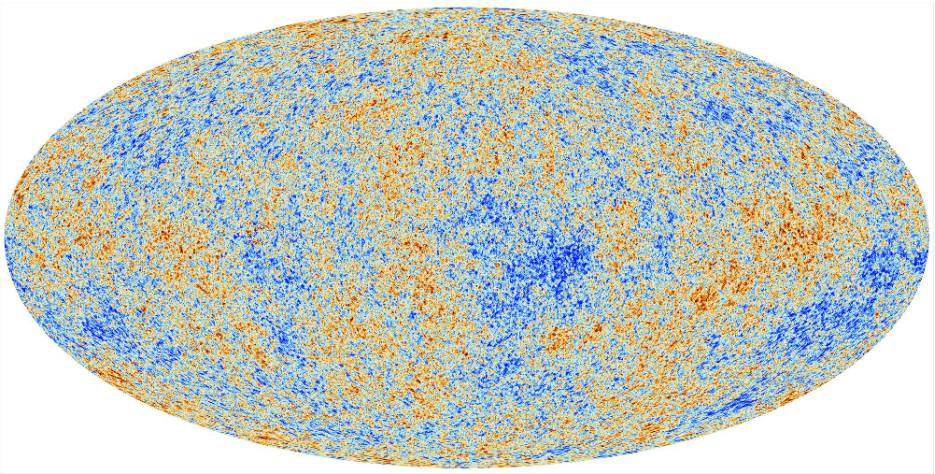

Figure 7.2: A map of the cosmic microwave background, made using data from the Planck satellite.

Table 7.1: Our data obtained from WMAP5, maximum likelihood.

Quantity	value	error
l_A	302.10	0.86
R	1.710	0.019
z_*	1090.04	0.93

The second quantity is called the "acoustic scale", which measures the ratio of the angular diameter distance r to recombination and the comoving sound horizon r_s at recombination. l_A is then given by

$$l_A = \pi \frac{r(z_*)}{r_s(z_*)}. \tag{7.2}$$

Here, $r_s(z_*)$ is given by Equation 6.5.

The third quantity we will use is the shift parameter, R. This measures the ratio of the angular diameter distance and the Hubble radius at the decoupling time [1]. It is given by

$$R = \sqrt{(\Omega_{b,0} + \Omega_{\mathrm{DM},0})} r(z_*). \tag{7.3}$$

If we look at the two last quantities l_A and R, and take the angular diameter distance $D_A(z_*)$ into account, we can express l_A and R as

$$l_A = (1 + z_*) \frac{\pi D_A(z_*)}{r_s(z_*)}, \qquad R = D_A(z_*) H(z_*),$$

so as for the Baryon Acoustic Oscillations case, CMB uses standard rulers to constrain my interaction parameters with observational data. See [15] for more details about the parameters.

7.3 The CMB data

To obtain observational constraints from CMB, we will use CMB data from WMAP, a five-year fit to models with spatial curvature and dark energy [15]. The maximum likelihood values will be used. The data are given in Table 7.1. The entries of the inverse covariance matrix are given in Table 7.2 on the facing page.

7.4 Observational constraints from the CMB

Now that we have observational data to the CMB related quantities, we can compare them to our models. Having already done this with BAO,

[1] Do not confuse with the parameter R of the analytical solutions in Chapter 3

Table 7.2: The entries of the inverse covariance matrix for the CMB data.

1.800	27.968	-1.103
27.968	5667.577	-92.263
-1.103	-92.263	2.923

we can save a lot of work for the CMB case. We just copy the code, and insert computations of the CMB quantities into our code. In the BAO case, we used the comoving distance to the CMB, $r(z_*)$, and the comoving sound horizon at recombination, $r_s(z_*)$ directly, and entered our BAO data through the dilatation scale $D_V(z)$, where z was in our BAO data. This time, we first compute z_* from Equation 7.1, then we compute $r(z_*)$ and $r_s(z_*)$ using the computed value for z_*. Then we can easily compute $l_A(z_*)$ and $R(z_*)$ using $z_*, r(z_*)$ and $r_s(z_*)$. Then we make a column vector $\mathbf{X}$, with entries $l_A(z_*), R(z_*)$ and z_*, in that order. Using the inverse covariance matrix C^{-1} from Table 7.2, we compute χ^2 using the similar expression as in the BAO case:

$$\chi^2 = \mathbf{X}^T C^{-1} \mathbf{X} = \sum_i \sum_j X_i C_{ij}^{-1} X_j.$$

Now that we have the χ^2 estimator for a grid of interaction parameters, we write the values to a file and use matlab to make contour plots. As in the BAO case, we marginalize over $\Omega_{b,0}$. We have the measured quantity $\Omega_{b,0}h^2 = 0.023$, but we do not know what $\Omega_{b,0}$ and h should be separately. Since we are not directly interested in these quantities anyway, we just marginalize over $\Omega_{b,0}$, that is, for each combination of interaction parameters, we choose the value of $\Omega_{b,0}$ that gives the smallest value for χ^2.

7.5 Results

7.5.1 One interaction

For the one-interaction case, we let $\Omega_{\mathrm{DM},0}$ be a free parameter, as we did for supernovae type Ia and BAO. We then run our program three times, one with each interaction parameter varying, the two others being zero. We use matlab to make the contour plots of χ^2. The contours shows the 1, 2 and 3σ regions, according to Table B.1 on page 164. In Figure 7.3 on the next page, we have the contour plots where α is the active interaction parameter, β is the active interaction parameter for the contour plot in Figure 7.4, and γ is the active parameter in Figure 7.5 on page 81.

7.5.2 Two interactions

For the two-interactions case, we have fixed $\Omega_{\mathrm{DM},0}$ to 0.224, the best fit value for the ΛCDM model. We run the program three times, one time for

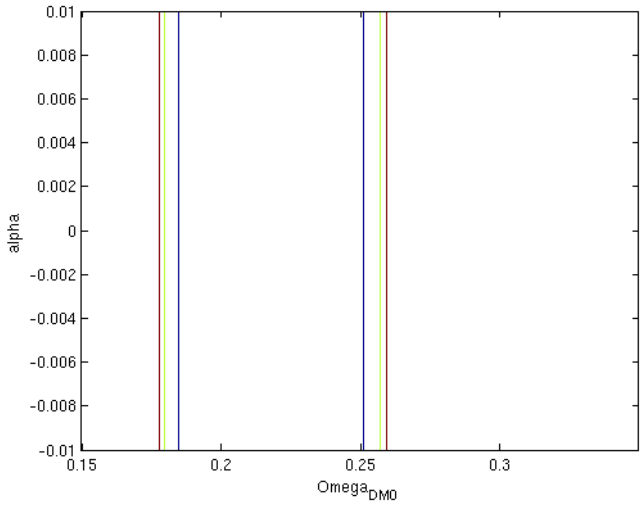

Figure 7.3: Contour plot of the χ^2-estimator with one interaction, showing the 1, 2 and 3σ regions. α is the active interaction parameter.

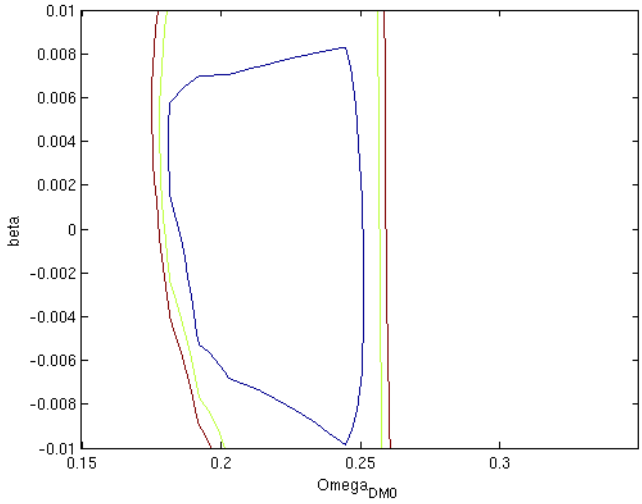

Figure 7.4: Contour plot of the χ^2-estimator with one interaction, showing the 1, 2 and 3σ regions. β is the active interaction parameter.

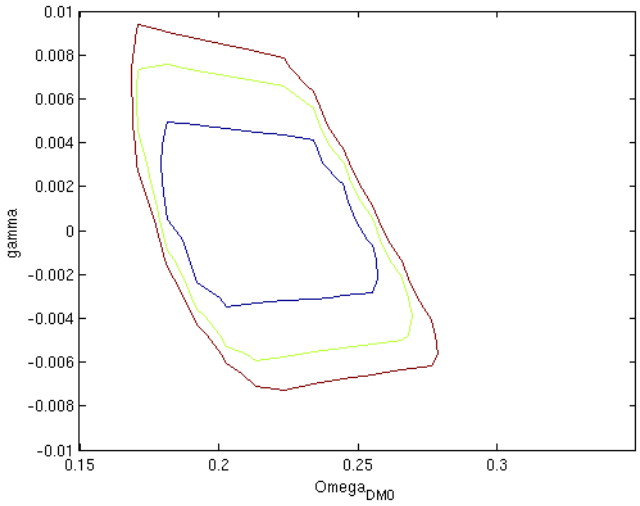

Figure 7.5: Contour plot of the χ^2-estimator with one interaction, showing the 1, 2 and 3σ regions. γ is the active interaction parameter.

each combination of non-zero interaction parameters (or one time for each interaction parameter being zero). We use matlab to make the contour plots, as in the one interaction case.

In Figure 7.6 on the next page, we have the contour plot for the case where α and β are active. In Figure 7.7 on the following page, we show the contours when α and γ are active, and in Figure 7.8 on page 83, we have the contour plot with β and γ as active interaction parameters.

7.6 Discussion

7.6.1 One interaction

When α is the active interaction parameter, representing interactions between baryonic matter and dark matter, we have a wide, but limited, 1σ contour for $\Omega_{\mathrm{DM},0}$, and small 2 and 3σ contours. We get no constraints on α itself. The explanation is the same as in the SNIa case and the BAO case: baryonic matter and dark matter affects the expansion rate in exactly the same way, so we can not use this to tell them apart, and the interaction paramater can be anything.

When β is the active parameter, we get one wide, but closed contour for the 1σ region, and smaller, but open regions for the 2 and 3σ regions. The regions are large since the abundance of baryonic matter is so small compared to the two dark components.

When γ is the active interaction parameter, giving us interaction between the two dark components, we get closed contours for all three σ-levels. These

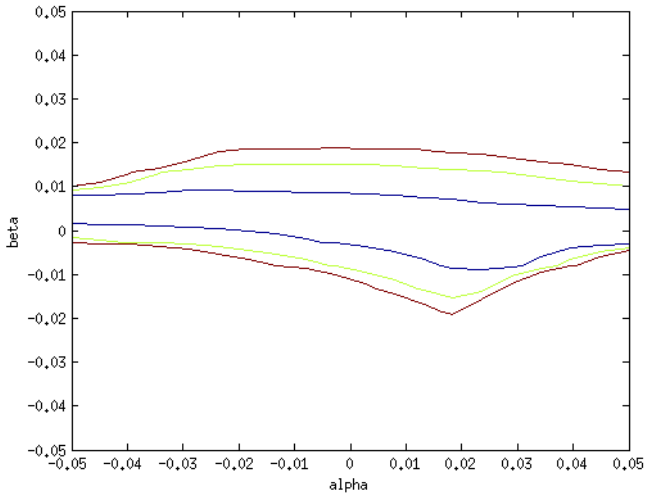

Figure 7.6: Contour plot of the χ^2-estimator with two interactions, showing the 1, 2 and 3σ regions. α and β are the two active interaction parameters.

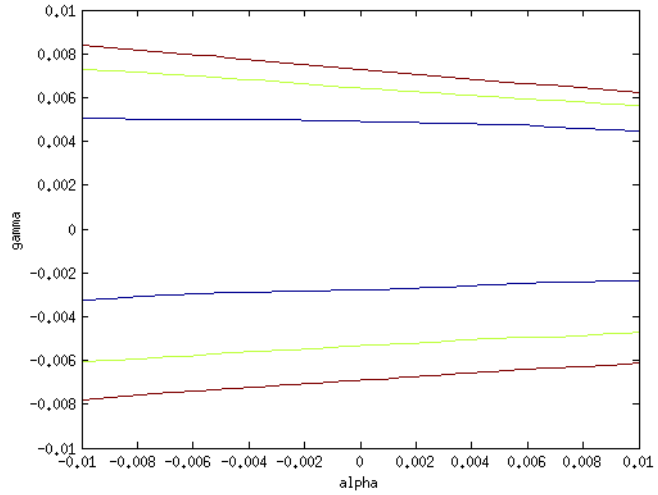

Figure 7.7: Contour plot of the χ^2-estimator with two interactions, showing the 1, 2 and 3σ regions. α and γ are the two active interaction parameters.

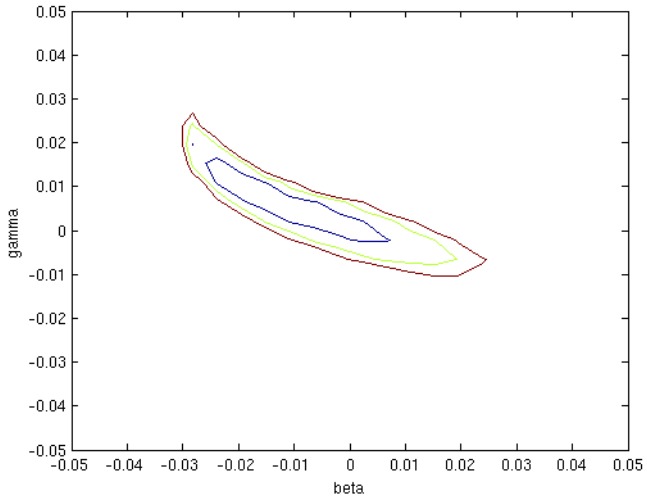

Figure 7.8: Contour plot of the χ^2-estimator with two interactions, showing the 1, 2 and 3σ regions. β and γ are the two active interaction parameters.

are all smaller than when α and β were active, and this is because γ is not related to baryonic matter, which there is way less of compared to the dark components.

The three contour plots all shows that the ΛCDM model, which all interaction parameters equal to zero and $\Omega_{\mathrm{DM},0} = 0.023$, is inside the 1σ contour, but the 1σ contour also covers an non-zero area. In other words, there are no statistical evidence for the interactions being present, but we can not exclude them either. But the contours are smaller compared to when we used SNIa and BAO data. This is because the CMB data are observations of the universe at way higher redshifts compared to SNIa and BAO, and so the interactions would eventually have more time to make its impact on the expansion rate.

7.6.2 Two interactions

The contour plots for two interactions shows much of the same as for one interaction: the ΛCDM model is inside the 1σ region in all cases, and so we have no statistical evidence for the interactions, but we can not exclude them either. We get some weak constraints on α, since it affects the abundance of baryonic and dark matter, which affects the efficiency of the other active interaction, and so α has an indirect effect on the expansion rate, when two interactions are active. The contours constraining β and γ are quite narrow, since β and γ affects the expansion rate directly, and the dark components are dominating over the baryons today.

Chapter 8

Interactions and the formation of structures

Now the time has come to study how our interactions will affect inhomogeneous perturbations in the metric and the energy densities of our universe components, which is what gives rise to cosmological structure formations. We will set up perturbations in the metric tensor, which together with our assumption that all the components of the universe are perfect fluids will give us the energy-momentum tensor for our components. Then we can use the equation for energy-momentum conservation in the general theory of relativity along with the Einstein equations and the Boltzmann equation for photons to get a set of coupeled, partial differential equations for how our perturbations evolve in space and time. By Fourier transforming our partial differential equations, we will get an infinite set of ordinary differential equations, which will tell us how our perturbations evolve in time on different length scales. The evolution in different length scales will then be decoupled from each other. These equations will be solved numerically, and we will be able to see how our interaction models affects an inhomogeneous universe.

8.1 The perturbed metric and the four velocity

When setting up perturbations, we need a background to perturb around. Our background is the universe we have worked with so far, with the usual FRW metric and our interaction models we get from that metric. This metric is defined in Equation 1.1, which in Cartesian coordinates reads

$$ds^2 = g_{\mu\nu}dx^\mu dx^\nu = -dt^2 + a^2(t)(dx^2 + dy^2 + dz^2).$$

Now, our metric is symmetric under the $SO(3)$ group, and so we use irreducible representations of $SO(3)$. We may then use the decomposition theorem, which says that perturbations of different tensor ranks (like scalars, vectors and tensor of higher ranks) will evolve independently to first order.

We will only deal with scalar perturbations, that is, our perturbation quantities will be scalar quantities, and then we do not have to worry about the perturbations of tensor rank one or higher. See [16] for more details and proof of the decomposition theorem.

Now we move on to the metric, and the choice of gauge. The most general way to write a metric with scalar perturbations is with the four functions A, B, E and ψ, all depending on x^μ:

$$g_{00} = -(1+2A), \qquad g_{0i} = -a\frac{\partial B}{\partial x^i} = g_{i0},$$

$$g_{ij} = a^2\left(\delta_{ij}(1+2\psi) - 2\frac{\partial^2 E}{\partial x^i \partial x^j}\right).$$

The four functions A, B, E and ψ are all perturbations, and when doing computations, we will only keep terms up to first order in these quantities. Now, we know that the line element ds^2, in general given by Equation A.1, is invariant. We use this to set up a coordinate transformation, from x^μ to $\tilde{x}^\mu$:

$$ds^2 = \tilde{g}_{\sigma\rho} d\tilde{x}^\sigma d\tilde{x}^\rho = g_{\mu\nu} dx^\mu dx^\nu$$
$$\Rightarrow g_{\mu\nu} = \tilde{g}_{\sigma\rho}\frac{\partial \tilde{x}^\sigma}{\partial x^\mu}\frac{\partial \tilde{x}^\rho}{\partial x^\nu}.$$

The most general, infinitesimal coordinate transformations generated by scalars (under the $SO(3)$ group) are given by two functions:

$$t \to \tilde{t} = t + \xi^0(x^\mu), \qquad x^i \to \tilde{x}^i = x^i + \delta^{ij}\frac{\partial \xi(x^\mu)}{\partial x^j},$$

where we also take the functions ξ^0 and ξ to be small quantities, and we only keep terms up to first order in ξ^0 and ξ. When we now do coordinate transformations, we can use these two functions to eliminate two of the functions in the metric, and so there are only two of the functions A, B, E and ψ in the metric that matters. When we choose which functions (or combination of functions) to use, we choose a gauge. We will set $A = \Psi$ and $\psi = \Phi$, and $B = E = 0$. This choice of gauge is called the conformal Newtonian gauge. The advantage of this gauge is that the metric is diagonal, which will be useful in some occasions later, and that the functions $\Psi(x^\mu)$ and $\Phi(x^\mu)$ are directly related to perturbations in the gravitational field and spatial curvature.

In the conformal Newtonian gauge, our perturbed metric looks like this:

$$g = (g_{\mu\nu}) = \begin{pmatrix} -(1+2\Psi) & 0 & 0 & 0 \\ 0 & a^2(1+2\Phi) & 0 & 0 \\ 0 & 0 & a^2(1+2\Phi) & 0 \\ 0 & 0 & 0 & a^2(1+2\Phi) \end{pmatrix}. \tag{8.1}$$

For more details about coordinate transformations and gauges, see [17], which this section is based on.

Next comes the four velocity. We start with the background (unperturbed) universe, assuming that we have a particle following the expansion of the universe. This particle will then be at rest in space, moving only in time. The background four-velocity $\bar{u}^\mu$ will then have components $\bar{u}^0 = 1$ and $\bar{u}^i = 0$ - time component is 1 and the three spatial components are 0. Then we introduce perturbations: $u^\mu = \bar{u}^\mu + \delta u^\mu$. We have $u^0 = 1 + \delta u^0$ and $u^i = \delta u^i$. Now we can use the four velocity identity, Equation A.3, to find the perturbation for the time component of the four velocity, δu^0:

$$\begin{aligned} -1 = u^\mu u_\mu = g_{\mu\nu} u^\mu u^\nu = g_{00}(u^0)^2 + g_{ij} u^i u^j \\ = -(1+2\Psi)(u^0)^2 + \delta_{ij} a^2 (1+2\Phi)(\delta u^i)^2. \end{aligned}$$

Now, since we are doing first order perturbation theory, we can neglect the last term on the right hand side, since it contains $(\delta u^i)^2$, which we assume is very small compared to the first term. We also Taylor-expand the part we are left with, and again only keep terms up to first order:

$$(u^0)^2 \approx \frac{1}{1+2\Psi} \Rightarrow u^0 \approx (1+2\Psi)^{-\frac{1}{2}} \approx 1 - \Psi. \tag{8.2}$$

Using the metric, we also get u_0:

$$u_0 = g_{\mu 0} u^\mu = -(1+2\Psi)(1-\Psi) \approx -(1+\Psi). \tag{8.3}$$

8.1.1 Perturbation decomposition

As mentioned, the decomposition theorem says that perturbations of different tensor ranks evolve independently to first order. We will be dealing with perturbations in the four velocity, and this brings in a point where we need to be careful, since the four velocity is a vector. We split the four velocity into a time component and a space component. We have already taken care of the time component. The perturbations in the space-components of the four velocity δu^i can be split up into a pure vector part v^i and a pure scalar part v, like this:

$$\delta u^i = v^i + \frac{\partial v}{\partial x^i} = v^i + \partial^i v. \tag{8.4}$$

Here, v^i has divergence zero:

$$\frac{\partial v^i}{\partial x^i} = \partial_i v^i = 0.$$

And using the decomposition theorem, we will only keep the scalar part of the perturbed four velocity $\partial_i v$. Now, I will actually write the other term instead, so $\delta v^i = v^i$ and $\delta u_i = v_i$. Not only does this save writing, but the equations will be easier to read, since I will use the partial differential operator for actual partial differentiation a lot.

8.1.2 The connection coefficients

With our new, perturbed metric comes connection coefficients $\Gamma^{\alpha}_{\mu\nu}$, defined in Equation A.4, and, since our basis is a coordinate basis, the connection coefficients are Christoffel symbols, and we can compute them by using Equation A.5. We divide the Christoffel symbols into groups, where each index takes zero or a Latin entry. We start with all indices being zero:

$$\Gamma^0_{00} = \frac{1}{-2(1+2\Psi)}\frac{\partial}{\partial t}(-(1+2\Psi)) = \frac{1}{1+2\Psi}\frac{\partial \Psi}{\partial t} \approx \frac{\partial \Psi}{\partial t},$$

where I in the last approximation only have kept terms up to first order. This will be done for all the other Christoffel symbols as well. Next, we let one of the lower indices be spatial:

$$\Gamma^0_{0j} = \frac{1}{-2(1+2\Psi)}\frac{\partial}{\partial x^j}(-(1+2\Psi)) \approx \frac{\partial \Psi}{\partial x^j} = \Gamma^0_{j0}.$$

Next we have two spatial lower indices:

$$\Gamma^0_{ij} = \frac{a^2\delta_{ij}}{1+2\Psi}\left(H(1+2\Phi) + \frac{\partial \Phi}{\partial t}\right) \approx a^2\delta_{ij}\left(H(1+2(\Phi-\Psi)) + \frac{\partial \Phi}{\partial t}\right).$$

Then we have the upper index spatial and the two lower indices zero:

$$\Gamma^i_{00} = \frac{-\delta^{ij}}{2a^2(1+2\Phi)}\frac{\partial}{\partial x^j}(-(1+2\Psi)) \approx \frac{\delta^{ij}}{a^2}\frac{\partial \Psi}{\partial x^j}.$$

Upper index spatial, one lower index spatial:

$$\Gamma^i_{j0} = \frac{\delta^i_j}{2(a^2(1+2\Phi))}\frac{\partial}{\partial t}\left(a^2(1+2\Phi)\right)$$

$$= \frac{\delta^i_j}{1+2\Phi}\left(H(1+2\Phi) + \frac{\partial \Phi}{\partial t}\right) \approx \delta^i_j\left(H + \frac{\partial \Phi}{\partial t}\right).$$

At last, three spatial indices:

$$\Gamma^i_{jk} = \frac{1}{2a^2(1+2\Phi)}$$

$$\cdot\left(\frac{\partial}{\partial x^k}\left(\delta^i_j a^2(1+2\Phi)\right) + \frac{\partial}{\partial x^j}\left(\delta^i_k a^2(1+2\Phi)\right) - \frac{\partial}{\partial x_i}\left(\delta_{jk} a^2(1+2\Phi)\right)\right)$$

$$\approx \delta^i_j\frac{\partial \Phi}{\partial x^k} + \delta^i_k\frac{\partial \Phi}{\partial x^j} - \delta_{jk}\frac{\partial \Phi}{\partial x_i}.$$

8.2 The energy-momentum tensor

The three components of the universe we are working with - baryonic matter, dark matter and dark energy, are all assumed to be perfect fluids, which means that there is no viscosity and no thermal conductivity. The energy-momentum tensor for each of the components is then given by Equation A.13. Written with one upper and one lower index, it reads

$$T^{\mu}_{\nu} = (\rho + p)u^{\mu}u_{\nu} + pg^{\mu}_{\nu}.$$

We need to introduce perturbations into our energy densities before we compute the components of the energy-momentum tensor. We use the density fluctuations δ to define our perturbations,

$$\rho(x^{\mu}) = \bar{\rho}(x^0)(1 + \delta(x^{\mu})), \tag{8.5}$$

so $\delta(x^{\mu})$ describes the deviation from the mean energy-density $\bar{\rho}(x^0)$. We will use the usual equation of state $\rho = wp$ to relate the energy-density to the pressure for all our components, and so we do not need to introduce separate perturbations in the pressure.

8.2.1 Baryons and dark matter

Baryonic matter and dark matter are both assumed to be pressureless, and so we have $w = p = 0$. The components of the energy-momentum tensor are then

$$T^0_0 = \rho u^0 u_0 = \bar{\rho}(1 + \delta)(1 - \Psi)(-1 - \Psi) \approx -\bar{\rho}(1 + \delta)$$

where, as usual, terms of second order and higher in the perturbation quantities (Ψ and δ) have been neglected. Continuing with the other components:

$$T^0_i = \rho u^0 u_i = \bar{\rho}(1 + \delta)(1 - \Psi)v_i \approx \bar{\rho}v_i,$$

$$T^i_0 = \rho u^i u_0 = \bar{\rho}(1 + \delta)v^i(-1 - \Psi) \approx -\bar{\rho}v^i,$$

$$T^i_j = \rho u^i u_j = \rho v^i v_j \approx 0.$$

And so the whole tensor written in matrix form reads

$$T(b, \mathrm{DM}) = (T^{\mu}_{\nu}) = \begin{pmatrix} -\bar{\rho}(1 + \delta) & \bar{\rho}v_x & \bar{\rho}v_y & \bar{\rho}v_z \\ -\bar{\rho}v^x & 0 & 0 & 0 \\ -\bar{\rho}v^y & 0 & 0 & 0 \\ -\bar{\rho}v^z & 0 & 0 & 0 \end{pmatrix}. \tag{8.6}$$

8.2.2 Dark energy

Dark energy has its usual equation of state: $p = w\rho$, where we take w as a constant. The energy-momentum tensor T^μ_ν for dark energy then has these components:

$$T^0_0 = (\rho+p)u^0u_0+w\rho g^0_0 = (1+w)\bar{\rho}(1+\delta)(1-\Psi)(-1-\Psi)+w\rho \approx -\bar{\rho}(1+\delta),$$

$$T^0_i = (\rho+p)u^0u_i + w\rho g^0_i = (1+w)\bar{\rho}(1+\delta)(1-\Psi)v_i \approx (1+w)\bar{\rho}v_i,$$

$$T^i_0 = (\rho+p)u^iu_0 + w\rho g^0_i = (1+w)\bar{\rho}(1+\delta)v^i(-1-\Psi) \approx -(1+w)\bar{\rho}v^i,$$

$$T^i_j = (\rho+p)u^iu_j + w\rho g^i_j \approx w\bar{\rho}(1+\delta)\delta^i_j.$$

And the whole tensor in matrix form reads

$$T(\mathrm{DE}) = (T^\mu_\nu) =$$

$$\begin{pmatrix} -\bar{\rho}(1+\delta) & (1+w)\bar{\rho}v_x & (1+w)\bar{\rho}v_y & (1+w)\bar{\rho}v_z \\ -(1+w)\bar{\rho}v^x & w\bar{\rho}(1+\delta) & 0 & 0 \\ -(1+w)\bar{\rho}v^y & 0 & w\bar{\rho}(1+\delta) & 0 \\ -(1+w)\bar{\rho}v^z & 0 & 0 & w\bar{\rho}(1+\delta) \end{pmatrix}. \tag{8.7}$$

8.3 The energy-momentum conservation equation

Now that we have the energy-momentum tensor of our three components, we can go back to our interaction equations in covariate form, which, if added, is nothing more than the conservation equation of the energy-momentum tensor. We start with the left hand side of the equations, which are the covariate derivatives of the energy-momentum tensors. Using Equation A.7, we have

$$\nabla_\mu T^\mu_\nu = T^\mu_{\nu,\mu} + \Gamma^\mu_{\alpha\mu}T^\alpha_\nu - \Gamma^\alpha_{\nu\mu}T^\mu_\alpha.$$

We can split this equation into two cases: the time component with ν being zero and the space components with ν being $1, 2$ or 3. In both cases, we split the sums over μ and α on the right hand side into time and space parts, in the terms with the connection coefficients (the partial derivative is left for later).

8.3.1 The time component equations

For the time component ($\nu = 0$), expanding α first, then μ, we have

$$\nabla_\mu T^\mu_0 = T^\mu_{0,\mu} + \Gamma^\mu_{0\mu}T^0_0 + \Gamma^\mu_{i\mu}T^i_0 - \Gamma^0_{0\mu}T^\mu_0 - \Gamma^i_{0\mu}T^\mu_i$$

$$= T^\mu_{0,\mu} + \Gamma^0_{00}T^0_0 + \Gamma^i_{0i}T^0_0 + \Gamma^0_{i0}T^i_0 + \Gamma^j_{ij}T^i_0 - \Gamma^0_{00}T^0_0 - \Gamma^0_{0i}T^i_0 - \Gamma^i_{00}T^0_i - \Gamma^i_{0j}T^j_i.$$

We see that some of the terms cancel each other, so we are left with

$$\nabla_\mu T^\mu_0 = T^\mu_{0,\mu} + \Gamma^i_{0i}T^0_0 + \Gamma^j_{ij}T^i_0 - \Gamma^i_{00}T^0_i - \Gamma^i_{0j}T^j_i. \tag{8.8}$$

Now we choose which component we want to work with. We start with baryons or dark matter - they have the same form of the energy momentum tensor. Since the pressure of these two components is zero, the last term will go away. Inserting for the connection coefficients and summing up in the other terms, we have

$$\begin{aligned}\nabla_\mu T_0^\mu &= T^\mu_{0,\mu} - 3\left(H + \frac{\partial\Phi}{\partial t}\right)\bar{\rho}(1+\delta) - \frac{\partial\Phi}{\partial x^i}(\bar{\rho}v^i) - \frac{1}{a^2}\frac{\partial\Psi}{\partial x^i}\bar{\rho}v^i \\ &\approx \frac{\partial T_0^0}{\partial t} + \frac{\partial T_0^i}{\partial x^i} - 3H\bar{\rho}(1+\delta) - 3\bar{\rho}\frac{\partial\Phi}{\partial t} \\ &= -\left(\delta\frac{\partial\bar{\rho}}{\partial t} + \bar{\rho}\left(\frac{\partial\delta}{\partial t} + \frac{\partial(v^i)}{\partial x^i} + 3H(1+\delta) + 3\frac{\partial\Phi}{\partial t}\right)\right), \end{aligned} \tag{8.9}$$

Where at the last equality, I have used the fact that the average energy density $\bar{\rho}$ does not depend on space, which cancels a term.

Over to dark energy, now we have pressure to account for, and we can not cancel so many terms as we could for the matter components. Going back to Equation 8.8, inserting for the connection coefficients and the energy-momentum tensor and summing up, we have

$$\begin{aligned}\nabla_\mu T_0^\mu &= T^\mu_{0,\mu} - 3\left(H + \frac{\partial\Phi}{\partial t}\right)\bar{\rho}(1+\delta) + \frac{\partial\Phi}{\partial x^i}(\bar{\rho}v^i) \\ &\quad -\frac{1}{a^2}\frac{\partial\Psi}{\partial x^i}\bar{\rho}v^i - 3\left(H + \frac{\partial\Phi}{\partial t}\right)w\bar{\rho}(1+\delta) \\ &\approx T^\mu_{0,\mu} - 3(1+w)H\bar{\rho}(1+\delta) - 3(1+w)\bar{\rho} + \frac{\partial\Phi}{\partial t} \\ &= -\left(\delta\frac{\partial\bar{\rho}}{\partial t} + \bar{\rho}\left(\frac{\partial\delta}{\partial t} + (1+w)\left(\frac{\partial(v^i)}{\partial x^i} + 3H(1+\delta) + \frac{\partial\Phi}{\partial t}\right)\right)\right). \end{aligned} \tag{8.10}$$

As a consistency check, we see that if we set $w = 0$, we get the same equation as for the matter case.

8.3.2 The space component equations

Now we go back to Equation A.7, setting ν to a spatial index k. Expanding the sums over α and μ, we have:

$$\nabla_\mu T_k^\mu = T^\mu_{k,\mu} + \Gamma^0_{00}T^0_k + \Gamma^i_{0i}T^0_k + \Gamma^0_{i0}T^i_k + \Gamma^j_{ij}T^i_k - \Gamma^0_{k0}T^0_0 - \Gamma^0_{ki}T^i_0 - \Gamma^i_{k0}T^0_i - \Gamma^i_{kj}T^j_i$$

This time, no terms cancel right away. Starting with the matter components, we have $T^i_j = 0$. Inserting for the connection coefficients and the energy-momentum tensor in the other terms, we have

$$\nabla_\mu T_k^\mu = T^\mu_{k,\mu} + \bar{\rho}\left(v_k\frac{\partial\Psi}{\partial t} + 3v_k\left(H + \frac{\partial\Phi}{\partial t}\right)\right.$$

$$+(1+\delta)\frac{\partial\Psi}{\partial x^k} - \delta^i_k v_i\left(H+\frac{\partial\Phi}{\partial t}\right) + a^2\delta_{ki}v^i\left(H(1+(\Phi-\Psi))+\frac{\partial\Phi}{\partial t}\right)\Bigg)$$
$$\approx v_k\frac{\partial\bar{\rho}}{\partial t} + \bar{\rho}\left(\frac{\partial(v_k)}{\partial t} + 3Hv_k + \frac{\partial\Psi}{\partial x^k}\right). \tag{8.11}$$

For dark energy, we have

$$\nabla_\mu T^\mu_k = T^\mu_{k,\mu} + \bar{\rho}\Bigg((1+w)\left(v_k\frac{\partial\Psi}{\partial t} + 3v_k\left(H+\frac{\partial\Phi}{\partial t}\right)\right.$$
$$+a^2\delta_{ki}v^i\left(H(1+2(\Phi-\Psi))+\frac{\partial\Phi}{\partial t}\right) - \delta^i_k v_i\left(H+\frac{\partial\Phi}{\partial t}\right)\Bigg)$$
$$-w(1+\delta)\delta^j_i\left(\delta_{ij}\frac{\partial\Phi}{\partial x^k} + \delta_{ik}\frac{\partial\Phi}{\partial x^j} - \delta_{jk}\frac{\partial\Phi}{\partial x^i}\right)$$
$$\left.+\delta^i_k(1+\delta)\frac{\partial\Psi}{\partial x^i} + 3\delta^i_k w(1+\delta)\frac{\partial\Phi}{\partial x^i} + (1+\delta)\frac{\partial\Psi}{\partial x^k}\right)$$
$$\approx T^\mu_{k,\mu} + \bar{\rho}\Bigg(3Hv_k(1+w) + w\frac{\partial\Psi}{\partial x^k} + 3w\frac{\partial\Phi}{\partial x^k} + \frac{\partial\Psi}{\partial x^k}$$
$$\left.+H(1+w)v_k - H(1+w) - 3w\frac{\partial\Phi}{\partial x^k}\right)$$
$$= (1+w)v_k\frac{\partial\bar{\rho}}{\partial t} + \bar{\rho}\left(\frac{\partial v_k}{\partial t} + w\frac{\partial\delta}{\partial x^k} + (1+w)\left(3Hv_k + \frac{\partial\Psi}{\partial x^k}\right)\right), \tag{8.12}$$

where we in the last step again have used that $\bar{\rho}$ is constant in space to eliminate a term.

8.4 The interaction terms

Now we are going to take a closer look at the interaction terms of two components x and y, $Q_\nu(x,y)$. These terms generate exchange of energy-momentum between the different components. The interaction terms have this form:

$$Q_\nu(x,y) = \zeta\nabla_\mu s^\mu(\rho(x)+\rho(y))s_\nu(x,y).$$

Here, $x, y \in \{b, \text{DM}, \text{DE}\}$, and $\zeta \in \{\alpha, \beta, \gamma\}$. We can divide the interaction term into four parts: First we have the interaction parameter ζ, which is directly related to the strength of the interaction. Then we have the four divergence, which is where the expansion of the universe comes in. Next we have the sum of the energy-densities of the two components interacting, and at last we have the four velocity factor. There are multiple possibilities for the four velocity factor, and we will use a simple case where s^μ is the average four velocity of the two interacting components x and y:

$$s^\mu(x,y) = \frac{u^\mu(x)+u^\mu(y)}{2},$$

and the same for $s_\nu(x,y)$. Now we can take a closer look at the four divergence. We use Equation A.8 to find this factor in terms of our perturbation quantities, to first order. First we need the determinant of the metric. Since the metric is diagonal, is is simply the product of the entries:

$$|\det(g_{\alpha\beta})| = (1+2\Psi)a^6(1+2\Phi)^6 \approx a^6(1+2\Psi+6\Phi),$$

where we have kept only zeroth and first order terms. Inserting this, we get

$$\nabla_\mu s^\mu \approx a^{-3}(1-\Psi-3\Phi)\frac{\partial}{\partial x^\mu}\left(a^3(1+\Psi+3\Phi)s^\mu\right)$$

$$= a^{-3}(1-\Psi-3\Phi)\left(\frac{\partial}{\partial t}(a^3(1+\Psi+3\Phi)(1-\Psi)) + \frac{\partial}{\partial x^i}(a^3(1+\Psi+3\Phi)s^i)\right)$$

$$\approx \frac{3}{a}\frac{da}{dt}(1-\Psi) + 3\frac{\partial\Phi}{\partial t} - \frac{\partial s^i}{\partial x^i}$$

$$= 3H - 3H\Psi + 3\frac{\partial\Phi}{\partial t} + \frac{\partial s^i}{\partial x^i}. \tag{8.13}$$

Here, we see that the zeroth order term is just three times the Hubble expansion, as we are used to in the background universe. Turning to the whole interaction term $Q_\nu(x,y)$, starting with the time component, $\nu = 0$:

$$Q_0(x,y)$$

$$= \zeta\left(3H(1-\Psi) + 3\frac{\partial\Phi}{\partial t} + \frac{1}{2}\frac{\partial}{\partial x^i}(v^i(x)+v^i(y))\right)$$

$$\cdot(\bar\rho_x(1+\delta_x) + \bar\rho_y(1+\delta_y))(-1-\Psi).$$

Here, we have inserted for s^i and used that $s_0 = -1-\Psi$ in our form of s. To first order, we get

$$Q_0(r,s) \approx$$

$$-\zeta\left((\bar\rho_x+\bar\rho_y)\left(3H + 3\frac{\partial\Phi}{\partial t} + \frac{1}{2}\frac{\partial}{\partial x^i}(v^i(x)+v^i(y))\right) + 3H(\bar\rho_x\delta_x + \bar\rho_y\delta_y)\right). \tag{8.14}$$

For the space component, we get

$$Q_k(x,y) = \zeta\left(3H - 3H\Psi + 3\frac{\partial\Phi}{\partial t} + \frac{1}{2}\frac{\partial}{\partial x^i}(v^i(x)+v^i(y))\right)$$

$$\cdot(\bar\rho_x(1+\delta_x) + \bar\rho_y(1+\delta_y))\frac{1}{2}(u_k(x)+u_k(y))$$

$$\approx \frac{3}{2}H\zeta(\bar\rho_y+\bar\rho_x)(u_k(x)+u_k(y)). \tag{8.15}$$

8.5 Interactions: the left hand side and the right hand side meet

Now that we have the left hand sides and the right hand side of all our equations, the time has come to let them meet each other.

8.5.1 Baryons

We start with the baryon equation:

$$\nabla_\mu T^\mu_\nu(b) = Q_\nu(b, \mathrm{DM}) + Q_\nu(b, \mathrm{DE}).$$

Time component

We start with the time component, $\nu = 0$:

$$\begin{aligned}\nabla_\mu T^\mu_\nu(b) &= -\left(\delta_b \frac{\partial \bar{\rho}_b}{\partial t} + \bar{\rho}_b \left(\frac{\partial \delta_b}{\partial t} + \frac{\partial (v^i)}{\partial x^i} + 3H(1+\delta_b) + 3\frac{\partial \Phi}{\partial t}\right)\right) \\ &= -\alpha(\bar{\rho}_b + \bar{\rho}_{\mathrm{DM}})\left(3H + 3\frac{\partial \Phi}{\partial t} + \frac{1}{2}\frac{\partial}{\partial x^i}(v^i_b + v^i_{\mathrm{DM}})\right) \\ &\quad -\beta(\bar{\rho}_b + \bar{\rho}_{\mathrm{DE}})\left(3H + 3\frac{\partial \Phi}{\partial t} + \frac{1}{2}\frac{\partial}{\partial x^i}(v^i_b + v^i_{\mathrm{DE}})\right) \\ &\quad +3H(\alpha(\bar{\rho}_b\delta_b + \bar{\rho}_{\mathrm{DM}}\delta_{\mathrm{DM}}) + \beta(\bar{\rho}_b\delta_b + \bar{\rho}_{\mathrm{DE}}\delta_{\mathrm{DE}})).\end{aligned}$$

We use the background equation to eliminate all terms with derivatives of $\bar{\rho}_b$:

$$\frac{\partial \bar{\rho}_b}{\partial t} + 3H\bar{\rho}_b = 3H(\alpha(\bar{\rho}_b + \bar{\rho}_{\mathrm{DM}}) + \beta(\bar{\rho}_b + \bar{\rho}_{\mathrm{DE}})).$$

Then we divide by $-\bar{\rho}_b$, and re-arrange terms, ending up with

$$\begin{aligned}&\frac{\partial \delta_b}{\partial t} + \frac{\partial v^i_b}{\partial x^i} + 3\frac{\partial \Phi}{\partial t} \\ &= 3H\left(2\delta_b(\alpha+\beta) + \alpha\frac{\bar{\rho}_{\mathrm{DM}}}{\bar{\rho}_b}(\delta_b + \delta_{\mathrm{DM}}) + \beta\frac{\bar{\rho}_{\mathrm{DE}}}{\bar{\rho}_b}(\delta_b + \delta_{\mathrm{DE}})\right) \\ &\quad +\alpha\left(1 + \frac{\bar{\rho}_{\mathrm{DM}}}{\bar{\rho}_b}\right)\left(3\frac{\partial \Phi}{\partial t} + \frac{1}{2}\frac{\partial}{\partial x^i}(v^i_b + v^i_{\mathrm{DM}})\right) \\ &\quad +\beta\left(1 + \frac{\bar{\rho}_{\mathrm{DE}}}{\bar{\rho}_b}\right)\left(3\frac{\partial \Phi}{\partial t} + \frac{1}{2}\frac{\partial}{\partial x^i}(v^i_b + v^i_{\mathrm{DE}})\right).\end{aligned}$$

Now we do a Fourier transformation of the whole equation, using Equation B.6, going from space x to wavenumber k. This will turn the partial differential equation into an infinite set of ordinary differential equations, one equation for each wavenumber k. These equations will be decoupled from

each other, meaning that perturbation evolutions on different lengthscales (by the wavenumber k) will evolve independently. The differential operators for ∂x^i goes to ik^i (where the i in front of k is now the imaginary unit). We also assume that the velocity field is irrotational, that is, it points in the same direction as k. Then we have $ik_i v^i = ikv$. We change integration variable, from cosmic time t to conformal time η, which will be useful later on. This change of variable is given by $dt = ad\eta$, where a is the scale factor from the metric tensor. Also, we re-scale the four velocity, replacing v by iv/a, which also will be useful later (the imaginary unit i now goes away). We end up with

$$\begin{aligned}\frac{\partial \delta_b}{\partial \eta} &= -kv_b - 3\frac{\partial \Phi}{\partial \eta} \\ &+\alpha\left(1+\frac{\bar{\rho}_{\rm DM}}{\bar{\rho}_b}\right)\left(3\frac{\partial \Phi}{\partial \eta}+\frac{k}{2}(v_b+v_{\rm DM})\right) \\ &+\beta\left(1+\frac{\bar{\rho}_{\rm DE}}{\bar{\rho}_b}\right)\left(3\frac{\partial \Phi}{\partial \eta}+\frac{k}{2}(v_b+v_{\rm DE})\right) \\ +3\mathcal{H}&\left(2\delta_b(\alpha+\beta)+\alpha\frac{\bar{\rho}_{\rm DM}}{\bar{\rho}_b}(\delta_b+\delta_{\rm DM})+\beta\frac{\bar{\rho}_{\rm DE}}{\bar{\rho}_b}(\delta_b+\delta_{\rm DE})\right). \qquad (8.16)\end{aligned}$$

Space component

When ν is a spatial index k, we get this interaction equation:

$$\begin{aligned}v_k^b\frac{\partial \bar{\rho}_b}{\partial t}+\bar{\rho}_b\left(\frac{\partial (v_k^b)}{\partial t}+3Hv_k^b+\frac{\partial \Psi}{\partial x^k}\right) \\ =\frac{3}{2}H\left(\alpha(\bar{\rho}_b+\bar{\rho}_{\rm DM})(v_k^b+v_k^{\rm DM})+\beta(\bar{\rho}_b+\bar{\rho}_{\rm DE})(v_k^b+v_k^{\rm DE})\right).\end{aligned}$$

As we have seen earlier, there is no background equation for the space component, since there are no zero-order terms in $Q_k(r,s)$. But we can still use the background equation of the time component to get rid of the terms with the time derivative of the background energy-density of the baryons, $\bar{\rho}_b$. We also divide by $\bar{\rho}_b$, which after some re-arrangements leaves this equation:

$$\frac{\partial v_k^b}{\partial t}+\frac{\partial \Psi}{\partial x^k}=3H\left(\alpha\left(1+\frac{\bar{\rho}_{\rm DM}}{\bar{\rho}_b}\right)\frac{3v_k^b+v_k^{\rm DM}}{2}+\beta\left(1+\frac{\bar{\rho}_{\rm DE}}{\bar{\rho}_b}\right)\frac{3v_k^b+v_k^{\rm DE}}{2}\right).$$

As for the time component equation, we Fourier transform to get ordinary differential equations, assume an irrotational velocity field, rescale v to iv/a (which brings a term $\mathcal{H}v_b$ into the equation through the derivative of v_k^b), and we change integration variable to conformal time η. We end up with this equation:

$$\begin{aligned}\frac{\partial v_b}{\partial \eta} &= -\mathcal{H}v_b - k\Psi \\ +3\mathcal{H}&\left(\alpha\left(1+\frac{\bar{\rho}_{\rm DM}}{\bar{\rho}_b}\right)\frac{3v_b+v_{\rm DM}}{2}+\beta\left(1+\frac{\bar{\rho}_{\rm DE}}{\bar{\rho}_b}\right)\frac{3v_b+v_{\rm DE}}{2}\right). \qquad (8.17)\end{aligned}$$

8.5.2 Dark matter

Now we have come to dark matter. The computations will be very similar to the baryonic case, but with β replaced by γ, and some of the signs will change.

The time component

The time component of the dark matter interaction equation is

$$
\begin{aligned}
-\left(\delta_{\mathrm{DM}}\frac{\partial\bar{\rho}_{\mathrm{DM}}}{\partial t}+\bar{\rho}_{\mathrm{DM}}\left(\frac{\partial\delta_{\mathrm{DM}}}{\partial t}+\frac{\partial(v^i)}{\partial x^i}+3H(1+\delta_{\mathrm{DM}})+3\frac{\partial\Phi}{\partial t}\right)\right)\\
=\alpha(\bar{\rho}_b+\bar{\rho}_{\mathrm{DM}})\left(3H+3\frac{\partial\Phi}{\partial t}+\frac{1}{2}\frac{\partial}{\partial x^i}(v_b^i+v_{\mathrm{DM}}^i)\right)\\
-\gamma(\bar{\rho}_{\mathrm{DM}}+\bar{\rho}_{\mathrm{DE}})\left(3H+3\frac{\partial\Phi}{\partial t}+\frac{1}{2}\frac{\partial}{\partial x^i}(v_{\mathrm{DM}}^i+v_{\mathrm{DE}}^i)\right)\\
+3H(-\alpha(\bar{\rho}_b\delta_b+\bar{\rho}_{\mathrm{DM}}\delta_{\mathrm{DM}})+\gamma(\bar{\rho}_{\mathrm{DM}}\delta_{\mathrm{DE}}+\bar{\rho}_{\mathrm{DE}}\delta_{\mathrm{DE}})).
\end{aligned}
$$

Now we use the background equation to get rid of terms with the time derivative of $\bar{\rho}_{\mathrm{DM}}$, we Fourier transform x to k, assume irrotational velocity fields, rescale v to iv/a, and change integration variable from t to η. This gives us

$$
\begin{aligned}
\frac{\partial\delta_{\mathrm{DM}}}{\partial\eta}=-kv_{\mathrm{DM}}-3\frac{\partial\Phi}{\partial\eta}\\
-\alpha\left(\frac{\bar{\rho}_b}{\bar{\rho}_{\mathrm{DM}}}+1\right)\left(3\frac{\partial\Phi}{\partial\eta}+\frac{k}{2}(v_b+v_{\mathrm{DM}})\right)\\
+\gamma\left(1+\frac{\bar{\rho}_{\mathrm{DE}}}{\bar{\rho}_{\mathrm{DM}}}\right)\left(3\frac{\partial\Phi}{\partial\eta}+\frac{k}{2}(v_{\mathrm{DM}}+v_{\mathrm{DE}})\right)\\
+3\mathcal{H}\left(2\delta_{\mathrm{DM}}(\gamma-\alpha)-\alpha\frac{\bar{\rho}_b}{\bar{\rho}_{\mathrm{DM}}}(\delta_b+\delta_{\mathrm{DM}})+\gamma\frac{\bar{\rho}_{\mathrm{DE}}}{\bar{\rho}_{\mathrm{DM}}}(\delta_{\mathrm{DM}}+\delta_{\mathrm{DE}})\right). \qquad (8.18)
\end{aligned}
$$

The space component

Now for the space component of the dark matter interaction equation:

$$
\begin{aligned}
v_k^{\mathrm{DM}}\frac{\partial\bar{\rho}_{\mathrm{DM}}}{\partial t}+\bar{\rho}_{\mathrm{DM}}\left(\frac{\partial v_k^{\mathrm{DM}}}{\partial t}+3Hv_k^{\mathrm{DM}}+\frac{\partial\Psi}{\partial x^k}\right)\\
=\frac{3}{2}H(-\alpha(\bar{\rho}_b+\bar{\rho}_{\mathrm{DM}})(v_k^b+v_k^{\mathrm{DM}})+\gamma(\bar{\rho}_{\mathrm{DM}}+\bar{\rho}_{\mathrm{DE}})(v_k^{\mathrm{DM}}-v_k^{\mathrm{DE}})).
\end{aligned}
$$

Again we Fourier transform, assume irrotational velocity fields, rescale v to iv/a, and change integration variable to η. We end up with

$$
\begin{aligned}
\frac{\partial v_{\mathrm{DM}}}{\partial\eta}=-\mathcal{H}v_{\mathrm{DM}}-k\Psi\\
+3\mathcal{H}\left(-\alpha\left(\frac{\bar{\rho}_b}{\bar{\rho}_{\mathrm{DM}}}+1\right)\frac{v_b+3v_{\mathrm{DM}}}{2}+\gamma\left(1+\frac{\bar{\rho}_{\mathrm{DE}}}{\bar{\rho}_{\mathrm{DM}}}\right)\frac{3v_{\mathrm{DM}}+v_{\mathrm{DE}}}{2}\right). \qquad (8.19)
\end{aligned}
$$

8.5.3 Dark energy

At last we have dark energy. To make things a lot simpler, I will set $w = -1$ straight away. When I am going to do numerical simulations, I must set a value for w, and then a very natural choice is $w = -1$. Setting w to something else is a whole field to explore, and I will not do that here, but see [18] and [19] for models with varying cosmological constants.

The time component

Putting together the time component of the dark energy interaction equation, with $w = -1$, we get

$$
\begin{aligned}
&-\left(\delta_{\mathrm{DE}}\frac{\partial\bar{\rho}_{\mathrm{DE}}}{\partial t}+\bar{\rho}_{\mathrm{DE}}\left(\frac{\partial\delta_{\mathrm{DE}}}{\partial t}\right)\right)\\
&=\beta(\bar{\rho}_b+\bar{\rho}_{\mathrm{DE}})\left(3H+3\frac{\partial\Phi}{\partial t}+\frac{1}{2}\frac{\partial}{\partial x^i}(v_b^i+v_{\mathrm{DE}}^i)\right)\\
&+\gamma(\bar{\rho}_{\mathrm{DM}}+\bar{\rho}_{\mathrm{DE}})\left(3H+3\frac{\partial\Phi}{\partial t}+\frac{1}{2}\frac{\partial}{\partial x^i}(v_{\mathrm{DM}}^i+v_{\mathrm{DE}}^i)\right)\\
&-3H(\beta(\bar{\rho}_b\delta_b+\bar{\rho}_{\mathrm{DE}}\delta_{\mathrm{DE}})+\gamma(\bar{\rho}_{\mathrm{DM}}\delta_{\mathrm{DM}}+\bar{\rho}_{\mathrm{DE}}\delta_{\mathrm{DE}})).
\end{aligned}
$$

For the fifth time, we Fourier transform, assume irrotational velocity fields, rescale v to iv/a, and change integration variable to η. We end up with this equation:

$$
\begin{aligned}
\frac{\partial\delta_{\mathrm{DE}}}{\partial\eta}&=-\beta\left(\frac{\bar{\rho}_b}{\bar{\rho}_{\mathrm{DE}}}+1\right)\left(3\frac{\partial\Phi}{\partial\eta}+\frac{k}{2}(v_b+v_{\mathrm{DE}})\right)\\
&\quad-\gamma\left(\frac{\bar{\rho}_{\mathrm{DM}}}{\bar{\rho}_{\mathrm{DE}}}+1\right)\left(3\frac{\partial\Phi}{\partial\eta}+\frac{k}{2}(v_{\mathrm{DM}}+v_{\mathrm{DE}})\right)\\
-3\mathcal{H}&\left(2\delta_{\mathrm{DE}}(\beta+\gamma)+\beta\frac{\bar{\rho}_b}{\bar{\rho}_{\mathrm{DE}}}(\delta_b+\delta_{\mathrm{DE}})+\gamma\frac{\bar{\rho}_{\mathrm{DM}}}{\bar{\rho}_{\mathrm{DE}}}(\delta_{\mathrm{DM}}+\delta_{\mathrm{DE}})\right). \qquad (8.20)
\end{aligned}
$$

The space component

At last, we have the space component for dark energy. This time, we start with the equation for a general w. Then it reads

$$
\begin{aligned}
&(1+w)v_k^{\mathrm{DE}}\frac{\partial\bar{\rho}_{\mathrm{DE}}}{\partial t}+\bar{\rho}_{\mathrm{DE}}\left(\frac{\partial v_k^{\mathrm{DE}}}{\partial t}+w\frac{\partial\delta}{\partial x^k}+(1+w)\left(3Hv_k^{\mathrm{DE}}+\frac{\partial\Psi}{\partial x^k}\right)\right)\\
&=-\frac{3}{2}H(\beta(\bar{\rho}_b+\bar{\rho}_{\mathrm{DE}})(v_k^b+v_k^{\mathrm{DE}})+\gamma(\bar{\rho}_{\mathrm{DE}}+\bar{\rho}_{\mathrm{DE}})(v_k^{\mathrm{DM}}+v_k^{\mathrm{DE}})).
\end{aligned}
$$

We see that when we set $w = -1$ in this equation, a lot of terms cancel - including the term with the time derivative of the dark energy velocity field. This means that we will not get a differential equation for v_k^{DE}, but we will

get an algebraic equation, since v_k^{DE} appears on the right hand side. Setting w to -1, Fourier transforming, and rescaling v to iv/a, we can solve for v_{DE}:

$$v_{\mathrm{DE}} = \frac{2k\delta_{\mathrm{DE}}}{3\mathcal{H}(\beta(\bar{\rho}_b/\bar{\rho}_{\mathrm{DE}}+1)+\gamma(\bar{\rho}_{\mathrm{DM}}/\bar{\rho}_{\mathrm{DE}}+1))} - \left(\beta\left(\frac{\bar{\rho}_b}{\bar{\rho}_{\mathrm{DE}}}+1\right)v_b + \gamma\left(\frac{\bar{\rho}_{\mathrm{DM}}}{\bar{\rho}_{\mathrm{DE}}}+1\right)v_{\mathrm{DM}}\right). \tag{8.21}$$

8.6 Let there be light

Photons play an important role in the evolution of the universe, and so we must see how they behave in our space with a perturbed metric. We will use the Boltzmann equation to see how all the photons in the universe statistically behave. Starting with the phase-space distribution function $f(x^\mu, p^\mu)$, the Boltzmann equation, which we have in Equation 1.17, tells us how the phase-space distribution evolves in time. In its most compact form, it reads

$$\frac{df}{dt} = C[f],$$

where $C[f]$ describes collisions, interactions with other particles. The strategy is to look at the two sides of the Boltzmann equation separately. We start with the left hand side, which tells us how the distribution of photons evolves in our space, with our perturbed metric given in Equation 8.1. This is the same as setting the right hand side to zero. Then we are going to study the collision term, which then will modify the evolution of the phase-space distribution function.

The Boltzmann equation for photons is not directly connected to my interaction model, so all this is well known from before. I will follow a set of lecture notes by Øystein Elgarøy [20] and parts of chapter 4 in Dodelson [17].

8.6.1 Left hand side: photons in a perturbed metric

We start with the left hand side: we expand the total time derivative into partial derivatives, and compute each factor we get. Then we expand the distribution function. First thing first, we have from Equation 1.18

$$\frac{df}{dt} = \frac{\partial f}{\partial t} + \frac{\partial f}{\partial x^i}\frac{dx^i}{dt} + \frac{\partial f}{\partial p}\frac{dp}{dt} + \frac{\partial f}{\partial \hat{p}^i}\frac{d\hat{p}^i}{dt}.$$

Then we go through each term. Starting with the last term, we know that photons follow a Bose-Einstein distribution at the background level, so f is given by

$$f(x^\mu, p^\mu) = \frac{1}{e^{p/T(t)}-1} = f(p, T(t)).$$

We see that f does not depend on the direction of p^μ, and so $\partial f/\partial \hat{p}$ has no zero-order terms. Also, since there are no potential for the photons to fall into at the background level, we have $d\hat{p}/dt = 0$. The conclusion is that the last term in the left hand side of the Boltzmann equation for photons has no zero or first order term, and so we can neglect it right from the start, since we are doing first order perturbation theory.

The other terms however will contribute. For the second term, we can use the kinematic of the photon, where the most important fact is that the photon is massless. When all the manipulations and cancellations are done, we end up with

$$\frac{\partial f}{\partial x^i}\frac{dx^i}{dt} \approx \frac{\partial f}{\partial x^i}\frac{\hat{p}^i}{a},$$

since f is independent of x^i to zeroth order. For the third term, we use the geodesic equation to manipulate with the time derivative of the magnitude of the momentum. One ends up with

$$\frac{dp}{dt} \approx -p\left(\frac{\hat{p}^i}{a}\frac{\partial \Psi}{\partial x^i} - \frac{\partial \Phi}{\partial t} - H\right).$$

Finlay, we need to expand the phase-space distribution function $f(x^\nu, p^\nu)$. We will expand around an average temperature, and so we introduce perturbations in the temperature field, Θ:

$$T(x^\mu, \hat{p}) = T(t)(1 + \Theta(x^\mu, \hat{p})).$$

Manipulating around, one ends up with this expansion:

$$f \approx f_{(0)} - p\frac{\partial f_{(0)}}{\partial p}\Theta.$$

Putting everything together, we get the left hand side of the Boltzmann equation:

$$\frac{df}{dt} \approx -p\frac{\partial f_{(0)}}{\partial p}\left(\frac{\partial \Theta}{\partial t} + \frac{\hat{p}^i}{a}\frac{\partial \Theta}{\partial x^i} + \frac{\partial \Phi}{\partial t} + \frac{\hat{p}^i}{a}\frac{\partial \Psi}{\partial x^i}\right). \tag{8.22}$$

8.6.2 Right hand side: Compton scattering

The collision term on the right hand side of the Boltzmann equation, $C[f]$, is non-zero for photons, since the photons interact with electrons through Compton scattering. Compton scattering is the process

$$e^-(\vec{q}) + \gamma(\vec{p}) \rightarrow e^-(\vec{q'}) + \gamma(\vec{p'}).$$

The collision term $C[f]$ is an integral:

$$C[f] = \frac{1}{8p(2\pi)^5}\int_q\int_{q'}\int_{p'}\frac{|\mathcal{M}|^2}{E_e(q)E_e(q')E_\gamma(p)}$$

$$\cdot\delta^3(\vec{p}+\vec{q}-\vec{p}'-\vec{q}')\delta(E_\gamma(p)+E_e(q)-E_\gamma(p')-E_\gamma(q'))$$
$$\cdot(f_e(\vec{q}')f_\gamma(\vec{p}')-f_e(\vec{q})f_\gamma(\vec{p}))d^3p'd^3q'd^3q.$$

After a lot of manipulations, and inserting Θ, one ends up with

$$C[f] = -p\frac{\partial f_{(0)}}{\partial p}n_e\sigma_T(\Theta_0 - \Theta(\hat{p}) + \hat{p}\cdot\vec{v}_b),$$

where we see the zeroth order expansion of Θ for the first time. It is defined in Equation B.8, with $F = \Theta$ and $l = 0$.

Now we are going to put the two sides together. We will write in terms of conformal time η, defined in Equation 1.10, and the optical depth:

$$\tau(\eta) = \int_\eta^{\eta_0} n_e\sigma_T a d\eta',$$

which we will work more with later. We will also Fourier transform the equation so we get it in terms of the wavenumber k, by using Equation B.6. μ is the angle between $\hat{p}^i$ and $\vec{v}_b$. We end up with

$$\frac{\partial\Theta}{\partial\eta} + ik\mu\Theta + \frac{\partial\Phi}{\partial\eta} + ik\mu\Psi = -\frac{\partial\tau}{\partial\eta}(\Theta_0 - \Theta + \mu v_b). \tag{8.23}$$

This is the Boltzmann equation for photons to first order, written in Fourier space and in terms of the conformal time.

8.7 The return of the Einstein tensor

To get enough equations to work with, we must know how the metric perturbations Ψ and Φ are related to the energy-density perturbations. Einsteins field equations, Equation A.15, gives us this relation. Now, the interaction are set up in such a way that the Einstein equations are unaltered, so there is really not much new in this section. I will follow the lecture notes by Øystein Elgarøy [21] closely, from where the section title is quoted.

From the metric, we can compute the Christoffel symbols. I have already done this, since I needed them to write out the expression for the covariate derivative of the energy-momentum tensor. To recap, they are (to first order

in the perturbations, as usual)

$$\begin{aligned}
\Gamma^0_{00} &\approx \frac{\partial\Psi}{\partial t},\\
\Gamma^0_{0j} = \Gamma^0_{j0} &\approx \frac{\partial\Psi}{\partial x^j},\\
\Gamma^0_{ij} &\approx a^2\delta_{ij}\left(H(1+2(\Phi-\Psi)) + \frac{\partial\Phi}{\partial t}\right),\\
\Gamma^i_{00} &\approx \frac{\delta^{ij}}{a^2}\frac{\partial\Psi}{\partial x^j},\\
\Gamma^i_{j0} = \Gamma^i_{0j} &\approx \delta^i_j\left(H + \frac{\partial\Phi}{\partial t}\right),\\
\Gamma^i_{jk} &\approx \delta_{ij}\frac{\partial\Phi}{\partial x^k} + \delta_{ik}\frac{\partial\Phi}{\partial x^j} - \delta_{jk}\frac{\partial\Phi}{\partial x^i}.
\end{aligned}$$

8.7.1 The Ricci tensor and scalar

The Ricci tensor can be computed using the Christoffel symbols using Equation A.9. The non-zero components are

$$R_{00} = -\frac{3}{a}\frac{d^2a}{dt^2} + \frac{1}{a^2}\frac{\partial^2\Psi}{\partial x^k\partial x_k} - 3\frac{\partial^2\Phi}{\partial t^2} + 3H\left(\frac{\partial\Psi}{\partial t} - 2\frac{\partial\Phi}{\partial t}\right),$$

$$\begin{aligned}
R_{ij} = -\frac{\partial^2}{\partial x^i\partial x^j}(\Phi-\Psi) + \delta_{ij}\left(\left(2a^2H^2 + a\frac{d^2a}{dt^2}\right)(1+2(\Phi-\Psi))\right.\\
\left.+a^2H\left(6\frac{\partial\Phi}{\partial t} - \frac{\partial\Psi}{\partial t}\right) + a^2\frac{\partial^2\Phi}{\partial t^2} - \frac{\partial^2\Phi}{\partial x^k\partial x_k}\right).
\end{aligned}$$

Now the time has come for the Ricci scalar, which we get by contracting the Ricci tensor:

$$\begin{aligned}
\mathcal{R} &= g^{\mu\nu}R_{\mu\nu}\\
&= (-1+2\Psi)\left(-\frac{3}{a}\frac{d^2a}{dt^2} + \frac{1}{a^2}\frac{\partial^2\Psi}{\partial x^k\partial x_k} - 3\frac{\partial^2\Phi}{\partial t^2} + 3H\left(\frac{\partial\Psi}{\partial t} - 2\frac{\partial\Phi}{\partial t}\right)\right)\\
&+\frac{1-2\Phi}{a^2}\left(-\frac{\partial^2}{\partial x^k\partial x_k}(\Phi+\Psi) + 3\left(\left(2a^2H^2 + a^2\frac{d^2a}{dt^2}\right)(1+2(\Phi-\Psi))\right.\right.\\
&\left.\left.+a^2H\left(6\frac{\partial\Phi}{\partial t} - \frac{\partial\Psi}{\partial t}\right) + a^2\frac{\partial^2\Phi}{\partial t^2} - \frac{\partial^2\Phi}{\partial x^k\partial x_k}\right)\right).
\end{aligned}$$

8.7.2 The Einstein tensor

Now that we have the Ricci tensor and the Ricci scalar, we can compute the Einstein tensor by Equation A.11. Now, for the energy momentum tensor, we have always worked with T^μ_ν, and we want to continue with that. Since the energy-momentum tensor is proportional to the Einstein tensor by the

Einstein equation, we need the Einstein tensor with one index upstairs and one index downstairs as well - E^μ_ν. So we can compute $E_{\mu\nu}$ from $R_{\mu\nu}$ and $\mathcal{R}$, which we already have, and then use $g^{\mu\nu}$ to raise one index. We end up with these non-zero components:

$$E^0_0 = -(1+2\Psi)\left(-\frac{3}{a}\frac{d^2a}{dt^2} + \frac{1}{a^2}\frac{\partial^2\Psi}{\partial x^k \partial x_k} - 3\frac{\partial^2\Phi}{\partial t^2} + 3H\left(\frac{\partial\Psi}{\partial t} - 2\frac{\partial\Phi}{\partial t}\right)\right)$$

$$+6\Psi\left(H^2 + \frac{1}{a}\frac{d^2a}{dt^2}\right) + \frac{1}{a^2}\frac{\partial^2\Psi}{\partial x^k\partial x_k} - 3\frac{\partial^2\Phi}{\partial t^2} + 3H\left(\frac{\partial\Psi}{\partial t} - 4\frac{\partial\Phi}{\partial t}\right) + \frac{2}{a^2}\frac{\partial^2\Phi}{\partial x^k\partial x_k},$$

$$E^i_j = g^{i\nu}\left(R_{j\nu} - \frac{1}{2}g_{\nu j}\mathcal{R}\right) = \delta^{ik}\frac{1-2\Phi}{a^2}R_{kj} - \frac{1}{2}\delta^i_j\mathcal{R}$$

$$= A\delta^i_j + \frac{1}{a^2}\frac{\partial^2}{\partial x^i\partial x^j}(\Phi - \Psi).$$

For the spatial components, I have written the Einstein tensor in a way that may appear a little bit strange now, with a factor A which contains a lot of terms. This way of writing E^i_j will be useful later. Now we split E^0_0 into zero and first order terms: $E^0_0 = \bar{E}^0_0 + \delta E^0_0$. The first-order term of E^0_0 is

$$\delta E^0_0 = -6H\frac{\partial\Phi}{\partial t} + 6H^2\Psi + \frac{2}{a^2}\frac{\partial^2\Phi}{\partial x^k\partial x_k}. \tag{8.24}$$

8.7.3 The energy-momentum tensor for photons

The Einstein tensor E^μ_ν is to be related to the energy-momentum tensor T^μ_ν. We already have the energy-momentum tensor for baryons, dark matter and dark energy, but not for photons, since we used the phase-space distribution function f directly when we worked with photons. The energy-momentum tensor is given by the phase-space distribution function in Equation A.12:

$$T^\mu_\nu = g\iiint_P \frac{1}{(2\pi)^3\sqrt{-\det(g_{\alpha\beta})}}\frac{P^\mu P_\nu}{P^0} f dP_1 dP_2 dP_3.$$

The determinant of the metric is easy to find, since the metric we use is diagonal in our gauge:

$$\det(g_{\alpha\beta}) \approx -a^6(1+2\Psi+6\Phi).$$

For photons, the degeneracy g is 2, and from the computations around the Botlzmann equation, we found

$$P_0 = -p(1+\Psi), \qquad P_i = ap\hat{p}^i(1+\Phi),$$

which gives us

$$T^0_0(\gamma) = -\frac{2}{(2\pi)^3}\int_P p f(x^\mu, P^\mu) d^3p.$$

Using our Taylor expansion for the phase-space distribution function f,

$$f \approx f_{(0)} - p\frac{\partial f_{(0)}}{\partial p}\Theta,$$

we simply get

$$T_0^0(\gamma) = -\bar{\rho}_\gamma(1 + 4\Theta_0).$$

Now that we have the energy-momentum tensor for all our components, we can find the Einstein equations.

8.7.4 The Einstein equations: space and the energy within

Now that we have both sides of the Einstein equation, the time has come to put them together. As usual, some terms will be of zeroth order and some of first order, and they make one equation each. The zeroth-order equation is just the first Firedmann-equation again, Equation 1.6 for the time component. The first order equation is

$$\delta E_0^0 = 8\pi G\delta T_0^0 \Rightarrow -6H\frac{\partial\Phi}{\partial t} + 6H^2\Psi + \frac{2}{a}\frac{\partial^2\Phi}{\partial x^k\partial x_k}$$

$$= -8\pi G(4(\bar{\rho}_\gamma\Theta_0 + \bar{\rho}_b\delta_b + \bar{\rho}_{\rm DM}\delta_{\rm DM} + \bar{\rho}_{\rm DE}\delta_{\rm DE}).$$

Using conformal time and Fourier transforming the equation, we end up with

$$k^2\Phi + 3\mathcal{H}\left(\frac{\partial\Phi}{\partial\eta} - \mathcal{H}\Psi\right)$$

$$= -4\pi G(4(\bar{\rho}_\gamma\Theta_0 + \bar{\rho}_b\delta_b + \bar{\rho}_{\rm DM}\delta_{\rm DM} + \bar{\rho}_{\rm DE}\delta_{\rm DE}). \tag{8.25}$$

Now we go to the space components. We start by Fourier transforming our expression for E_j^i:

$$E_j^i = A\delta_j^i + \frac{k^ik_j}{a^2}(\Phi + \Psi).$$

Now we are going apply a projection operator on E_j^i:

$$\left(\hat{k}_i\hat{k}^j - \frac{1}{3}\delta_i^j\right)E_j^i = \frac{2k^2}{3a^2}(\Phi + \Psi),$$

where the A-term has gone away. Now we also need to let this projection operator act on T_j^i. We have

$$\left(\hat{k}_i\hat{k}^j - \frac{1}{3}\delta_i^j\right)\hat{p}^i\hat{p}_j = \frac{3}{2}\mathcal{P}_2(\mu).$$

with $\mu = \hat{k} \cdot \hat{p}$, and $\mathcal{P}_2(\mu)$ is the second order Legendre polynomial with argument μ. We then have

$$\left(\hat{k}_i\hat{k}^j - \frac{1}{3}\delta_i^j\right) T_j^i = \frac{g}{(2\pi)^3}\int_P \frac{2}{3}\mathcal{P}_2(\mu)\frac{p^2}{E}f(x^\mu, P^\mu)d^3p.$$

This is non-zero only for photons, since $T_j^i = 0$ for baryonic matter and dark matter, and $T_j^i \propto \delta_j^i$ for dark energy. In the end, the space component of the Einstein equation is

$$k^2(\Phi + \Psi) = -32\pi G a^2 \bar{\rho}_\gamma \Theta_2. \tag{8.26}$$

8.8 Some last pieces

Now we have gone through the energy-momentum conservation equations for baryons, dark matter and dark energy, we have seen the Boltzmann equation for photons, and we have looked at the Einstein equations. There are still a few things left: Polarization will have a small contribution in the Boltzmann equation for photons, the perturbations in the photon temperature Θ must be expanded in to multipoles, and we will look at the term for Compton scattering that enters the equations for the baryons.

8.8.1 Polarization

Polarization of the photon field has to be taken account for. I will do it the simple way by adding polarization contribution through Θ_2 in the Boltzmann equation for photons. With this modification, Equation 8.23 takes this form:

$$\frac{\partial\Theta}{\partial\eta} + ik\mu\Theta + \frac{\partial\Phi}{\partial\eta} + ik\mu\Psi = -\frac{\partial\tau}{\partial\eta}\left(\Theta_0 - \Theta + \mu v_b - \frac{1}{2}\mathcal{P}_2(\mu)\Theta_2\right), \tag{8.27}$$

where $\mathcal{P}_2(\mu) = 1/2(3\mu^2 - 1)$ is the second order Legendre polynomial, which we can get from Equation B.7. See [17], chapter 10 for more details.

8.8.2 Multipole expansion of the temperature perturbations

We have seen multiple examples already on the multipole expansion of the radiation field Θ_l for photons. In the Boltzmann equation, the zeroth order multipoles - the monopoles, came in, and in Equations 8.26 and 8.27, the second order multipole moment, the quadrupole, came in. In this section, we will expand all Θ into multipoles, so only Θ_l will enter our equations - not Θ. The Legendre expansion is given by Equation B.8, and we will also use the recursion relation in Equation B.9. to find the higher order moments in terms of the lower ones. Using the zeroth and first order Legendre polynomials and integrating, we get these two equations for Θ_0 and Θ_1:

$$\frac{\partial\Theta_0}{\partial\eta} + k\Theta_1 = -\frac{\partial\Phi}{\partial\eta},$$

$$\frac{\partial\Theta_1}{\partial\eta} - \frac{k}{3}\Theta_0 + \frac{2k}{3}\Theta_2 = \frac{k}{3}\Psi + \frac{\partial\tau}{\partial\eta}\left(\Theta_1 + \frac{1}{3}v_b\right). \tag{8.28}$$

For the higher moments ($l \geq 2$), we have

$$\frac{\partial\Theta_l}{\partial\eta} - \frac{lk}{2l+1}\Theta_{l-1} + \frac{k(l+1)}{2l+1}\Theta_{l+1} = \frac{\partial\tau}{\partial\eta}\left(\Theta_l - \frac{\Theta_2}{10}\delta_{l,2}\right). \tag{8.29}$$

Now we can see a general problem that we will have if we are going to solve this numerically - the equation for every moment depends on the moment above. This is solved pretty simply by setting a cut-off value for l. We will come back to this in the next chapter.

8.8.3 Compton scattering

In addition to interactions with dark matter and dark energy through our interaction models, the baryons also interact with the photons through Compton scattering. We have seen this all the time when working with the photons, but we must also include this the other way, by adding a collision term in the equation for the baryons. We have two equations for baryons - one time component, Equation 8.16, which tells us how the energy-density perturbation evolves, and one space component, Equation 8.17, which tells us how the velocity perturbation evolves in time. Due to symmetry, we only get a non-zero interaction term in the space component equation. With this interaction term, the space-component of the interaction equation for baryons takes this form:

$$\frac{\partial v_b}{\partial\eta} = -v_b - \frac{k}{\mathcal{H}}\Psi + \frac{\partial\tau}{\partial\eta}\frac{4\bar{\rho}_\gamma}{3\bar{\rho}_b}\left(3\Theta_1 + v_b\right)$$

$$+3\left(\alpha\left(1 + \frac{\bar{\rho}_{\mathrm{DM}}}{\bar{\rho}_b}\right)\frac{3v_b + v_{\mathrm{DM}}}{2} + \beta\left(1 + \frac{\bar{\rho}_{\mathrm{DE}}}{\bar{\rho}_b}\right)\frac{3v_b + v_{\mathrm{DE}}}{2}\right). \tag{8.30}$$

8.9 In the beginning, there was ϕ

In this section, I will set up the initial conditions to our set of differential equations. I will neglect the interactions models here to make matters simpler (I will defend this later), and set up the initial conditions according to the ΛCDM model. This is then all done before, and I will follow the lecture notes by Øystein Elgarøy [22] (from which again, the section title is quoted) and Dodelson [17].

The first question is what time we are to set our initial conditions at. We can not set them at big bang (cosmic time $t = 0$), because we do not know the physics of that event. But we will choose a time in the very early universe, so early that a chosen wave number times conformal time η is way smaller than 1. This will of course depend on the chosen wavenumber, so we

will choose the η that fullfills this for the largest interesting wavenumber. We will come back to specific quantities later, but now we can state that we will set initial conditions to length scales that are way larger than the particle horizon. We then know that the distribution of photons is very smooth, and we will only consider the monopole contribution, so $\Theta \approx \Theta_0$. Also in this era, the universe is radiation dominated, and the Friedmann equations then tells us that $\eta \propto a$.

Using $k\eta \ll 1$ and $\Theta \approx \Theta_0$, we can simplify Equation 8.23 to this:

$$\frac{\partial \Theta_0}{\partial \eta} = -\frac{\partial \Phi}{\partial \eta}.$$

For the energy-density perturbations, the δ's, we simplify Equations 8.16 on page 95, 8.18 on page 96 and 8.20 on page 97 to this:

$$\frac{\partial \delta_b}{\partial \eta} = \frac{\partial \delta_{\mathrm{DM}}}{\partial \eta} = -3\frac{\partial \Phi}{\partial \eta},$$

$$\frac{\partial \delta_{\mathrm{DE}}}{\partial \eta} = -3(1+w)\frac{\partial \Phi}{\partial \eta}.$$

The velocities are comparable to the first order moments Θ, and so we can set

$$v^b = v^{\mathrm{DM}} = 0$$

since we are only keeping Θ_0. Now we take a closer look at Equation 8.25: We can neglect the $k^2\Phi$ term since it contains k^2, and we can neglect the terms with contributions from baryons, dark matter and dark energy, since the universe is radiation dominated in the epoch we work with now. So this equations first simplifies to

$$3\mathcal{H}\left(\frac{\partial \Phi}{\partial \eta} - \mathcal{H}\Psi\right) = 16\pi G a^2 \bar{\rho}_r \Theta_0$$

In the radiation dominated epoch, we have $\mathcal{H} = 1/\eta$. We use the first Friedmann equation, Equation 1.6, to relate η to the background energy-density of radiation:

$$\frac{1}{\eta^2} = \frac{8\pi G}{3}\bar{\rho}_r a^2.$$

We then have

$$\frac{1}{\eta}\frac{\partial \Phi}{\partial \eta} - \frac{\Psi}{\eta^2} = \frac{2\Theta_0}{\eta}$$

Next, we differentiate with respect to η and re-organize the terms, which gives us

$$\eta\frac{\partial^2 \Phi}{\partial \eta^2} + 3\frac{\partial \Phi}{\partial \eta} - \frac{\partial \Psi}{\partial \eta} = 0.$$

The second Einstein equation, Equation 8.26, is now

$$k^2(\Phi - \Psi) = -32\pi G a^2 \bar{\rho}_r \Theta_2 \approx 0,$$

since we neglect higher order moments of Θ. This equations gives us $\Psi \approx -\Phi$, and our second order differential equation reads

$$\eta \frac{\partial^2 \Phi}{\partial \eta^2} + 4\frac{\partial \Phi}{\partial \eta} = 0.$$

This equation has a solution on the form $\Phi = \eta^p$, and the equation then gives

$$p(p+3) = 0.$$

The solution $p = -3$ corresponds to a quickly dying mode, so we are interested in the $p = 0$ solution. This corresponds to a constant mode. Then we get

$$\frac{\partial \Phi}{\partial \eta} = 0 \Rightarrow \Phi = -\Psi = 2\Theta_0.$$

Since Φ is constant, Θ_0 is also a constant. And so we have $\Phi(k, \eta_i) = 2\Theta_0(k, \eta_i)$ for an initial conformal time η_i. Moving on to the energy-density fluctuations:

$$\frac{\partial \delta_b}{\partial \eta} = \frac{\partial \delta_{\mathrm{DM}}}{\partial \eta} = 3\frac{\partial \Theta}{\partial \eta}$$

Which means that $\delta_b(k, \eta_i) = \delta_{\mathrm{DM}}(k, \eta_i) = 3\Theta_0$ plus a constant of integration. We will work with adiabatic initial conditions, which are favored by observations, and this means that this constant of integration is zero. For dark energy, we get a similar expression:

$$\frac{\partial \delta_{\mathrm{DE}}}{\partial \eta} = 3(1+w)\Theta_0 \Rightarrow \delta_{\mathrm{DE}}(k, \eta_i) = 3(1+w)\Theta_0$$

We move on to the velocity perturbations. The terms with k must now be accounted for again - if not, we will just get zero everywhere, and then the equations are useless. For baryons and dark matter, $v = v_b$ and $v = v_{\mathrm{DM}}$, we have

$$\frac{\partial v}{\partial \eta} + \mathcal{H} v = -ik\Psi.$$

Since the universe is radiation-dominated at the time epoch we work with now, we have $\mathcal{H} = 1/\eta$. Combined with $\Psi = -\Phi$, we have

$$\frac{\partial v}{\partial \eta} + \frac{v}{\eta} = ik\Phi$$

We multiply with η and use the product rule on the left hand side:

$$\frac{\partial}{\partial \eta}(nv\eta) = ik\Phi\eta.$$

Now we integrate and divide by η, reinset $\eta = 1/\mathcal{H}$, and set up our initial conditions:

$$v_b(k, \eta_i) = v_{\mathrm{DM}}(k, \eta_i) = \frac{ik\Phi}{2\mathcal{H}}$$

Now for the multipole expansion of the radiation field, Θ_l. We know the initial condition for Θ_0. We use the recursion relation for the Legendre polynomials, Equation B.9, and the quantity ϵ to express Θ_{l+1} in terms of Θ_l, when $l \geq 1$:

$$\epsilon = \frac{k}{\mathcal{H}\dot{\tau}},$$

where $\dot{\tau}$ is the optical depth differentiated with respect to the conformal time, which we will look more at later. First, the initial condition for Θ_1 is

$$\Theta_1(k, \eta_i) = -\frac{k}{6\mathcal{H}}\Phi.$$

Early on, the optical depth (and also its derivative) will be very large, and so the number ϵ will be very small. The number ϵ can therefore be used as an expansion parameter for Θ_l when $l \geq 1$: $\Theta_{l+1} \approx \epsilon\Theta_l$. The initial conditions for Θ_l when $l > 2$ are then

$$\Theta_2 = -\frac{20k}{45\mathcal{H}\dot{\tau}}\Theta_1,$$

$$\Theta_l = \frac{l}{2l+1}\Theta_{l-1}, \quad l > 2.$$

Now our initial conditions are ready. We set an initial conformal time η_i:

$$\delta_b(k, \eta_i) = \delta_{\mathrm{DM}}(k, \eta_i) = 3\Theta_0(k, \eta_i), \tag{8.31}$$

$$\delta_{\mathrm{DE}}(k, \eta_i) = 3(1+w)\Theta_0(k, \eta_i), \tag{8.32}$$

$$v_b(k, \eta_i) = v_{\mathrm{DM}}(k, \eta_i) = -\frac{k\Phi}{2\mathcal{H}}, \tag{8.33}$$

$$\Theta_0(k, \eta_i) = \frac{1}{2}\Phi(k, \eta_i), \tag{8.34}$$

$$\Theta_1(k, \eta_i) = -\frac{k}{6\mathcal{H}}\Phi, \tag{8.35}$$

$$\Theta_2 = -\frac{20k}{45\mathcal{H}\dot{\tau}}\Theta_1, \tag{8.36}$$

$$\Theta_l = \frac{l}{2l+1}\Theta_{l-1}, \quad l > 2. \tag{8.37}$$

Now, what physical mechanism sets up these initial conditions? The answer lies in the concept of inflation, and our best model for inflation is a scalar field ϕ that leaks energy. However, we do not get any useful equations for this thesis if we go further on, so I will not go anymore into inflation here. But there lies the explanation to the section title.

Remember that I have neglected the interaction models when I have set the initial conditions. This will of course have some consequences, but trial and errors shows that the solutions will converge towards the true solutions, independent of the initial conditions - if they do not deviate a lot from the ΛCDM model, of course. I will come back to this when we are looking at the results.

Chapter 9

Numerical simulations of structure formations

In the last chapter, we set up the equations for the perturbations in the metric tensor and the energy-densities, using the energy-momentum conservation equation (this is where our interaction model entered), the Einstein equation and the Boltzmann equation. The perturbation in the temperature field for photons were expanded into multipoles, and we have set initial conditions to our equations. Fourier transforming our equations turned partial differential equations into an infinite number of ordinary differential equations.

In this chapter, we will solve our set of equations. Before we do that, some of the equations will have to be rewritten, due to limitations (multipole moments) and numerical instabilities (tight coupling). We will start with this. Then we will go through the whole recipe for the numerical simulations, going from our theoretical setup from the last chapter with the modifications, and the background quantities we have been working on earlier, through the recombination area and all the way to the solution of our equation system. Then we will look at results we get along the way, and compare these to the ΛCDM model, where none of my interactions are present.

9.1 Preparations

Before we can start simulating, there are a set of preparations we must do. We need to put some limitations on our multipole expansion, and we must look at some numerical instabilities that we will run into. There are quantities in the background universe we must look at, and we must study some detailed physics that took place during recombination. In the theoretical work we did in the previous chapter, we started out with cosmic time t, and then we changed to conformal time η. The conformal time will still pop up a few places, but from now on, we will use the number of e-foldings $N = \ln a$ as our time variable, which will give us more accurate results when

we integrate.

9.1.1 The background universe

In the background universe, there are some quantities that we need as a function of N: the density parameters $\{\Omega_b, \Omega_{\rm DM}, \Omega_{\rm DE}, \Omega_r\}$, the conformal time η, the Hubble parameter H, the scaled Hubble parameter $\mathcal{H} = Ha$ and its derivative $\mathcal{H}'$ with respect to N. For the density parameters, we go back to Equation 2.16, and for the Hubble parameter, we use Equation 2.17. The scaled Hubble parameter $\mathcal{H} = Ha$ is given by this differential equation:

$$\frac{d\mathcal{H}}{dN} = e^N \left(H + \frac{dH}{dN} \right), \tag{9.1}$$

and the conformal time η is given by this differential equation:

$$\frac{d\eta}{dN} = \frac{1}{e^N H}. \tag{9.2}$$

9.1.2 Recombination

In the early universe, the temperature was so high that the electrons and photons were tightly coupled together. Today, they are not, which means that at some point, things changed. The time the photons and electrons decoupled is called recombination. At this time, the temperature had decreased to a point where the protons and electrons could form neutral atoms without the photons destroying them over and over again. Since there were so many more photons than baryons, recombination did not occur until the temperature of the universe had cooled down to 3000K. Now the photons were free to move as far as they wanted to, so the universe became transparent, and the cosmic microwave background was created.

In this section, I will go through some important points from the physics of recombination, since we will integrate our equations through this era. What we really need to know is the optical depth $\tau(\eta)$, which we have seen before:

$$\tau(\eta) = \int_{\eta}^{\eta_0} n_e \sigma_T a d\eta'. \tag{9.3}$$

From these definitions, we can set up these two useful expression with τ:

$$\frac{d\tau}{d\eta} = -n_e \sigma_T a \qquad \frac{d\tau}{dx} = -\frac{n_e \sigma_T a}{\mathcal{H}}$$

In these equations, a is the scale factor as we know from before, n_e is the electron number density, and σ_T is the Thomson scattering cross section:

$$\sigma_T = \frac{8\pi\alpha^2}{3m_e^2},$$

where α is the hydrogen fine structure constant, and m_e is the electron mass. The Thomson scattering cross section is a constant, and we get the scale factor a through the Friedmann equations. The problem is the electron number density, which is dramatically changed during recombination. We start by defining the free electron fraction:

$$X_e = \frac{n_e}{n_H} = \frac{n_e}{n_b}, \tag{9.4}$$

where we have ignored helium, setting the proton number density equal to the hydrogen number density. If we also ignore the small mass difference between neutral hydrogen and free protons, we have

$$n_H = n_b \approx \frac{\bar{\rho}_b}{m_H} = \frac{\Omega_b \rho_c}{m_H a^3}, \quad \rho_c = \frac{3H_0^2}{8\pi G},$$

where ρ_c is the critical energy-density of the universe. Before recombination, the universe is completely ionized, so $X_e = 1$, and $n_e \propto a^{-3}$. After recombination, the universe is almost completely neutral, so $X_e \ll 1$. So our questions is how X_e changes during recombination. When the change in X_e goes slowly, we can use the Saha equation, which is an algebraic equation:

$$\frac{X_e^2}{1 - X_e} \approx \frac{1}{n_b} \left(\frac{m_e T_b}{2\pi} \right)^{\frac{3}{2}} e^{\frac{\epsilon_0}{T_b}}. \tag{9.5}$$

When we do our numerical simulations, we will use the Saha equation when $X_e \geq 0.99$. When $X_e < 0.99$, we will use the Peebles equation:

$$\frac{dX_e}{dN} = \frac{C_r(T_b)}{H} \left(\beta(T_b)(1 - X_e) - n_H \alpha^{(2)}(T_b) X_e^2 \right). \tag{9.6}$$

See [17] for more details about the Saha equation and the Peebles equation. Now, we need the baryon temperature T_b. This is given by a differential equation that couples to X_e, but it is a good approximation to just set it equal to the photon temperature:

$$T_b \approx T_\gamma = \frac{T_0}{a}, \quad T_0 = 2.725 \text{ K}.$$

As mentioned, we expect X_e to be equal to 1 before recombination, and during recombination, it will decrease and approach zero (but it will always be greater than zero). Later on, it will actually rise towards 1 again, and today, the universe is more or less ionized again. This is due to star formation, and most of the electrons today are in stars. This process is called re-ionization. We will not take re-ionization into account, and so we will expect X_e to approach zero after recombination.

When we have X_e, we also have n_e, and we can compute the optical depth, which tells us how transparent the universe is. And when we have

the optical depth (and its first order derivative), we can compute *the visibility function* g. We define it and scale it like this:

$$g(\eta) = g(N) = -\mathcal{H}\tau' e^{-\tau(N)}$$

$$\tilde{g} = -\tau' e^{-\tau(N)} = \frac{g(N)}{\mathcal{H}(N)}. \tag{9.7}$$

The scaled version is what we will use in our simulations. The visibility function is normalized:

$$\int_0^{\eta_0} g(\eta) d\eta = \int_{-\infty}^{0} \tilde{g}(N) dN = 1,$$

and so we can use it as a probability distribution. $\tilde{g}(N)$ is then the probability that a given photon were last scattered at time N. We expext $\tilde{g}$ to have a peak around redshift $z = 1100$, the redshift of recombination.

9.1.3 An l above all else

Looking back at Equation 8.29, we see that in order to find the evolution of Θ_l, we need to know the evolutions for both Θ_{l-1} and Θ_{l+1}. We can not solve for an infinite number of multipoles, and so we must find a cutoff value for l. For large l, the time dependence of $\Theta_l(k, \eta)$ can be approximated by the spherical Bessel functions, as discussed in [23]:

$$\lim_{l \to \infty} \Theta_l(k, \eta) = j_l(k\eta)$$

Using a recurrence relation for the spherical Bessel functions, Equation B.11, we get

$$\Theta_{l+1} \approx \frac{2l+1}{k\eta}\Theta_l(k, \eta) - \Theta_{l-1}(k, \eta), \quad l = l_m.$$

Putting this into Equation 8.29, with N as our free variable, we get

$$\frac{\partial \Theta_l}{\partial N} \approx \frac{k}{\mathcal{H}}\Theta_{l-1} - \left(\frac{l+1}{\mathcal{H}\eta(N)} - \frac{\partial \tau}{\partial N}\right)\Theta_l, \quad l = l_m. \tag{9.8}$$

Previous testings of this shows that the low value $l_m = 6$ is actually a good cutoff value for l. See [24] for more details.

9.1.4 Tight coupling

Early on, when the photons and baryons were tightly coupeled to each other, the optical depth, and also its derivative, was very large. This time epoch is called tight coupling, and there is a numerical instability in the tight

coupling regime that we must take care of. When written in terms of N, the differential equation for Θ_1 takes this form:

$$\frac{\partial\Theta_1}{\partial N} = \Theta_1' = \frac{k}{3\mathcal{H}}\Theta_0 - \frac{2k}{3\mathcal{H}}\Theta_2 + \frac{k\Psi}{3\mathcal{H}} + \tau'\left(\Theta_1 + \frac{v_b}{3}\right)$$

Early on, the quantity in the brackets, $\Theta_1 + v_b/3$, is very small, and this is to be multiplied with τ', which, as mentioned, is very large. This can cause a numerical instability. To solve this, we expand $3\Theta_1 + v_b$ in powers of $1/\tau'$. We define R as $4\bar{\rho}_r/3\bar{\rho}_b$. Then we set up a parameter q:

$$q = \frac{-((1-2R)\tau' + (1+R)\tau'')(3\Theta_1 + v_b) - \frac{k\Psi}{\mathcal{H}}}{(1+R)\tau' + \mathcal{H}'/\mathcal{H} - 1}$$

$$+\frac{(1+\frac{\mathcal{H}'}{\mathcal{H}})\frac{k}{\mathcal{H}}(2\Theta_2 - \Theta_0) - \frac{k}{\mathcal{H}}\Theta_0'}{(1+R)\tau' + \mathcal{H}'/\mathcal{H} - 1}. \tag{9.9}$$

In terms of q, we can write v_b' like this:

$$v_b' = \frac{1}{1+R}\left(-v_b - \frac{k}{\mathcal{H}}\Psi + R\left(q + \frac{k}{\mathcal{H}}\left(2\Theta_2 - \Theta_0\right) - \frac{k}{\mathcal{H}}\Psi\right)\right).$$

With q and v_b', the differential equation for Θ_1 during the tight coupling regime can be written like this:

$$\Theta_1' = \frac{q - v_b'}{3}. \tag{9.10}$$

With this "new" differential equation for Θ_1 and our modified multipole expansion, we have obtained our modifications for the tight coupling regime. For the higher order moments, it is a good approximation to set $\Theta_l' = 0$ when $l \geq 2$. Therefore, we just use the initial conditions through the whole tight coupling for these moments.

We now need to state when the tight coupling regime is. A good estimate is to set that if

$$\left|\frac{k}{\mathcal{H}\tau'}\right| < \frac{1}{10} \quad \text{and} \quad |\tau'| > 10, \tag{9.11}$$

we use the tight coupling equations. Also, when we reach the start of the recombination era, we switch to the full set of equations, even if the above conditions gives a later time.

9.2 The true final form of our differential equations

As the title says, I am now going to present the true final form of our differential equations, which are to be put straight into our program for numerical simulations. From our theoretical setup to the final form, we have

- Changed the free variable from conformal time η to the e-fold number $N = \ln a$.
- Expanded Θ into multipoles, using the Legendre expansion.
- Set a cutoff value at $l_m = 6$ for the multipole expansions, since the equation for one multipole depends on the one above and the one below.
- Explored numerical instabilities in the tight coupling regime, where we have taken care of a numerical instability with a large τ', and modified the multipole expansion for Θ.
- Set the equation of state parameter w for dark energy to -1.
- For the Einstein equations, we use the density-parameters Ω in stead of the energy-densities ρ.
- We set the initial condition for Φ to 1, since we are not interested in the physical values of our quantities, we will only compare our interaction models to the ΛCDM model.
- To save some writing, we define these rations as well:

$$R_{b,\mathrm{DM}} = \frac{\bar{\rho}_b}{\bar{\rho}_{\mathrm{DM}}} \quad R_{b,\mathrm{DE}} = \frac{\bar{\rho}_b}{\bar{\rho}_{\mathrm{DE}}} \quad R_{\mathrm{DM,DE}} = \frac{\bar{\rho}_{\mathrm{DM}}}{\bar{\rho}_{\mathrm{DE}}}.$$

9.2.1 Full equation set

In its final form, our complete set of equations outside the tight coupling regime looks like this:

$$\Theta_0' = -\frac{\Theta_1}{\mathcal{H}} - \Psi'.$$

$$\Theta_1' = \frac{k}{3\mathcal{H}}\Theta_0 - \frac{2k}{3\mathcal{H}}\Theta_2 + \frac{k}{2\mathcal{H}}\Psi + \tau'\left(\Theta_1 + \frac{v_b}{3}\right).$$

$$\Theta_l' = \frac{lk}{(2l+1)\mathcal{H}}\Theta_{l-1} - \frac{(l+1)k}{(2l+1)\mathcal{H}}\Theta_{l+1} + \tau'\left(\Theta_l - \frac{\Theta_l}{10}\delta_{l,2}\right), \quad l \in [2, l_m).$$

$$\Theta_l' = \frac{k}{\mathcal{H}}\Theta_{l-1} - \frac{l+1}{\mathcal{H}\eta(N)}\Theta_l + \tau'\Theta_l, \quad l = l_m.$$

$$\delta_b' = \frac{k}{\mathcal{H}}v_b - 3\Phi'$$

$$-3\left(2\delta_b(\alpha+\beta) + \alpha R_{b,\mathrm{DM}}^{-1}(\delta_b + \delta_{\mathrm{DM}}) + \beta R_{b,\mathrm{DE}}^{-1}(\delta_b + \delta_{\mathrm{DE}})\right)$$

$$+\alpha\left(1 + R_{b,\mathrm{DM}}^{-1}\right)\left(3\Phi' - \frac{k}{2\mathcal{H}}(v_b + v_{\mathrm{DM}})\right)$$

$$+\beta\left(1 + R_{b,\mathrm{DE}}^{-1}\right)\left(3\Phi' - \frac{k}{2\mathcal{H}}(v_b + v_{\mathrm{DE}})\right).$$

$$v_b' = -v_b - \frac{k}{\mathcal{H}}\Psi + \tau' R(3\Theta_1 + v_b)$$
$$-\alpha(1 + R_{b,\mathrm{DM}}^{-1})\frac{3v_b + v_{\mathrm{DM}}}{2}.$$
$$\delta_{\mathrm{DM}}' = \frac{k}{\mathcal{H}}v_{\mathrm{DM}} - 3\Phi'$$
$$-3\left(2\delta_{\mathrm{DM}}(\gamma - \alpha) - \alpha R_{b,\mathrm{DM}}(\delta_b + \delta_{\mathrm{DM}}) + \gamma R_{\mathrm{DM,DE}}^{-1}(\delta_{\mathrm{DM}} + \delta_{\mathrm{DE}})\right)$$
$$-\alpha(R_{b,\mathrm{DM}} + 1)\left(3\Phi' - \frac{k}{2\mathcal{H}}(v_b + v_{\mathrm{DM}})\right)$$
$$+\gamma(1 + R_{\mathrm{DM,DE}}^{-1})\left(3\Phi' - \frac{k}{2\mathcal{H}}(v_{\mathrm{DM}} + v_{\mathrm{DE}})\right).$$
$$v_{\mathrm{DM}}' = -v_{\mathrm{DM}} - \frac{k}{\mathcal{H}}\Psi - 3\alpha(R_{b,\mathrm{DM}} + 1)\frac{v_b + 3v_{\mathrm{DM}}}{2}.$$
$$\delta_{\mathrm{DE}}' = +3(2\delta_{\mathrm{DE}}(\beta + \gamma) + \beta R_{b,\mathrm{DE}}(\delta_b + \delta_{\mathrm{DE}}) + \gamma R_{\mathrm{DM,DE}}(\delta_{\mathrm{DM}} + \delta_{\mathrm{DE}}))$$
$$-\beta(R_{b,\mathrm{DE}} + 1)\left(3\Phi' - \frac{k}{2\mathcal{H}}(v_b + v_{\mathrm{DE}})\right)$$
$$-\gamma(R_{\mathrm{DM,DE}} + 1)\left(3\Phi' - \frac{k}{2\mathcal{H}}(v_{\mathrm{DM}} + v_{\mathrm{DE}}\right).$$
$$v_{\mathrm{DE}} = \frac{2k\delta_{\mathrm{DE}}}{3\mathcal{H}(\beta(R_{b,\mathrm{DE}} + 1) + \gamma(R_{\mathrm{DM,\ DE}} + 1))}$$
$$-\left(\beta\left(R_{b,\mathrm{DE}} + 1\right)v_b + \gamma\left(R_{\mathrm{DM,\ DE}} + 1\right)v_{\mathrm{DM}}\right).$$
$$\Phi' = \Psi - \frac{k^2}{3\mathcal{H}^2}\Phi + \frac{H_0^2}{2\mathcal{H}^2}\left(\Omega_b\delta_b + \Omega_{\mathrm{DM}}\delta_{\mathrm{DM}} + \Omega_{\mathrm{DE}}\delta_{\mathrm{DE}} + 4\Omega_r\Theta_0\right).$$
$$\Psi = -\Phi - \frac{12H_0^2}{k^2a^2}\Omega_{r0}\Theta_2.$$

The initial conditions comes from Equation 8.37:

$$\Phi = 1.$$
$$\delta_b = \delta_{\mathrm{DM}} = \frac{3}{2}\Phi, \qquad \delta_{\mathrm{DE}} = \frac{3(1+w)}{2}\Phi.$$
$$v_b = v_{\mathrm{DM}} = \frac{k}{2\mathcal{H}}\Phi.$$
$$\Theta_0 = \frac{1}{2}\Phi, \quad \Theta_1 = -\frac{k}{6\mathcal{H}}\Phi, \quad \Theta_2 = -\frac{8k}{15\mathcal{H}\tau'}\Theta_1, \quad \Theta_l = -\frac{l}{2l+1}\frac{k}{\mathcal{H}\tau'}\Theta_{l-1}.$$

9.2.2 Tight coupling

In the tight coupling regime, we will have some modifications. The equations for Θ_1 and v_b are modified, using the parameter q from Equation 9.9:

$$v_b' = \frac{1}{1+R}\left(-v_b - \frac{k}{\mathcal{H}}\Psi + R\left(q + \frac{k}{\mathcal{H}}\left(2\Theta_2 - \Theta_0\right) - \frac{k}{\mathcal{H}}\Psi\right)\right),$$

$$\Theta_1' = \frac{q - v_b'}{3}.$$

For the higher order moments of Θ, we just use the initial conditions:

$$\Theta_2 = -\frac{8k}{45\mathcal{H}\tau'}\Theta_1 \quad \Theta_l = -\frac{lk}{(2l+1)\mathcal{H}\tau'}\Theta_{l-1}.$$

9.3 Simulations

Now we are ready to actually start the simulations. The simulations are divided into three steps: the background universe, recombination, and structure evolution. After the simulations are set up, we must set values for our interaction parameters, and this is done in the end.

9.3.1 The background universe

We start with the background universe, by setting up a N grid from the start of recombination at $N = -7.39658$ (redshift $z = 1630.4$) and to the end of recombination at $N = -6.4220$ (redshift $z = 614.2$), with a 200 points resolution. Then we continue to today, $N = 0$, with 300 points resolution. This is the grid we will use when we display our results. But to compute them, we must actually start a lot earlier, at $N = -23.0259$, far into the radiation dominated era. In this grid, we compute the energy-density parameters Ω from Equation 2.16 and the Hubble parameter H from Equation 2.17. Now we can easily compute the scaled Hubble parameter $\mathcal{H}$ and its derivative $\mathcal{H}'$ from Equation 9.1. When we have the Hubble parameter, we can compute the conformal time using Equation 9.2. Note that when we compute the density parameters and the Hubble parameter, we set initial conditions today, at $N = 0$, and we integrate backwards. We use the ΛCDM values for the density parameters and Hubble parameter as initial conditions, so $\Omega_b(N=0) = 0.046, \Omega_{\mathrm{DM}}(N=0) = 0.224, \Omega_r(N=0) = 8.3{\cdot}10^{-5}$, and $\Omega_{\mathrm{DE}}(N=0) = 0.7299$, which is one minus the sum of the three others. $H(N=0) = H_0 = 70$ km/s/Mpc. When we compute the conformal time η, we set initial condition $\eta(N=-23.0259) = H_0\sqrt{\Omega_r(N=0) * a^{-10}}$, since we assume that the universe is radiation dominated that early, and we neglect our interaction models and use ΛCDM. Next, we use a cubic spline,

so that when we later need to know any of these quantities at a time N that is not in our grid, we use a cubic spline method to interpolate to our point using a third degree polynomial. The routine that does these computations was given to me by an earlier lecturer, and I will not go into more details about those.

9.3.2 Recombination

Next, we look at recombination. We set up another grid over N that runs through recombination (from -7.3966 to -6.4220), using 1000 points. We are going to compute the free electron fraction, defined in Equation 9.4 in our recombination grid. The initial condition is $X_e(N = -7.3966) = 1$ - the universe is completely ionized before recombination. Then we use the Saha Equation 9.5, which is algebraic, when $X_e \geq 0.99$. When $X_e < 0.99$, we use the Peebles Equation 9.6, which is a differential equation. When we have the free electron fraction, we can compute the electron number density, the optical depth τ and its first and second derivative, Equation 9.3, and the visibility function g and its first and second derivative, Equation 9.7. We spline each of these functions, so we can use them for any value of N later on.

9.3.3 Structure evolution

So comes our perturbation quantities. We start by setting up a set of wavenumbers that we wish to use. We start at $k_0 = 0.0001H_0$ and end at $k_n = 10H_0$, using this distribution:

$$k_i = k_0 \cdot \left(\frac{k_n}{k_0}\right)^{\frac{i}{n}}.$$

When we then start counting at $i = 1$, we see that our lowest wavenumber, k_1, is 0.0011. Now we can set our initial conditions (some of which depends on k). Then we need to know at which N the tight coupling regime ends. We use the condition in Equation 9.11. We solve the tight coupling equations up to this point, then we turn to the full set of equations, solving through our grid that we set in the beginning. We end up with $\Theta_l(k, N), \delta_b(k, N), \delta_{\mathrm{DM}}(k, N), \delta_{\mathrm{DE}}(k, N), v_b(k, N), v_{\mathrm{DM}}(k, N)$, $v_{\mathrm{DE}}(k, N)$, $\Phi(k, N)$ and $\Psi(k, N)$. We will look closer at the energy-density perturbations, and so we write out these with varying wavenumber for redshift $z = 1100$ (recombination) and $z = 0$ (today), and as a function of N (or redshift), for the smallest and largest wavenumber I have used.

9.3.4 Interaction strength

At last, we must set values for the interaction parameters. We start with the ΛCDM model: $\alpha = \beta = \gamma = 0$ - no interactions at all. Then we will study

models with one interaction active, and then models with two interactions active.

An important question is then what non-zero values we should use for the interaction parameters. With three different interaction parameters, there are a whole lot of different models to study. First, I have limited γ to be non-negative, since there will be an instability if γ is negative [25]. I also think it is more interesting to study how the universe models differs when the signs of the interaction parameters change, and so I have chosen, by trial and error, to set the absolute value of any non-zero interaction parameter to 0.01. The observational constraints we looked at earlier suggests that the interaction parameters should be even smaller, but let us look at more hypothetical universes for now. The stronger the interactions are, the more exotic the universe models can be. So with a set value of the magnitude of the interaction parameters, and the stability criteria for γ, we get five different universe models when one interaction is active, which I will label $\{\alpha+, \alpha-, \beta+, \beta-, \gamma\}$, and eight different universe models when two interactions are present, which I will label $\{\alpha+\beta+, \alpha+\beta-, \alpha-\beta+, \alpha-\beta-, \alpha+\gamma, \alpha-\gamma, \beta+\gamma, \beta-\gamma\}$.

When displaying the results, we are always interested in comparing them to the ΛCDM model. Therefore, for the two matter components, I will plot the ratio of the density fluctuation $\delta_{b,\mathrm{DM}}$ in my model to the density fluctuation $\delta_{(b,\mathrm{DM}),0}$ for the ΛCDM model. We also square to make the quantity positive (I want to use logarithmic axes), and to smooth out some of the curves:

$$\Delta^2 = \frac{\delta^2}{\delta_0^2}. \tag{9.12}$$

For dark energy, there are no perturbations in the ΛCDM model, and so I will plot δ_{DE}^2 directly. I will also plot the sign of δ_{DE}, which is given by $\delta_{\mathrm{DE}}/|\delta_{\mathrm{DE}}|$, so we can see when we have overdensity or underdensity of dark energy.

9.4 Results

Now we can run our simulations and see what kind of universes we get. We start with no interactions, the ΛCDM model, then we turn on one interaction, then two interactions.

9.4.1 No interactions

For the ΛCDM model, we have $\alpha = \beta = \gamma = 0$. In this case, we will look at some of quantities in the background universe and the recombination era as well, these are displayed on Figure 9.1 on the next page: The energy-density parameters Ω follow the well-known evolutions, as in the upper left plot. The evolution of the free electron fraction X_e is shown on the upper right

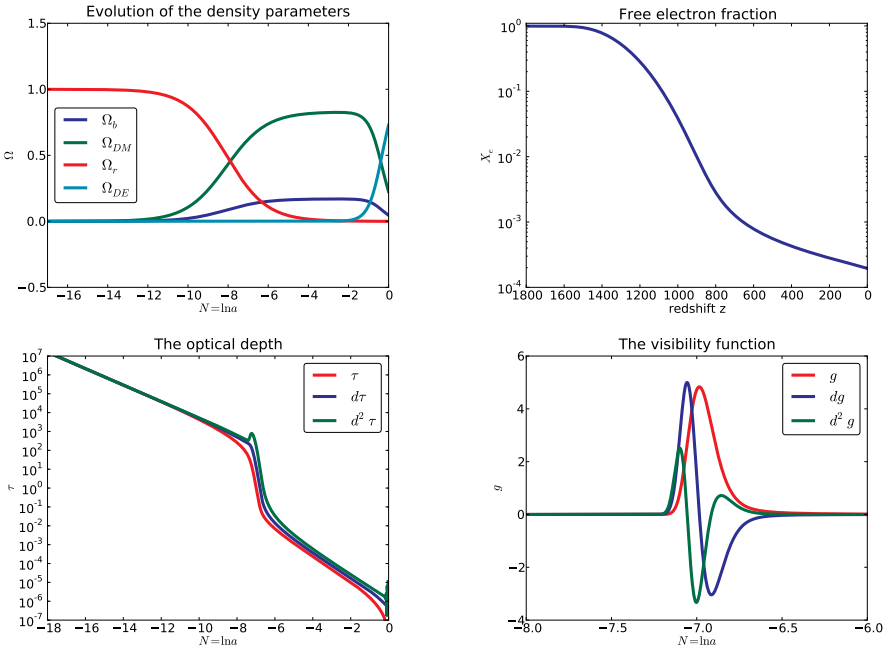

Figure 9.1: The density parameters, the free electron fraction, the optical depth and the visibility function, all for the ΛCDM model.

plot. In the lower left plot is the optical depth τ and its first and second derivative, and in the lower right is the visibility function and its first and second derivative, the latter two scaled by $1/10$ and $1/300$ so they all fit the same scale.

Moving on to the energy-density perturbations, we see from our equations that if β and γ are both zero, there are no perturbations for dark energy. So these will not be plotted for those cases. We now plot the perturbations Δ_b^2 for baryons and Δ_{DM}^2 for dark matter according to Equation 9.12, in four cases: varying redshift for two wavenumbers, and varying wavenumber for two redshifts. The fluctuations are squared to avoid negative values, since we want to use logarithmic scales. All plots are shown on Figure 9.2 on the following page, note that the line for Δ_{DM}^2 is multiplied by 10, to avoid overlapping.

At last, we want to study how the perturbation Ψ in the gravitational potential evolve. For the ΛCDM case, it is shown on Figure 9.3.

9.4.2 One interaction

Now we turn on one of the interaction parameters. As mentioned earlier, I have set the magnitude of the interaction parameter to 0.01, and will study how the perturbations evolve with different signs on the interaction parameters. Due to the instability mentioned earlier, γ will always be non-negative,

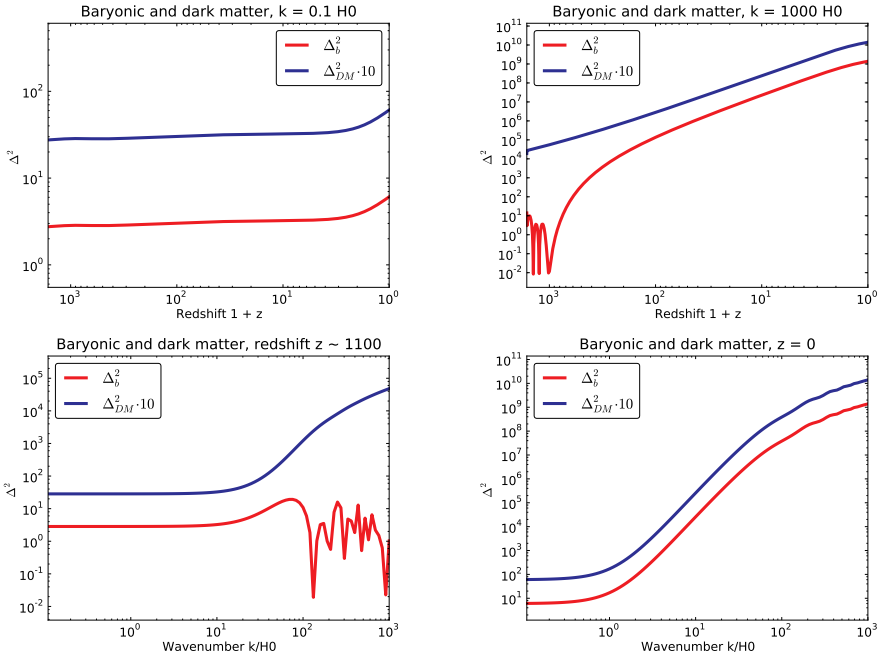

Figure 9.2: δ_b and δ_{DM} for the ΛCDM model. All plots have logarithmic axes.

and so we have five different models with one interaction. The two models where α is active will not touch the dark energy, and so there will be no perturbations in the dark energy density. Therefore, δ_{DE} will not be studied for these cases. When displaying the results, I will plot Δ^2 defined in Equation 9.12 for the matter components, and δ^2_{DE} and $\delta_{\mathrm{DE}}/|\delta_{\mathrm{DE}}|$for dark energy, comparing all five models in the same plot (three models for dark energy).

It may also be interesting to study the evolution of the density parameters Ω for the different models. I have picked out two of them, the one with $\alpha = 0.01$ and the one with $\beta = -0.01$. The evolutions are shown on Figure 9.4 on the next page. Remember that we here have used the ΛCDM values today as initial conditions, and integrated backwards in time.

Baryonic matter

We first look at the density fluctuation ratio for baryonic matter, Δ_b^2. We have four cases, two with constant wavenumber $k = 0.1H_0$ and $k = 1000H_0$, and two with constant redshifts $z = 1100$ and $z = 0$. All cases is shown in Figure 9.5 on page 124.

Dark matter

Turning to dark matter, we plot Δ^2_{DM}. Again we have four cases, two with contant wavenumbers and two with constant redshift. The plots are in Fig-

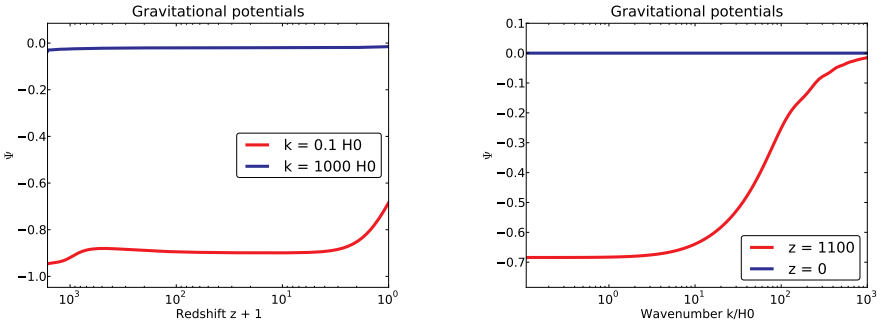

Figure 9.3: Perturbations in the gravitational potentials, for two fixed wavenumbers and two fixed redshifts.

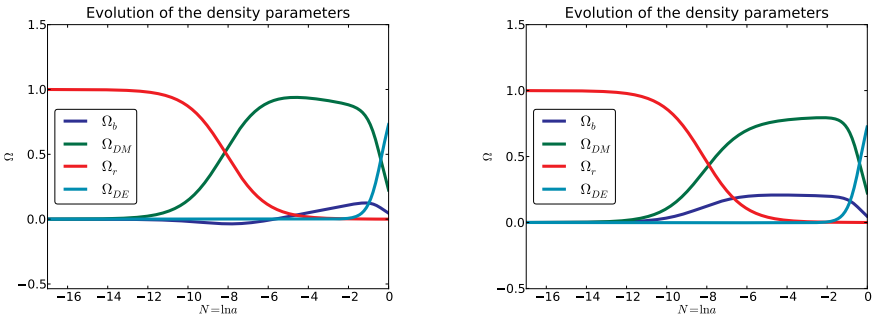

Figure 9.4: The evolution of the density parameters $\Omega(N)$, integrated backwards. On the left plot, we have $\alpha = 0.01$ and on the right plot, we have $\beta = -0.01$.

ure 9.6 on the next page.

Dark energy

Now we will look at dark energy. Since there are no density fluctuations to compare with in the ΛCDM model, I will plot δ^2_{DE} directly. The square is there to make all values non-negative, so that I can have logarithmic scales. The plots for the four cases (each case now having only three models) is displayed in Figure 9.7 on page 125. Now, δ_{DE} may also be negative, which represents an underdensity of dark energy. It is important so wee when that is the case, and so I have plotted the sign of δ_{DE} as well, in Figure 9.8 on page 125.

The gravitational potential

At last we will look at the perturbations in the gravitational potentials. They are shown on Figure 9.9 on page 126. For the two cases with fixed wavenumbers and the first case with fixed redshift, I have plotted the difference $\Psi - \Psi_{\Lambda\text{CDM}}$, and used linear y-axis. For the second case with fixed

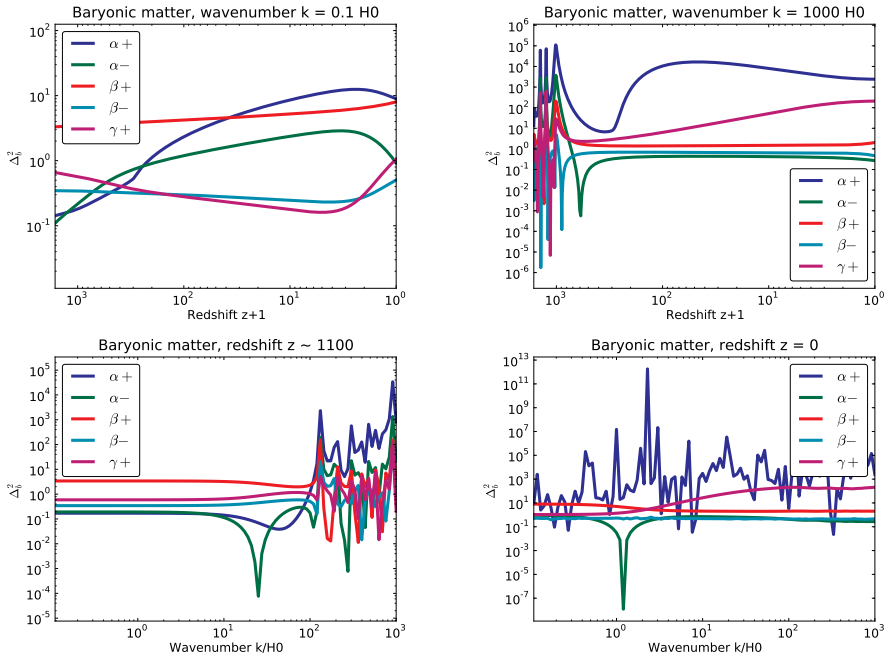

Figure 9.5: Baryonic matter density fluctuation ratio. Upper plots have fixed wavenumber, lower plots have fixed redshifts. All plots have logarithmic axes.

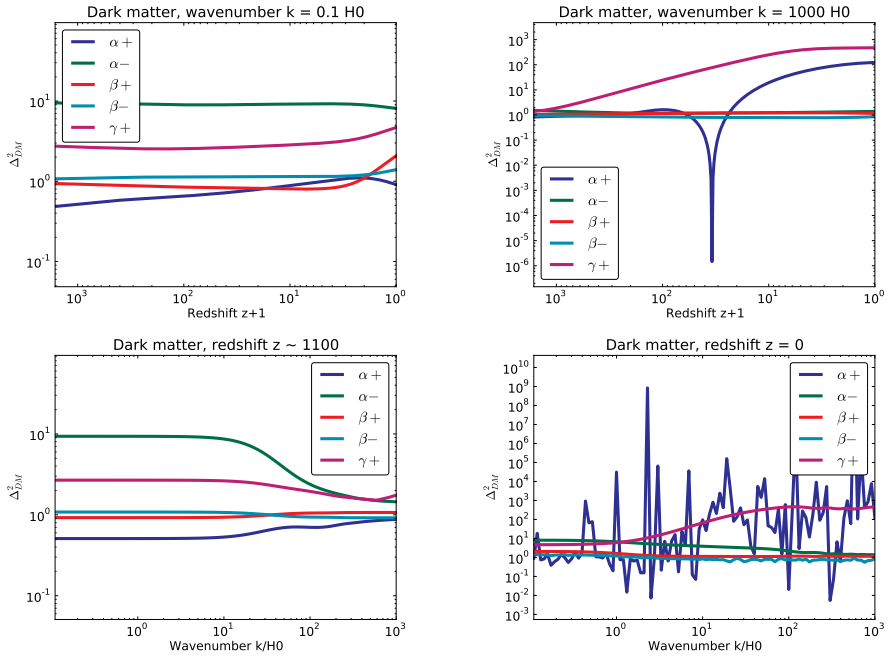

Figure 9.6: Dark matter density fluctuation ratio. Upper plots have fixed wavenumber, lower plots have fixed redshifts. All plots have logarithmic axes.

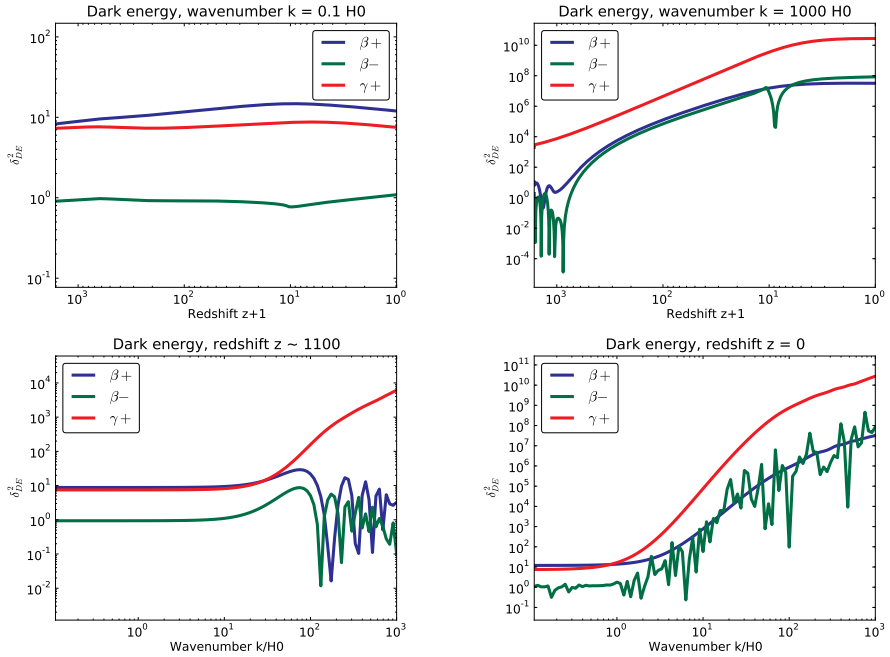

Figure 9.7: Dark energy density fluctuations. Upper plots have fixed wavenumber, lower plots have fixed redshifts. All plots have logarithmic axes.

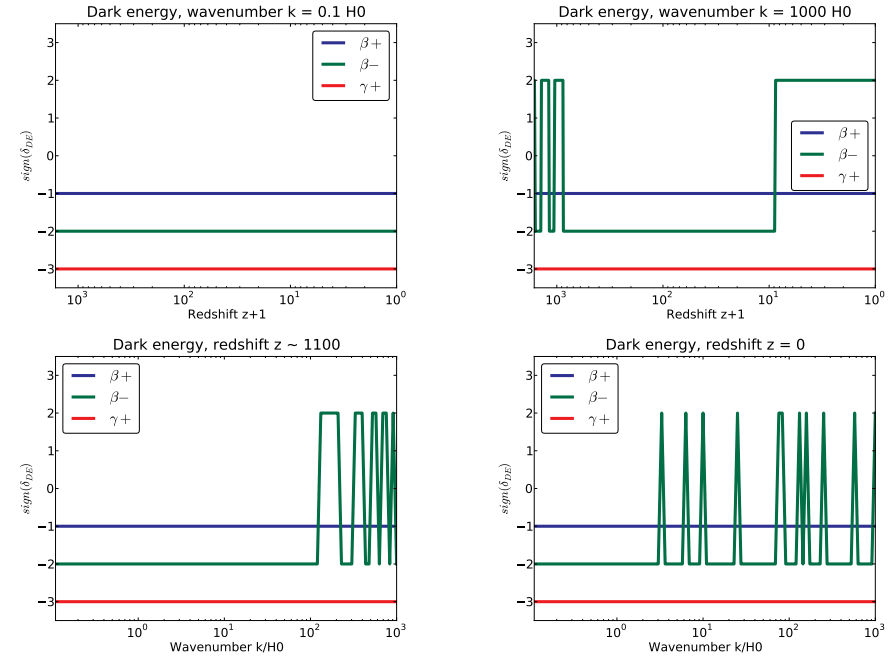

Figure 9.8: The sign of δ_{DE}, enhanced with different factors so we can tell the lines apart. Upper plots have fixed wavenumber, lower plots have fixed redshifts. Logarithmic x-axis.

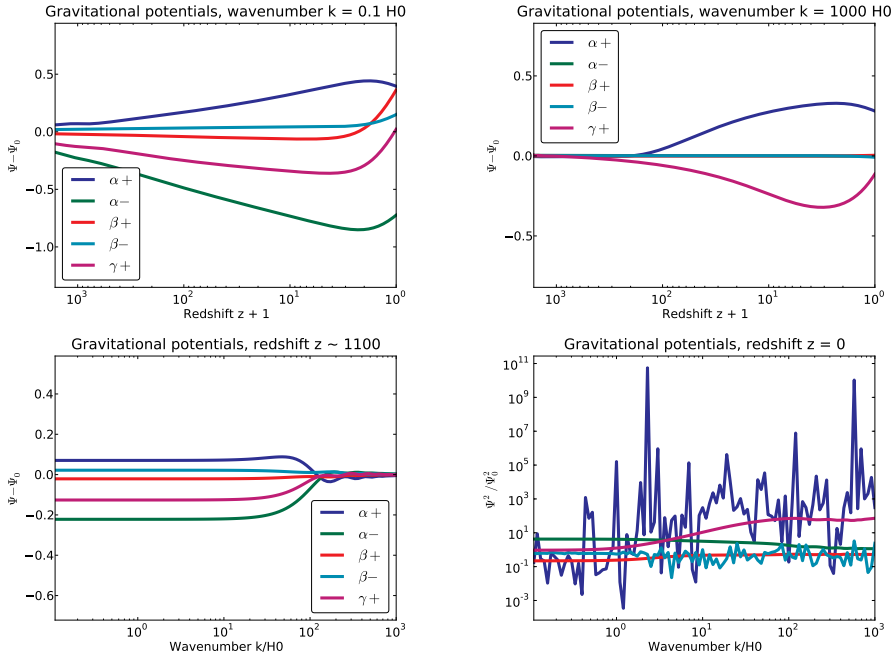

Figure 9.9: Perturbations in the gravitational potential Ψ, compared to the ΛCDM model. All plots have logarithmic x-axis, lower right plot have logarithmic y-axis.

redshift, I have plotted the ratio $\Psi^2/\Psi^2_{\Lambda\text{CDM}}$, and used logarithmic y-axis.

9.4.3 Two interactions

Now we turn on two of the interactions. Here we have are eight different models to look at, and all the models will produce dark energy density fluctuations. All plots will be divided into two parts, one where α and β are active, and one where γ and either α or β are active. For the matter components, we will study Δ^2 according to Equation 9.12, and for dark energy, we will study δ^2_{DE} directly, and the sign of δ_{DE}.

For the evolution of the density parameters Ω, we have looked at four of the models: $\alpha = \beta = 0.01$, $\alpha = -\beta = 0.01$, $\alpha = \beta = -0.01$ and $\alpha = \gamma = 0.01$. Again, we have used the ΛCDM values today as initial conditions and integrated backwards in time. The evolutions are displayed on Figure 9.10 on the next page.

Baryonic matter

We study Δ^2_b for a total of eight models, and the usual four cases: two with fixed wavenumber, and two with fixed redshift. The plots with fixed wavenumber are on Figure 9.11 on page 128, and the plots with fixed redshift are on Figure 9.12 on page 128.

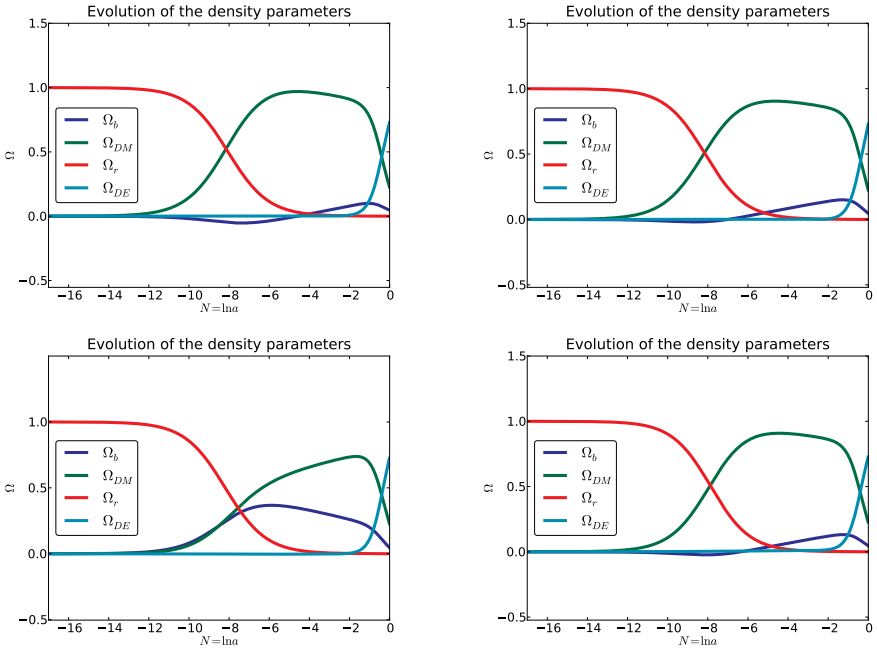

Figure 9.10: The evolution of the density parameters $\Omega(N)$ for four different models: top left is $\alpha + \beta+$, top right is $\alpha + \beta-$, bottom left is $\alpha - \beta-$ and bottom right is $\alpha + \gamma+$.

Dark matter

Here we study Δ^2_{DM} for the eight models and four cases. For fixed wavenumber, look at Figure 9.13 on page 129, and for fixed redshift, see Figure 9.14 on page 129.

Dark energy

Now we will study the dark energy density fluctuation δ_{DE}, both the magnitude through δ^2_{DE}, and the sign through $\delta_{\mathrm{DE}}/|\delta_{\mathrm{DE}}|$. For fixed wavenumber, see Figure 9.15 on page 130 for the magnitude, and Figure 9.18 on page 131 for the sign. For fixed redshift, have a look at Figure 9.17 on page 131 for the magnitude and Figure 9.18 on page 131 for the sign.

The gravitational potential

Finally, we will look at the perturbations in the gravitational potentials, Ψ. On Figure 9.19 on page 132, we have the cases where the wavenumber k is fixed, and on Figure 9.20 on page 132, we have the cases where the redshift z is fixed. In most of the plots, I have plotted the difference $\Psi - \Psi_{\Lambda\mathrm{CDM}}$ and used linear y-axis, but in a few plots were the differences were greater, I have plotted the ratio $\Psi^2/\Psi^2_{\Lambda\mathrm{CDM}}$, and used logarithmic y-axis.

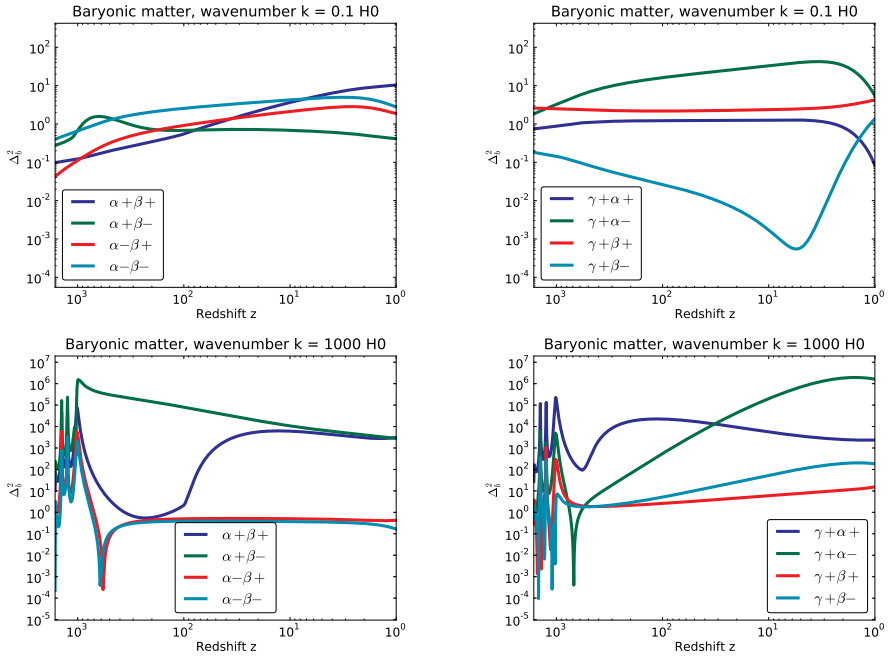

Figure 9.11: Baryonic matter density fluctuation ratios, fixed wavenumber. Upper plot have wavenumber $0.0011H_0$, lower plot have wavenumber $10H_0$. Logarithmic axes.

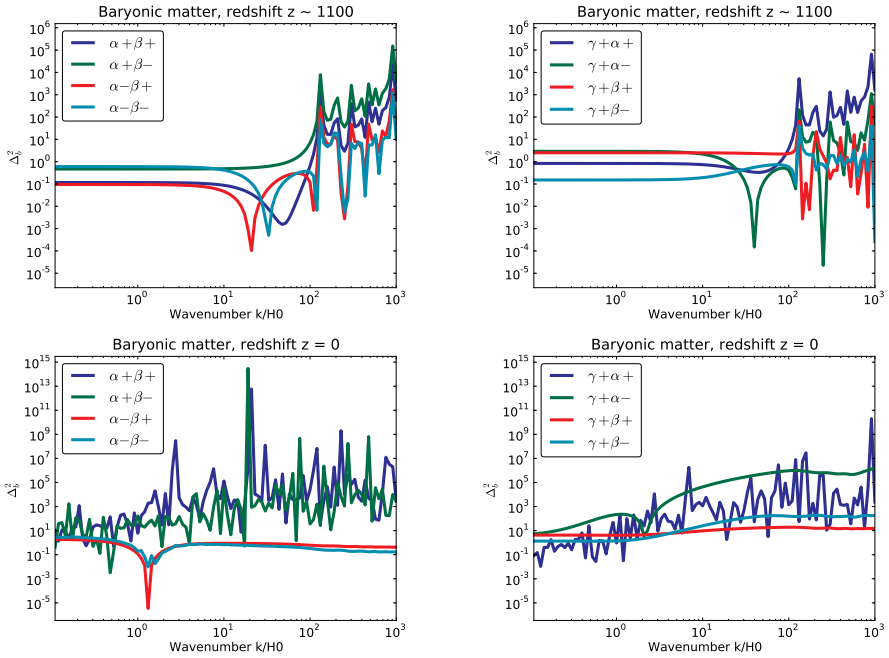

Figure 9.12: Baryonic matter density fluctuation ratios, fixed redshift. Upper plots have redshift 1100, lower plots have redshift 10. Logarithmic axes.

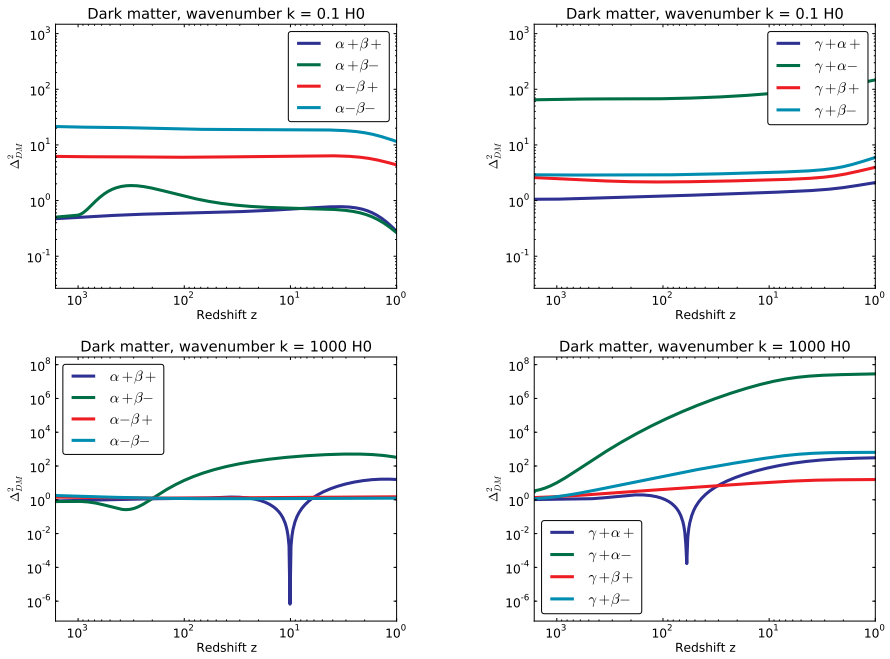

Figure 9.13: Dark matter density fluctuation ratios, fixed wavenumber. Upper plot have wavenumber $0.0011H_0$, lower plot have wavenumber $10H_0$. Logarithmic axes.

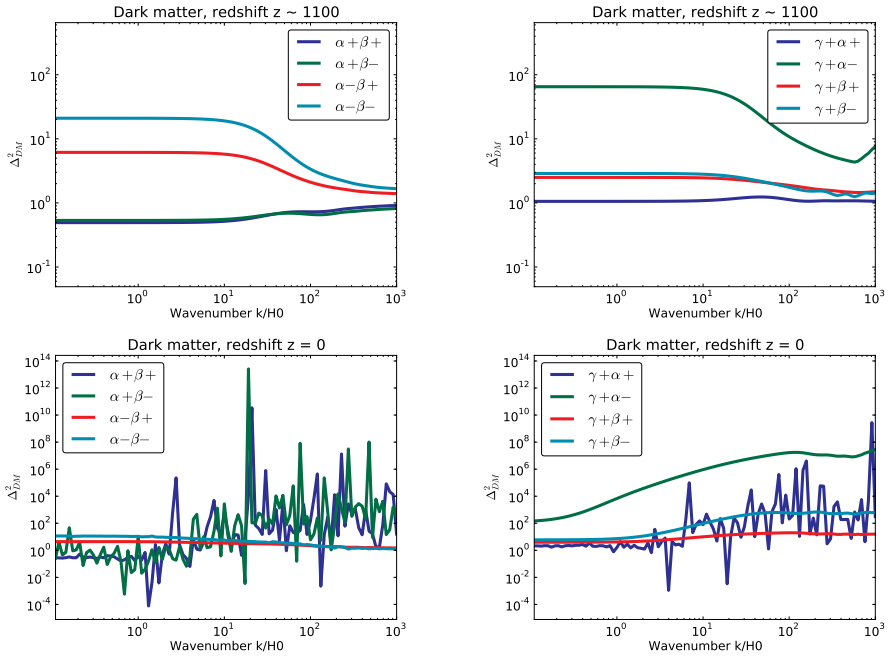

Figure 9.14: Dark matter density fluctuation ratios, fixed redshift. Upper plots have redshift 1100, lower plots have redshift 10. Logarithmic axes.

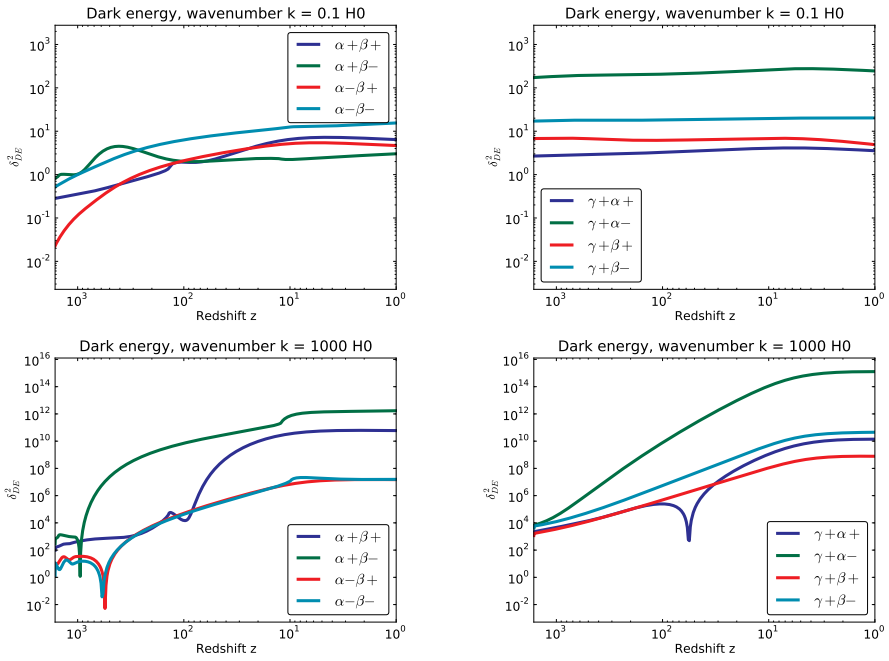

Figure 9.15: Plots of δ^2_{DE}, fixed wavenumber. Upper plot have wavenumber $0.0011H_0$, lower plot have wavenumber $10H_0$. Logarithmic axes.

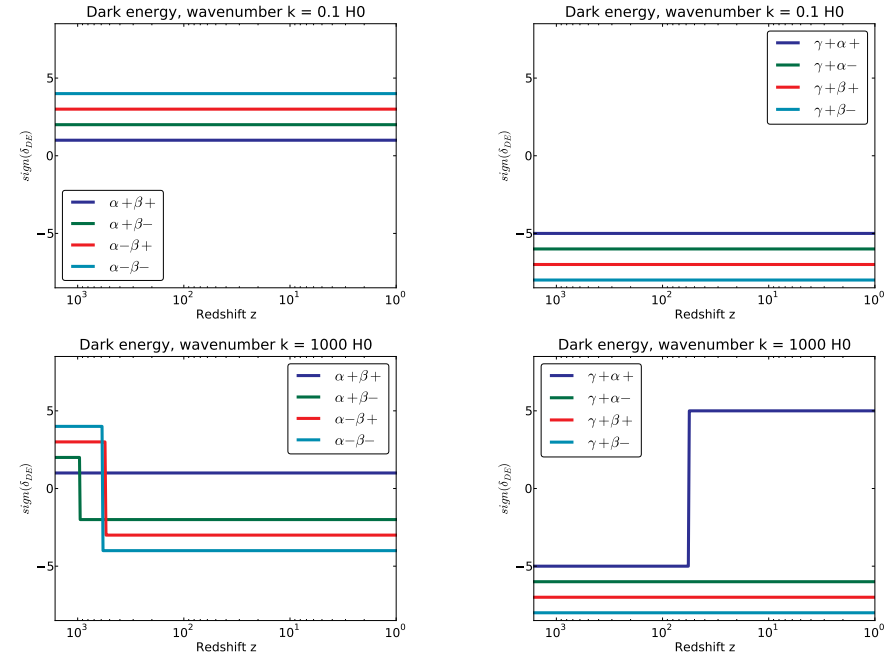

Figure 9.16: Sign of δ_{DE}, fixed wavenumber. Upper plot have wavenumber $0.0011H_0$, lower plot have wavenumber $10H_0$. The values are scaled differently so we can tell the lines apart. Logarithmic x-axis.

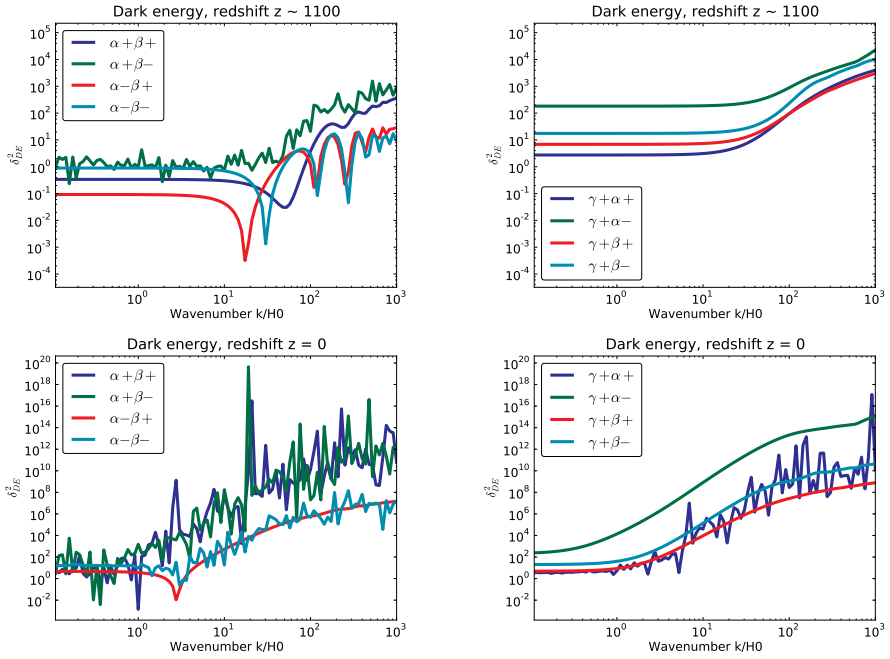

Figure 9.17: Plots of δ^2_{DE}, fixed redshift. Upper plots have redshift 1100, lower plots have redshift 10. Logarithmic axes.

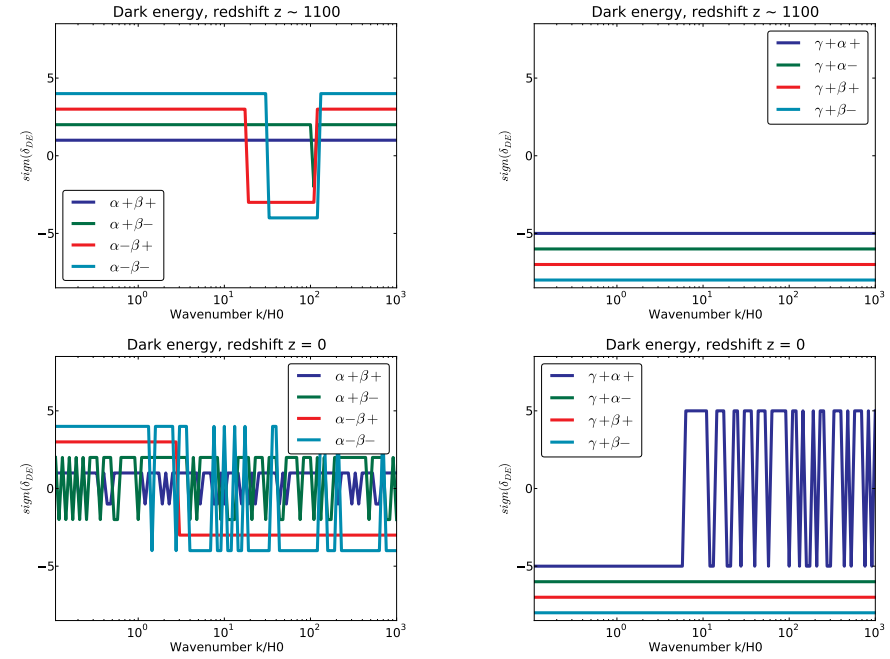

Figure 9.18: Sign of δ_{DE}, fixed redshift. Upper plots have redshift 1100, lower plots have redshift 10. The values are scaled differently so we can tell the lines apart. Logarithmic x-axis.

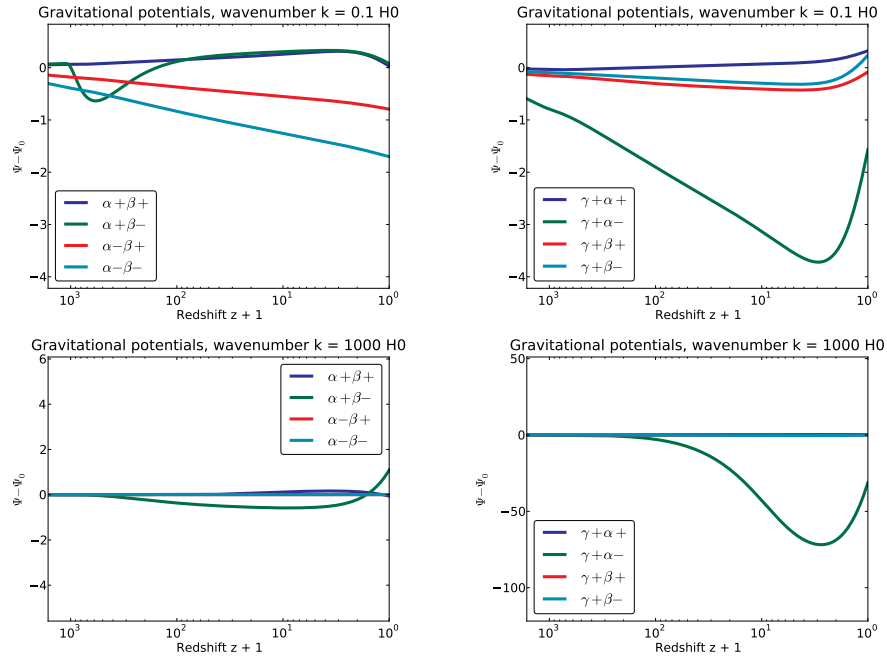

Figure 9.19: Perturbations in the gravitational potential Ψ, fixed wavenumber. Upper plots have wavenumber $0.0011H_0$, lower plot have wavenumber $10H_0$.

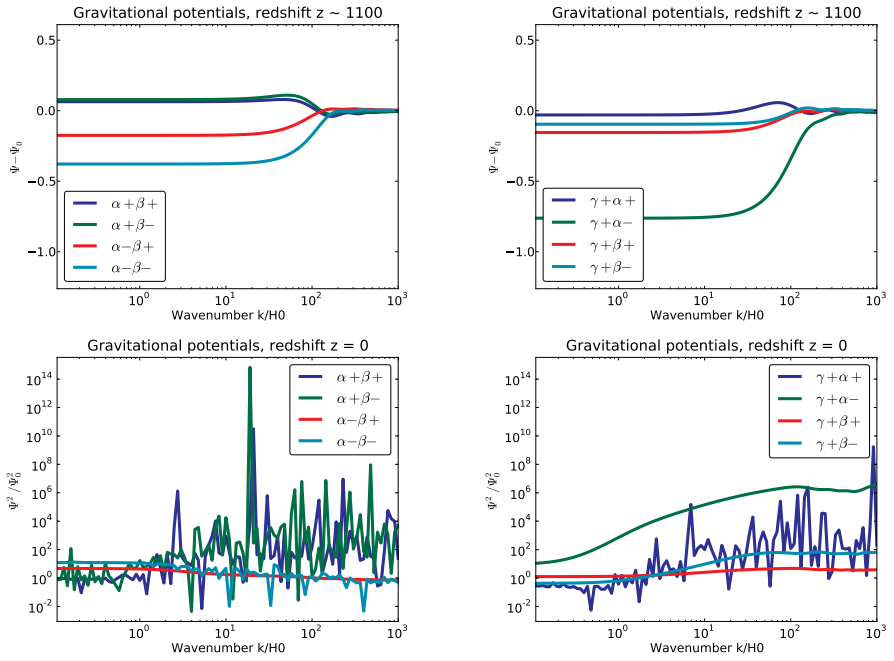

Figure 9.20: Perturbations in the gravitational potential Ψ, fixed wavenumber. Upper plots have wavenumber $0.0011H_0$, lower plot have wavenumber $10H_0$.

Chapter 10

Structure formation analysis

Now we have went through the energy-momentum conservation equations and the Einstein equations for a universe described by the perturbed metric in Equation 8.1, and we have solved them numerically, giving us the evolution of the energy-densities when we have interaction between the components of the universe. It is time to look at these results, to see what they tell us about the basics of structure formations, and how the interaction models affect the structure formations compared to the ΛCDM model.

10.1 No interactions

We started out with a model where none of our interactions were present. We first look at the energy-density contrasts, defined in Equation 8.5, and plotted in Figure 9.2 on page 122. From the upper plots, we see that the fluctuations grow in time, and they grow faster for the higher wavenumbers. This is due to the horizon growing, so causal physics can act over more than one wavelength. The smaller the wavelength (larger wavenumber) is, the earlier the horizon covers the whole wavelength, and the perturbations can grow more. Also notice the oscillations in the upper right plot, these are baryon acoustic oscillations. The same features can bee seen in the lower plots, that the perturbations grows more for large wavenumbers, and grow monotonically in time for the wavenumbers I look at. We also see BAO at early times for high wavenumbers. Note that since there are no interactions active, there will be no perturbations for dark energy, and so there are no lines for that component. At last, we have the perturbations in the gravitational Ψ in Figure 9.3 on page 123. For high wavenumbers and low redshifts, Ψ is close to zero, while for low wavenumbers and high redshifts, it is closer to 0.7. When we look back, we know that the initial value is -1, and so we see that Ψ goes towards zero, but slower at lower wavenumbers, since causal physics affects over one wavelength at later times than at higher wavenumbers.

Now we look back to the plots in Figure 9.1 on page 121. The evolution of the energy-density parameters $\{\Omega_b, \Omega_{\rm DM}, \Omega_{\rm DE}, \Omega_r\}$ are plotted in the upper left, and we see the well-known evolution from early radiation domination, through the matter domination and all the way to the dark energy domination today. I have plotted the free electron fraction X_e as a function of redshift (notice that this z-axis goes the other way) in the upper right, and we see the usual evolution that the universe goes towards being neutral through recombination. The optical depth τ, along with τ' and τ'', is plotted in the lower left, and there we see that the universe goes from being opaque ($\tau \gg 1$) to transparent ($\tau \ll 1$) during recombination. On the plot in the lower left, we have the visibility function g, and we can see that a given photon from space was most probable last scattered during recombination.

Our results agree with Dodelson [17], where more details about structure formations in the ΛCDM model can be found.

10.2 One interaction

Now we turn one one interaction. As before, we are studying five different models. The magnitude of the active interaction parameter is always 0.01.

10.2.1 The baryons

For the baryons, we have plotted Δ_b^2 as defined in Equation 9.12, both as a function of redshift for two fixed wavenumbers, and as a function of wavenumber for two fixed redshifts. All the plots are in Figure 9.5 on page 124.

The main feature we see is that we get more baryons if α or β is positive than if they are negative. There are stronger variations for the largest wavenumbers (smallest length scales) and the lowest redshift, since causal physics have had more time to act at small scales and late times. At redshift $z = 1100$, we can see oscillations when k is larger than $100H0$ for all five models, while at $z = 0$, we can see oscillations at all length scales when α is positive. There might be oscillations for some other models as well, but they are way weaker. These large oscillations are probably caused by a numerical instability, since it would be very strange that δ_b^2 in this model should be a factor of 10^3 larger than the ΛCDM case. We also see oscillations when z is varying, more at larger wavenumbers and higher redshifts - these may be related to the baryon acoustic oscillations that we see in the ΛCDM model.

Now, the way that the matter components affect the expansion of the universe differently than dark energy gives some exceptions, and that is also why γ being non-zero gives Δ_b^2 different from one, even though γ is not directly connected to the baryons. The abundance of baryons and of the other two components also plays a role, of course. The evolution of the abundance is shown on Figure 9.4 on page 123 for two models.

10.2.2 Dark matter

For dark matter, we have plotted $\Delta^2_{\rm DM}$, with the usual two wavenumbers and redshift, as a function of the other variable. The plots are displayed on Figure 9.6 on page 124.

As in the baryon case, we get more dark matter than in the ΛCDM model if α is negative or γ is positive, since these values directly gives more dark matter. We see that β have only very weak effect on $\Delta_{\rm DM}$, as expected. As usual, there are almost no variations at small wavenumbers/large scales and high redshifts. Today, we can see a lot of oscillations when α is positive. These are the same oscillations as we saw in the baryonic matter case, and are probably caused by a numerical instability, due to the huge amplitudes. Also notice the huge variation when $k = 1000H_0$ and $\alpha = 0.01$ - we actually get a higher dark matter fluctuation after $z = 40$ here compared to when $\alpha = -0.01$. This may again be related to the abundance of baryonic matter and dark matter.

10.2.3 Dark energy

When we study dark energy, we look directly at $\delta_{\rm DE}$, since there are no fluctuations in for dark energy in the ΛCDM model we can compare to. In figure 9.7 on page 125, we have the magnitude of $\delta_{\rm DE}$ through $\delta^2_{\rm DE}$, and in Figure 9.8 on page 125, we have the sign of $\delta_{\rm DE}$.

Starting with the sign of $\delta_{\rm DE}$, we see that when β or γ are positive, we always get a negative sign - which means negative fluctuations. This is because these models goes from dark energy to the other components. When β is negative, we have a model that gives more energy in dark energy, and the sign can be positive, giving overdensities. We also see a lot of oscillations in this model, which may be related to BAO, or numerical instabilibies.

For the magnitude, we see that when β or γ are positive, the underdensity grows, the growth being stronger at higher wavenumbers and lower redshifts. During recombination, there are also some oscillations when β is positive at low redshifts. These are connected with the oscillations in the baryon fluctuations. The same goes for the oscillations we see when β is negative. When $k = 1000H_0$, the oscillations die out at low redshifts, when the dark energy starts to dominate because of the expansion of the universe. At $z = 1100$, the oscillations are only present at the highest wavenumbers, since causal physics have had longer time to work on those scales than on the larger scales.

10.2.4 The gravitational potential

In Figure 9.9 on page 126, we compare the inhomogeneities in the gravitational potential, Ψ, to the ΛCDM model. When the differences are small, I have plotted the difference $\Psi - \Psi_{\Lambda\rm CDM}$ directly, using linear scales. When

the differences are larger, I have plotted the ratio $\Psi^2/\Psi^2_{\Lambda\text{CDM}}$, and used logarithmic axes.

We can see that when we have interaction that goes towards dark matter ($\alpha-$ and $\gamma+$), we get a lower value for Ψ, while if we have interactions going away from dark matter (only $\alpha+$), we get a higher value for Ψ, compared to the ΛCDM model. Now, remember that Ψ is usually negative in the ΛCDM model, so we get stronger inhomogeneities in the gravitational potentials when we have more dark matter. This is logical, since dark matter is the most important source of gravitational potentials, especially at the largest scales. This brings me over to the next point - the differences are smaller at smaller scales, especially early on, like at $z = 1100$. At later times, dark energy has started to dominate, and the differences vary a lot more, as we can see in the lower right plot.

10.3 Two interactions

When we now have seen how one active interaction affects our perturbations, let us turn on one more interaction. Both active interaction parameters will have magnitude 0.01. Since we have eight different models, I have splitted the plots into two parts, one with α and β active, and one with γ and either α or β active. Much of the analysis will be the same as in the one interaction case, and I will mostly try to point out the differences to the one interaction case.

10.3.1 The baryons

For the baryons, the cases with fixed wavenumber is in Figure 9.11 on page 128, and the cases with fixed redshift is in Figure 9.12 on page 128.

As in the one interaction case, we see see oscillations in the baryonic matter density fluctuations at high redshift and high wavenumbers. These are related to the baryonic acoustic oscillations we have in the ΛCDM case, but they are shifted either upwards or downwards, depending on the interaction parameters. In the plots where γ is active together with either α or β, we see that α gives a larger difference to the ΛCDM model than β does at late times. This is connected to the abundance of dark matter being greater than the abundance of dark energy earlier, giving more time for the interaction to have an impact on the fluctuations.

10.3.2 Dark matter

For dark matter, the cases with fixed wavenumber is shown on Figure 9.13 on page 129, and the cases with fixed redshift is in Figure 9.14 on page 129.

We see that there are larger differences to the ΛCDM model at late times and large wavenumbers, since causal physics have had more time to act on

these scales. During recombination, the differences are largest for the largest wavenumbers, since the clustering goes slower at these scales. Today, we see oscillations when α is positive, these are again realted to BAO. As expected, β does not have a very large impact in the dark matter cases.

10.3.3 Dark energy

Now we look at the dark energy. For fixed wavenumber, the magnitude of δ_{DE} is illustrated on Figure 9.15 and the sign on Figure 9.16 on page 130. For fixed redshift, see Figure 9.17 for the magnitude and Figure 9.18 on page 131 for the sign.

Again, when the interactions are active, we do get fluctuations in the dark matter energy-density. These fluctuations are mostly positive when γ is zero, and mostly negative when $\gamma = 0.01$, and some cases of oscillations today, redshift $z = 0$, when coupeled to baryons. We see that the oscillations are stronger when also α is positive, even though α is not directly related to the dark energy. These strong oscillations is most probably caused by numerical instabilities.

For all cases, we see that the magnitude of the fluctuations are larger for smaller scales and later times.

10.3.4 The gravitational potential

Finally, we look at the fluctuations in the gravitational potential Ψ. See Figure 9.19 on page 132 for the cases with fixed wavenumbers, and Figure 9.20 on page 132 for the cases with fixed redshift.

When the wavenumber is fixed, we see that the deviations from the ΛCDM model are fairly small early on, and growing later. For the $(\alpha-, \gamma+)$ model, the deviations are great compared to the other ones. In this model, both interactions goes towards dark matter, the most important source of gravitational potentials, so this may be expected.

When the redshift is fixed, we see that the differences are largest at the largest scales, and pretty small at the smaller scales, during recombination. This again has to do with causality. Today, we see oscillations when α is positive. For the same reason as before, the model $(\alpha-, \gamma+)$ has the largest impact on Ψ.

Epilogue

The time is almost out, and there are still lots of stuff that can be done in the studies of a universe with interacting components. I will now put up a summary of what we have done with the interaction models, and then I will write some words of what can be done in the future.

Summary and conclusions

The background universe

We now go all the way back to the background universe, which starts with the FRW metric in Equation 1.1 and the interaction model in this metric, Equation 2.6. We studied universe models where either one or two of the interactions were present, and in those cases, we found the analytical solutions to the equations, and we studied the stability of these solutions.

One interaction

For the three cases with one active interaction, which we looked at in Chapter 3, I make this conclusion:

- To get the analytical solution in a straight forward way, we use methods from linear algebra by writing the equation set as a matrix equation and find the eigenvalues and eigenvectors of the matrix. We also make some substitutions to decouple the system and get analytical solutions that are easier to interpret.

- To study the stability of the solutions, we write the equations in terms of the density parameters. The Friedmann constraint, Equation 2.7, can be used to eliminate one of the equations. We then use Equation 2.9 to study the stability of the solutions.

- When α is active, we make the substitutions $\rho_{\mathrm{M}} = \rho_b + \rho_{\mathrm{DM}}$ and $S = \rho_{\mathrm{DM}}/\rho_{\mathrm{M}}$. Since both matter components are pressureless, we get the simple solutions $\rho_{\mathrm{M}} = \rho_{\mathrm{M}}^{(0)}(1+z)^3$ and $S = 3\alpha N + S_0$. For the stability, we either get $\Omega_{\mathrm{DE}} = 0$, which also gives $\alpha = 0$, and we have no

interaction, or $\Omega_{\mathrm{DE}} = 1$, a universe totally dominated by dark energy, independent of α. Both these critical points are stable.

- When β or γ is active, we get analytical solutions on the same form. We make a common energy density of the two components $\rho = \rho_{b,\mathrm{DE}} + \rho_{\mathrm{DE}}$ and a ratio $R = \rho_{\mathrm{DE}}/\rho_{b,\mathrm{DM}}$. When β is active, $\rho(N)$ is given in Equation 3.10, and $R(N)$ is given in Equation 3.11. When γ is active, we get $\rho(N)$ from Equation 3.7 and $R(N)$ from Equation 3.8.

- For the stability, we can get two critical points with different stability depending on the interaction strength. If γ or β is between 0 and $1/4$, we can have a stable solution.

Two interactions

For the three cases with two active interactions, which we looked at in Chapter 4, I make this conclusion:

- We use methods from linear algebra to find the analytical solutions.

- When studying the stability, we make region plots, showing where each of the three critical points exists, and what kind of stability they have. We also show where the critical points are real, and where the Friedmann constraint is fulfilled, and we make some phase maps to show the evolution of the system for a given combination of interaction parameters.

- In all three cases, we could always find a stable critical point where the Friedmann constraint is fulfilled.

Observational constraints

For the second part of this thesis, we worked with observational data to see if the interaction models could be used to describe the universe we live in, and how strong they could be.

Supernova Ia

We started with the Union2 data set comprising 557 supernova type Ia, which we looked at in Chapter 5.

- Supernovae type Ia are exploding white dwarfs, which all are very similar. They then have approximately the same absolute magnitude, and they are standardazible candles.

- Our data set, the union two, consisted of redshift and apparent magnitude of 557 type Ia supernovae.

- We worked with models with one and two active interactions. When one interaction was active, we also included $\Omega_{\mathrm{DM},0}$ as a free parameter, and got some constraints on that as well. In the two interaction case, $\Omega_{\mathrm{DM},0}$ was fixed to 0.224, the best fit value in the ΛCDM model.

- In the one interaction case, we got no constraints on α, since baryonic matter and dark energy affects the expansion of the universe in the same way. When α was active, the best value for $\Omega_{\mathrm{DM},0}$ seemed to be around 0.22, close to the ΛCDM value for $\Omega_{\mathrm{DM},0}$.

- We got some weak constraints on β, γ and $\Omega_{\mathrm{DM},0}$ with one interaction active, with higher value for the active interaction parameter giving a higher value for $\Omega_{\mathrm{DM},0}$.

- In the two interaction case, we got some weak constraints on α, since it indirectly affects the other interaction. We got stronger constraints on β and γ, one balancing for the other.

- We concluded that we get no statistical evidence proving that the interactions are present, but such models are possible. Supernova Ia gives rather weak constraints, allowing quite strong interactions. This is due to the supernovae in the data set being rather close to us, all below a redshift of 1.5.

Baryon acoustic oscillations

In Chapter 6, we used data from observations of baryon acoustic oscillations (BAO) to constrain our models.

- We used a total of six data points of BAO from three different surveys.

- The model constraints were based on the comoving sound horizon at recombination, and is an example of a standard ruler. The data were obtained through observations of galaxies.

- In contrast to the supernovae Ia studies, we included correlations in our data, which makes this case a little bit more complicated.

- We did two cases, the first with one interaction active together with having $\Omega_{\mathrm{DM},0}$ as a free parameter, and one with two active interactions with $\Omega_{\mathrm{DM},0} = 0.224$, the best-fit value in the ΛCDM model.

- In the one interaction case we got no constraints on α, since the matter components affects the expansion of the universe in the same way. For $\Omega_{\mathrm{DM},0}$, a value around 0.22 seemed to be favored. We got some weak constraints on β, and stronger constraints on γ, since the dark components are the dominating components of the universe in the time eras we are working with here.

- In the two interaction case, we get some weak constraints on α, since it indirectly affects the other active interaction. When β and γ were active, they seem to balance each other.
- As in the supernovae Ia case, we get no statistical evidence for or against my interaction models: they can be present, but the ΛCDM model also fit.
- The constraints from BAO are also weak, allowing quite strong interactions, but the constraints are stronger than in the supernovae Ia case.

The cosmic microwave background

In Chapter 7, we used data based on the cosmic microwave background to constrain our models.

- We used data from the WMAP satellite for three quantities related to the CMB: The redshift of the CMB, the acoustic scale, and the shift parameter.
- The data were correlated, as in the BAO case.
- We studied models with one and two interactions active, the first with $\Omega_{\mathrm{DM},0}$ being a free parameter as well.
- When one interaction was active, we got no constraints on α for the same reasons as in the supernovae Ia and BAO cases, and $\Omega_{\mathrm{DM},0}$ should be around 0.22. We did get constraints on β and γ, the magnitude should be smaller than 0.01.
- With two interactions active, we got some weak constraints on α for the same reasons as before, and we got constraints on both β and γ.
- As in the supernovae Ia and BAO cases, we can not conclude anything about the presence of my interaction models.
- Compared to the supernova Ia and BAO cases, we get significantly stronger constraints now, since the observations we are working with are at way higher redshifts than the supernovae Ia and BAO.

Structure formations

In the third part of the thesis, I studied how my interaction models would affect the evolution of inhomogeneous perturbations in the metric and the energy-densities of the components, which is what makes structures in our universe.

- In Chapter 8, we set up perturbations in the metric tensor and the energy-densities of the components.
- We used the interaction models in a covariante form to see how they looked in our new metric.
- Then we went through the energy-momentum conservation equations to get equations for the evolutions of the density fluctuations with the interactions present.
- We gave a summary of the deviations of the Boltzmann equation for photons and the Einstein equations, which are known from the ΛCDM model, and we set initial conditions to our equations based on the ΛCDM model.
- Fourier transforming our equations got us from coupeled partial differential equations to an infinite set of ordinary differential equations, which were decoupled on different length scales.
- In Chapter 9, we rewrote our equations to a form fitted for numerical simulations.
- Then we looked at numerical instabilities in the tight coupling regime, and we studied some of the physics in the recombination era, which we needed to know.
- Next, we solved our equations through time and at different length scales.
- We plotted our results using the ratio to the ΛCDM model for easy comparison.
- In the end, we saw that my interaction models had a lot of impact on the structure formation, which interactions were active and which way they were going gave way different universes.
- Numerical issues also seemed to be present in my results, giving oscillations with very large amplitudes in some cases.

The road ahead

Even though I have gone through studies of the background universe, observational constraints and structure formations, there are still a lot of things that can be done connected to my interaction models.

Three interactions

As we have went through this thesis, I have never worked with cases where all three interactions have been present at once. There are numerous reasons for that, the most important one being time. The priority was to get through all three parts, and then the cases with one and two interactions took time enough. Also, since a third interaction makes up a dimension, a lot of the results must be displayed in another way, and I never did any exploration in this area. I was considering going further with observations, doing Monte Carlo simulations and such, but I did not get the time.

A fourth interaction

We saw in Chapter 8 that the baryons were interacting with the photons through Compton scattering, and this was not included in my interaction models from the beginning. It is possible, and maybe interesting, to study models were the components couple to photons as well, which we know that they do. Baryons couples directly to the photons through Compton scattering as we have seen, dark matter sets up gravitational potentials that we know affect the photons, and dark energy drives the acceleration of the expansion of the universe, which redshifts the photons within it. Interactions to photons can be implemented as the three other interactions were by adding a new term in the interactions, and setting up a new equation for the photons, but one has to be careful when doing this. Changing the physics of the photons will have a large impact on almost every area of astrophysics, since photons make up all the observations we have. The luminosity distance and the black body spectrum of the CMB are among the things that can change. Still, such interaction models may be something to study in the future.

Big Bang Nucleosynthesis

We used data from supernovae Ia, baryon acoustic oscillations and the cosmic microwave background to get constraints for the strength of our interactions. These never gave any direct constraints on the parameter α, since baryonic matter and dark matter affects the expansion of the universe in the same way after recombination. However, data based on the time epoch called Big Bang Nucleosynthesis (BBN), where nucleis of hydrogen, helium and some lithium were formed, could tell us something about the abundance of baryonic matter compared to dark matter, and this could then directly tell us something about α. The standard constraint from BBN is that the Hubble expansion rate at that time cannot vary more than about 10 % from the standard model.

A model for the interactions

Through the studies of my interaction models in this thesis, I have only focused on how the interaction models affects our universe. I have never mentioned how the interaction models work, the mechanisms that drive the interactions. A possibility would be some kind of scalar field. Again, there were not enough time to do this, since it was not a priority, but it may be interesting to study this sometime.

Appendix A

The general theory of relativity

In this appendix, I will give a short summary of the general theory of relativity, which will go from the basic assumptions to the results we need in this thesis. I have set the speed of light c equal to one. The text in this appendix is based on some small parts of the book by Grøn and Hervik [26], and some lecture notes by Øystein Elgarøy [27].

A.1 The principle of equivalence

One of the most difficult concepts in physics is *mass*. In one way, everyone knows what mass is, since we use it every day from the day we are born. Mass then tells us how heavy something is. But if one looks closer to this, it can actually be quite difficult to define precisely what mass really is, and the easiest way of thinking of mass is how we measure it.

In Newtonian mechanics, the mass of an object appears in two ways: as inertial mass in Newton's second law $F = ma$, which applies to any force, and as gravitational mass in Newton's law of gravitation $F_G = GMm/r^2$, which only applies to the force of gravity. If an object is only affected by gravity, then one can combine the two laws, which, with a suitable choice of units, tells us that the two masses are the same, even though they actually are defined through way different physical phenomena. The principle of equivalence says that these two masses are equal.

From this, and the definition of a gravitational field as the force of gravity acting on an object divided by the objects mass, the combination of Newton's second law and Newton's law of gravitation along with the principle of equivalence then says that a gravitational field is equal to an acceleration. And so, the principle of equivalence also states that a gravitational field is equivalent to an accelerated reference frame. The related acceleration is locally called the acceleration of gravity.

A.2 Distances and the metric tensor

If we want to do specific physical computations, we need a coordinate system. In the theory of relativity, such a coordinate system needs four dimensions, one time dimension, labeled by 0, and three spatial dimensions, labeled by 1, 2 and 3. Physical quantities will have to be labeled by the basis of this coordinate system, using subscrips and superscrips as indices. A Greek index can be any dimension, and runs from 0 to 3. A Latin index is always a spatial dimension, and runs from 1 to 3.

When choosing a coordinate system, we choose a *basis*, a set of vectors $\mathbf{e}_\mu$ that span our coordinate system. From the basis vectors, we obtain the *metric tensor* through the scalar product: $g_{\mu\nu} = \mathbf{e}_\mu \cdot \mathbf{e}_\nu$. The metric tensor is actually the definition of the dot product between two basis vectors, and it has two main purposes:

- Measure distances through the invariant line elemend ds^2.
- Isomorphism between a tangent plane and its dual.

We take the first one first. The coordinates of points in space depends on our coordinate system, but the distance between two points does not - if we define this distance properly, using all four dimensions. If we have two points in our space with an infinitesimal separation dx^μ in our coordinate system, we can define the line element ds^2:

$$ds^2 = \sum_\mu \sum_\nu g_{\mu\nu} dx^\mu dx^\nu = g_{\mu\nu} dx^\mu dx^\nu. \tag{A.1}$$

Now, ds^2 does not depend on what basis we have - it is invariant. By the way, here is the first example of Einstein's summing convection - repeated indices are summed over.

The metric tensor is also used for raising and lowering indices. If we have a component v^μ of a vector or a component v_μ of a one-form (a function that acts on a vector to produce a real number), we can use the metric tensor to find the components of the corresponding one-form/vector:

$$v_\mu = g_{\mu\nu} v^\nu \qquad v^\mu = g^{\mu\nu} v_\nu.$$

This can be extended to tensors of higher rank by adding more factors of the metric tensor. So for this mixed tensor of rank three, for example, we have

$$T^{\beta\gamma}_\alpha = g_{\alpha\rho} g^{\beta\sigma} g^{\gamma\tau} T^\rho_{\sigma\tau}.$$

The metric tensor then allows us to establish a correspondence between covariant and contravariant tensors. From this, we also see that $g_{\mu\nu}$ is the inverse of $g^{\mu\nu}$.

A.3 Proper time and four velocity

In this section, I will define two important concepts: the invariant quantity called the *proper time*, and the four vector quantity called the *four velocity*. First, we choose a coordinate system (which then has a given basis), and label points in our coordinate system by x^μ. Now we imagine that we have a particle in our coordinate system with fixed spatial position x^i, but with changing time $t = x^0$ of course. The line element ds^2 then reads

$$ds^2 = g_{\mu\nu} dx^\mu dx^\nu = g_{00} dt = -d\tau^2.$$

To the last equality, I have used that only one term survives, $(dx^0)^2$, which I then have labeled dt^2. The line element is then a time component, the time measured on a clock following this particle (which does not move through the three-space in our coordinate system). This quantity is then also invariant, and we call it the proper time, labeled by τ. The sign is there only for convenience. Now we set up a particle that moves in our coordinate system. This particle will also have a proper time, since we can have another coordinate system that follows this particle. We want to compute the velocity of this particle in our coordinate system. We then define the four velocity u^μ of the particle as the position x^μ differentiated with respect to the proper time τ of the particle:

$$u^\mu = \frac{dx^\mu}{d\tau}. \tag{A.2}$$

From this definition, one can show a useful relation called the *four velocity identity*:

$$u_\mu u^\mu = g_{\mu\nu} u^\mu u^\nu = -1. \tag{A.3}$$

A.4 Covariant differentiation

Covariant differentiation deals with differentiating tensors in a way that is independent of basis. The tensor must then be differentiated with respect to an invariant parameter. We will use the proper time τ as this invariant parameter. For a scalar - a tensor of rank zero, this would be straight forward, and may serve as a good example for introducing useful notation: a comma denotes partial derivative with respect to the corresponding coordinate. So if we have a scalar field $\phi(x^\mu)$, we can write

$$\frac{d\phi}{d\tau} = \frac{\partial \phi}{\partial x^\mu} \frac{dx^\mu}{d\tau} = u^\mu \partial_\mu \phi = u^\mu \phi_{,\mu}.$$

Here, I have used the four velocity, and introduced two alternative ways to label the partial derivative (comma and ∂^μ). Also note that an upper index in a denominator corresponds to a lower index in a numerator.

Now, let us move on to a vector $\mathbf{A}$, a tensor of rank one. We write it as a linear combination of our basis vectors: $\mathbf{A} = A^\mu \mathbf{e}_\mu$. Differentiating, we get

$$\frac{d\mathbf{A}}{d\tau} = \frac{d}{\tau}(A^\mu \mathbf{e}_\mu) = \mathbf{e}_\mu \frac{dA^\mu}{d\tau} + A^\mu \frac{d\mathbf{e}_\mu}{d\tau}.$$

We take a closer look at the last term, defining the connection coefficients $\Gamma^\alpha_{\mu\nu}$:

$$\frac{d\mathbf{e}_\mu}{d\tau} = \Gamma^\alpha_{\mu\nu} \frac{dx^\nu}{d\tau} \mathbf{e}_\alpha = \Gamma^\alpha_{\mu\nu} u^\nu \mathbf{e}_\alpha. \tag{A.4}$$

If our basis is a coordinate basis (which means that the basis vectors are partial derivative operators), we call the connection coefficients the Christoffel symbols. The Christoffel symbols are symmetric in the two lower indices: $\Gamma^\alpha_{\mu\nu} = \Gamma^\alpha_{\nu\mu}$. By using Hamilton's principle and the Lagrange equation, one finds this useful expression for the Christoffel symbols in terms of the metric tensor:

$$\Gamma^\alpha_{\mu\nu} = \frac{g^{\alpha\beta}}{2} \left(g_{\mu\beta,\nu} + g_{\beta\nu,\mu} - g_{\mu\nu,\beta} \right). \tag{A.5}$$

Back to the covariant derivative, inserting the four velocity and the connection coefficients, we have

$$\frac{d\mathbf{A}}{d\tau} = A^\mu_{,\nu} u^\nu \mathbf{e}_\mu + \Gamma^\mu_{\nu\alpha} u^\nu A^\alpha \mathbf{e}_\mu$$

Now we remove the four velocity and the basis vector, and introduce two notations for the covariant derivative, the ∇ and the semicolon:

$$\nabla_\nu A^\mu = A^\mu_{;\nu} = A^\mu_{,\nu} + \Gamma^\mu_{\alpha\nu} A^\alpha. \tag{A.6}$$

This is then the covariate derivative of a vector component. This expression can be generalized to a tensor of any rank. We will need this expression for a mixed tensor of rank two. It will look like this:

$$\nabla_\mu T^\alpha_\beta = T^\alpha_{\beta;\mu} = T^\alpha_{\beta,\mu} + \Gamma\alpha_{\sigma\mu} T^\sigma_\beta - \Gamma^\sigma_{\beta\mu} T^\alpha_\sigma. \tag{A.7}$$

When $\nu = \mu$ in Equation A.6, we have this useful formula for the covariant derivative, which now is a divergence:

$$\nabla_\mu A^\mu = \frac{1}{\sqrt{|\det(g_{\alpha\beta})|}} \frac{\partial}{\partial x^\mu} \left(\sqrt{|\det(g_{\alpha\beta})|} A^\mu \right). \tag{A.8}$$

Note that α and β are not free indices, they are just there to label which version of the metric we use.

A.5 Some useful tensors

A tensor is a mathematical object which follows a specific transformation rule: a component of a tensor written in one basis is a linear combination of the tensor components written in another basis. All tensors have a rank, which is zero or greater. A tensor of rank zero is a scalar, and a tensor of rank one is a vector. For example, if we have a contravariant tensor T of rank 3 written in the basis $(\mathbf{e}_\mu, \mathbf{e}_\nu, \mathbf{e}_\sigma)$, we write the components as $T^{\mu\nu\sigma}$, and if we want to know the components of T in the basis $(\mathbf{e}_{\mu'}, \mathbf{e}_{\nu'}, \mathbf{e}_{\sigma'})$, we transform like this:

$$T^{\mu'\nu'\sigma'} = \frac{\partial x^{\mu'}}{\partial x^\mu}\frac{\partial x^{\nu'}}{\partial x^\nu}\frac{\partial x^{\sigma'}}{\partial x^\sigma}T^{\mu\nu\sigma}.$$

From this, we can also see that if T has rank zero, there are no coefficients, and so a scalar has the same value in all coordinate systems.

We have already met one tensor of rank 2, the metric tensor $g_{\mu\nu}$. Another tensor we need is the Ricci tensor $R_{\mu\nu}$. To define it, we first define the Riemann curvature tensor, which is given by the connection coefficients and the structure coefficients:

$$R^\alpha_{\beta\gamma\delta} = \Gamma^\alpha_{\beta\delta,\gamma} - \Gamma^\alpha_{\beta\gamma,\delta} + \Gamma^\mu_{\alpha\delta}\Gamma^\alpha_{\mu\gamma} - \Gamma^\nu_{\beta\gamma}\Gamma^\alpha_{\nu\delta} - c^\rho_{\gamma\delta}\Gamma^\alpha_{\gamma\rho}.$$

Here, the structure coefficients $c^\alpha_{\mu\nu}$ comes into play, which are defined through this commutator:

$$[\mathbf{e}_\mu, \mathbf{e}_\nu] = c^\alpha_{\mu\nu}\mathbf{e}_\alpha.$$

When we work with a coordinate basis, the connection coefficients reduce to the Christoffel symbols, all structure coefficients are zero, and we can ignore the last term in the Riemann curvature tensor.

If we contract the upper index with the middle lower index in the Riemann curvature tensor (that is, setting them equal and summing over), we get the Ricci tensor:

$$R_{\mu\nu} = R^\rho_{\mu\rho\nu}.$$

The Ricci tensor can be found using the Christoffel symbols, by this formula:

$$R_{\mu\nu} = \Gamma^\alpha_{\mu\nu,\alpha} - \Gamma^\alpha_{\mu\alpha,\nu} + \Gamma^\alpha_{\beta\alpha}\Gamma^\beta_{\mu\nu} - \Gamma^\alpha_{\beta\nu}\Gamma^\beta_{\mu\alpha}. \tag{A.9}$$

If we contract the Ricci tensor, we get the Ricci scalar:

$$\mathcal{R} = R^\mu_\mu = g_{\mu\nu}R^{\mu\nu}. \tag{A.10}$$

The Ricci tensor minus one half times the metric times the Ricci scalar gives us the Einstein tensor:

$$E_{\mu\nu} = R_{\mu\nu} - \frac{1}{2}g_{\mu\nu}\mathcal{R}. \tag{A.11}$$

The Einstein tensor fulfills this equation:

$$\nabla_\mu E^{\mu\nu} = 0,$$

or, in other words, the Einstein tensor has zero covariant divergence. This is an important point in Einstein's field equations.

Next comes the energy-momentum tensor $T_{\mu\nu}$. There are multiple ways to define it, and I will define it by the phase-space distribution function $f(x^\mu, P^\mu)$

$$T^\mu_\nu = g \iiint_P \frac{1}{(2\pi)^3\sqrt{-\det(g_{\alpha\beta})}} \frac{P^\mu P_\nu}{P^0} f dP_1 dP_2 dP_3. \tag{A.12}$$

Here, the factor g is the degeneracy level, and is related to the internal degrees of freedom of the component we are working with. Also note that the determinant of the metric tensor is also basis-independent, so the indices α and β are not free indices, they are just there to label the metric tensor. The integral goes over the spatial momentum space. Now, if we have a component that is a perfect fluid (a fluid that has no viscosity and no thermal conduction), the expression for the energy-momentum tensor is way easier:

$$T_{\mu\nu} = (\rho + p)u_\mu u_\nu + p g_{\mu\nu}. \tag{A.13}$$

Using covariant differentiation, conservation of energy and momentum takes on a very simple form:

$$\nabla_\mu T^\mu_\nu = 0. \tag{A.14}$$

As in the case for the Einstein tensor, the energy-momentum tensor also has zero covariant divergence.

A.6 Einstein's field equations

In classical mechanics, we use Newton's laws to find the equation of motion for an object. Einstein's field equations are the equation of motion in the general theory of relativity. There is a way to deduce Einstein's field equations from the variational principle, but I am not going to do that. I will simply state that the two tensor with zero covariant divergence we now have, the Einstein tensor and the energy-momentum tensor, are proportional. The constant of proportionality is $8\pi G$, where G is the universal constant of gravity. This is the constant of proportionality that gives us the correct result when we look at the limits between Newton's law of gravity and Einstein's field equations. So, Einstein's field equations, also called the Einstein equations, reads

$$E^\mu_\nu + g^\mu_\nu \Lambda = 8\pi G T^\mu_\nu, \tag{A.15}$$

where I have used one index upstairs and one index downstairs, since T^{μ}_{ν} is the easiest form of T to work with. Now, we get the Einstein from Riemann's curvature tensor, which we again get from the metric tensor. The Einstein tensor contains the geometry of space. We get the energy-momentum tensor from the energy-densities and pressure of what we have in our space, and the Einstein equation then relates geometry of space and the contents of the space. Or as Taylor and Wheeler says it in [28] - space tells matter how to move, and matter tells space how to curve, through the Einstein equation.

Note the term with Λ in Einstein's field equations- Einstein noticed that one could add a constant to one side of the equation, and the equation would still be fulfilled.

Appendix B

Mathematical, numerical and statistical methods

In this appendix, I will write about some of the mathematical, numerical and statistical methods that we have used in this thesis.

B.1 Mathematical methods

Through the thesis, I have used a set of mathematical methods that I feel needs a little bit more explanation, and that is what one finds in this section. I will start with the linear algebra used for solving systems of differential equations and studying the stability of the solutions, then I will explain more details of some tricks used for manipulating equations, named after some famous mathematicians.

B.1.1 Eigenvalues and eigenvectors

Two important concepts in linear algebra, which are strongly related, are eigenvalues and eigenvectors. If one has an $n \times n$ matrix A, an eigenvalue $u \in \mathbb{C}$ and an eigenvector $\mathbf{v}$, which is a column vector with n rows, fulfills this equation:

$$A\mathbf{v} = u\mathbf{v}. \tag{B.1}$$

We see that $\mathbf{v} = 0$ fulfills this equation for any u, and so $\mathbf{v} = 0$ is not considered an eigenvector. However, the eigenvalue u may be zero with a non-zero eigenvector (then the eigenvector belongs to the kernel of A, since it fulfills the equation $A\mathbf{v} = 0$).

If we have the matrix A, we can find the eigenvalues through the characteristic polynomial, since we know that the eigenvalues must fulfill this equation, I_n being an $n \times n$ identity matrix:

$$(A - uI_n)\mathbf{v} = 0. \tag{B.2}$$

Since $\mathbf{v}$ is always non-zero, we know that the matrix $A - uI_n$ is not invertible, and so the determinant of this matrix must be zero. This sets up the characteristic polynomial, since the determinant of an $n \times n$ matrix is a polynomial of degree n. So a $n \times n$ matrix have n complex eigenvalues, but some of them may be equal. The characteristic equation is then

$$\begin{vmatrix} a_{11} - u & a_{12} & \dots & a_{1n} \\ a_{21} & a_{22} - u & & \\ \vdots & \ddots & & \\ a_{n1} & & & a_{nn} - u \end{vmatrix}. \tag{B.3}$$

The eigenvectors $\mathbf{v}$ are found through the equation set $A\mathbf{v} = u\mathbf{v}$, when we now know the eigenvalues u.

B.1.2 Differential equations

Now we have the eigenvalues and eigenvectors, let us use them to solve differential equations. In this report, we will be looking at systems of first order, linear ordinary differential equations with constant coefficients. Assume we have a set of n functions $y_i(x)$, where $i \in \{1, 2, \dots, n\}$, that we wish to find, and we have differential equations for them. Since we are talking about first order, ordinary linear differential equations with constant coefficients, we can write the system like this:

$$\begin{aligned} y_1' &= a_{11}y_1 + a_{12}y_2 + \ldots + a_{1n}y_n, \\ y_2' &= a_{21}y_1 + a_{22}y_2 + \ldots + a_{2n}y_n, \\ &\vdots \\ y_n' &= a_{n1}y_1 + a_{2n}y_2 + \ldots + a_{nn}y_n. \end{aligned}$$

Here, the prime denotes differentiation with respect to the variable x. If we now let the coefficients a_{ij} (which are constants) make up a matrix A, we can write this system as $\mathbf{y}' = A\mathbf{y}$. If we now let u_i be the eigenvalues of A (which we assume are different, see below), and $\mathbf{v}$ the corresponding eigenvectors, the solution is simply given by

$$\mathbf{y}(x) = \sum_{i=1}^{n} c_i \mathbf{v}_i e^{u_i x}. \tag{B.4}$$

Here, the coefficients c_i are integration constants, and are determined using the initial conditions. So solving such a system of differential equations is essentially the same as finding the eigenvalues and eigenvectors of the matrix A.

Now, we assumed that all the eigenvalues were different. If some of the eigenvalues are equal, and the corresponding eigenvectors are linear dependent, we get fewer solutions than the number of equations in our set. For

an eigenvalue u that appears more than once, one can find a solution on the form

$$y(x) = cxe^{ux},$$

where c is a constant to be determined by the initial conditions.

B.1.3 Stability and fixed points

When solving systems of differential equations using the linear algebra methods we have just explained, they can turn out to be very complex, and it can be hard so see how the system behave just by looking at solutions. Another thing we can do to study the behavior of the system is to find the fixed points, and from them see what kind of stability we have. Assume we have a set of $n \in \mathbb{N}$ functions $x_i(t), i \in \{1, 2, \ldots, n\}$, that are given through a set of differential equations

$$\frac{dx_i}{dt} = f_i(\mathbf{x}),$$

so each of the total derivatives with respect to t is a function of all the components, but not explicitly dependent on the parameter t. We say that such a system is *autonomous*. In vector form, we can write

$$\frac{d\mathbf{x}}{dt} = \mathbf{f}(\mathbf{x}).$$

A *fixed point* is a point $\mathbf{x}_*$ where $f_i(\mathbf{x}_*) = 0 \forall i$. To study the stability of such a point, we make this matrix M:

$$M = \begin{pmatrix} \frac{\partial f_1}{\partial x_1} & \frac{\partial f_1}{\partial x_2} & \cdots & \frac{\partial f_1}{\partial x_n} \\ \frac{\partial f_2}{\partial x_1} & \frac{\partial f_2}{\partial x_2} & \cdots & \frac{\partial f_2}{\partial x_n} \\ \vdots & \vdots & \ddots & \vdots \\ \frac{\partial f_n}{\partial x_1} & \frac{\partial f_n}{\partial x_2} & \cdots & \frac{\partial f_n}{\partial x_n} \end{pmatrix}, \tag{B.5}$$

so we take all the functions and differentiate with respect to all the variables. This corresponds to linearizing the system, so we Taylor expand the system around $\mathbf{x}_*$ and study small perturbations around $\mathbf{x}_*$. The stability of a fixed points is determined by the eigenvalues of the matrix M evaluated at the corresponding fixed point. A fixed point is said to be stable if the system ends up in this point if we let the time go long enough, provided the initial conditions are right. Think of it as a bottom of a potential well. In the same way, a fixed point is said to be unstable if the system goes further and further away from this point as time goes. A saddle point then is like a saddle: if one views it from one angle, is is a stable point, from another angle, it is unstable, like the saddle on a horse. Depending on the initial conditions, the system can then first approach this point, and then turn around and go away from this point at some time. We can also have spirals, meaning that

the system will approach or leave the fixed points following a spiral path - or it can just orbit the fixed point following an elliptical path.

To simplify, we will now constrain ourselves to two dimensions, since this is what we will use this for in this thesis. The matrix M then have two eigenvalues, which may be complex, and we get these possible cases for the fixed point in question:

- If the eigenvalues are real, and both are positive, we have an unstable fixed point.
- If the eigenvalues are real, and both are negative, we have a stable fixed point.
- If the eigenvalues are real, and one is negative and the other is positive, we have a saddle point.
- If the eigenvalues are complex with a positive real part, we have an unstable spiral.
- If the eigenvalues are complex with a negative real part, we have a stable spiral.
- If the eigenvalues are complex with real part zero (pure imaginary), we will have an ellipse around the fixed point.

Note that if one of the eigenvalues is complex, the other eigenvalue is the complex conjugate of the first, and hence their real parts are the same.

B.1.4 Fourier, Legendre and Bessel

In this section, I will look at some useful mathematical methods named after Joseph Fourier, Adrien-Marie Legendre and Friedrich Bessel. These methods are useful for analyzing some functions and manipulating equations. This section is based on parts of [29].

Fourier transforms

We start with Fourier. We will use what we call a *Fourier transform* of a function. A Fourier transform is defined simply: If you have a function $f(x)$, you can Fourier transform this function to get a function $g(k)$ by multiplying $f(x)$ with $e^{\pm ikx}$ and integrate over x. Also, a factor of 2π or $(2\pi)^{-1}$ should also be present - this factor (and the sign in the exponent) depends on which way we transform (one could also have a factor of $(2\pi)^{-1/2}$ for both ways). However, if we start with f and transform to g, this is the most common definition:

$$g(k) = \int_{-\infty}^{\infty} f(x)e^{-ikx}dx. \tag{B.6}$$

Then, to get from g back to f, we have

$$f(x) = \frac{1}{2\pi} \int_{-\infty}^{\infty} g(k) e^{ikx} dk,$$

with the sign in the exponent reversed and a factor of $(2\pi)^{-1}$ in front.

Since the number in the exponent should be dimensionless, x and k must have inverse units - so if x is a length, units meters, k will be associated with a wave number, unit inverse meter. If x has unit time, unit seconds, k will be a frequency, unit inverse seconds. This is important when we use Fourier transforms in physics.

We will Fourier transform the terms in partial differential equations. Since the integral of a sum is the sum of the integrals, this just corresponds to Fouriertransforming term by term (if the coefficients in the equation does not depend on the variable we are Fourier transforming). What happens if our term contains a differential operator, differentiating with respect to x? We use integration by parts to test:

$$\int_{-\infty}^{\infty} \frac{\partial f}{\partial x} e^{-ikx} dx = \left[f e^{-ikx} \right]_{-\infty}^{\infty} - \int_{\infty}^{\infty} ikf e^{-ikx} dx$$

$$= ik \int_{-\infty}^{\infty} f(x) e^{ikx} dx = ikg,$$

where g is the Fourier transform of f. Dropping f (and g), we see that the differential operator goes away under the Fourier transformation, and we just multiply the Fourier transformed function with ik. And so an ordinary differential equation in our first space is an algebraic equation in Fourier space, and a partial differential equation in our first space is a set of decoupled, ordinary differential equations in Fourier space. So if a quantity $f(x,t)$ is given through a partial differential equation in x and t, and we Fourier transform, going from x to k, we get an infinite set of decoupled, ordinary differential equations - one for each value of k.

Legendre expansions

Now turning to Legendre. We start with a differential equation, *Legendre's equation*, where we have a function $y(x)$, and l is a constant:

$$(1 - x^2) \frac{d^2 y}{dx^2} - 2x \frac{dy}{dx} + l(l+1) y = 0.$$

The solution can be found using power series, and one then finds that the series always converges for $|x| < 1$. When $l \in \mathbb{Z}$, the series also converges if $|x| = 1$. These are the cases we are interested in. The solution $y(x)$ is a

polynomial of degree l. These are the Legendre polynomials $\mathcal{P}_l(x)$, and they are given by the Rodrigues' formula:

$$\mathcal{P}_l(x) = \frac{1}{2^l l!} \frac{d^l}{dx^l} \left((x^2 - 1)^l \right). \tag{B.7}$$

Note that l must be non-negative now - this is no problem, since Legendre's equation will have the same solution for l as for $-l$, and so we only need to consider $l \in \mathbb{N}_0$, that is, $l = 0$ or $l \in \mathbb{N}$.

When $x \in [-1, 1]$, the Legendre polynomials form a complete set of orthogonal functions. This means two things:

- A function $F(x)$ can be expressed as a linear combination of Legendre polynomials:

  $$F(x) = \sum_{l=0}^{\infty} c_l \mathcal{P}_l(x).$$

  (This formula becomes a little bit more complicated when F is not continuous, but we will not worry about that.) The coefficients are given by

  $$c_l = \frac{2l+1}{2} \int_{-1}^{1} F(x) \mathcal{P}_l(x) dx.$$

- The integral of the product of two Legendre polynomials of degree m and l over the interval $x \in [-1, 1]$ has a Kroenecker delta: the orthogonality relation is

  $$\frac{2l+1}{2} \int_{-1}^{1} \mathcal{P}_l(x) \mathcal{P}_m(x) dx = \delta_{lm}.$$

Now, we need the Legendre expansion formula using the variable μ:

$$\mu = \frac{\vec{x} \cdot \hat{p}}{|\vec{x}|} = \cos\theta,$$

where θ is the angle between a unit vector $\hat{p}$ (the hat means that the length of the vector is 1: $|\hat{p}| = 1$) a the vector $\vec{x}$. The expansion is then

$$c_l = \frac{1}{2(-i)^l} \int_{-1}^{1} F(\mu) \mathcal{P}_l(\mu) d\mu. \tag{B.8}$$

The Legendre polynomials also have this useful recursion formula ([17], page 418):

$$(l+1)\mathcal{P}_{l+1}(\mu) = (2l+1)\mu \mathcal{P}_l(\mu) - l\mathcal{P}_{l-1}(\mu). \tag{B.9}$$

Spherical Bessel functions

The Bessel functions are solutions to Bessle's equation. In Its standard form, it reads

$$x^2\frac{d^2y}{dx^2} + x\frac{dy}{dx} + (x^2 - l^2)y = 0,$$

where $l \in \mathbb{R}$ is called the order of the Bessel function $J_l(x)$, which solves the equation. The solution $J_l(x)$ can be written in terms of the Γ functions:

$$J_l(x) = \sum_{n=0}^{\infty} \frac{(-1)^n}{\Gamma(n+1)\Gamma(n+1+l)} \left(\frac{x}{2}\right)^{2n+l},$$

where the Γ function is

$$\Gamma(p) = \int_0^\infty x^{p-1}e^{-x}dx, \quad p > 0.$$

When $l = (2n+1)/2, n \in \mathbb{Z}$, we label the Bessel function by $j_l(x)$, and we have the spherical Bessel functions. They are related to the ordinary Bessel functions by

$$j_l(x) = \sqrt{\frac{\pi}{2x}} J_{(2l+1)/2}(x). \tag{B.10}$$

We will need this useful recursion relation for $j_l(x)$:

$$j_{l+1}(x) = \frac{2l+1}{x} j_l(x) - j_{l-1}(x). \tag{B.11}$$

Bessel functions are used in a lot of ways in physics, and we are going to use them as a limit in an expansion.

B.2 Numerical simulations

When I use observational data to constrain parameters in a model, I do a lot of numerical simulations, which I write from the bottom. In this section, I will write about the methods I use when I solve differential equations, interpolate and integrate numerically. In the part where I work with structure formations, I used more advanced methods for numerical simulations, such as the Burlich Stoer algorithm for solving differential equations and cubic splines for interpolation. These methods were given to me in modules that were ready to use, so I have not gone into them in details, and I will not write more about them here.

B.2.1 Ordinary differential equations

When we are working with observational data, we will use a different kind of variable and different functions than what we do when we study the model

alone. It turns out that the equations we will solve becomes non-linear when we do this substitution, and therefore, we will solve the equations numerically. I will use a straight forward fourth order Runge Kutta method for solving my differential equations, which are on the form

$$\frac{dy_j}{dx} = f(x, y_1, y_2, \ldots, y_n)$$

for $j \in \{1, 2, \ldots, n\}$. This method is just a more complicated version of the classical Euler method. Now, let us gather all the unknown functions y_j in a vector $\mathbf{y}$. When I later add a number to this vector, it is to be understood that we add this number to all of the components. Now, if we have $\mathbf{y}_i$ at point x_i, we use this algorithm for getting $\mathbf{y}_{i+1}$, at point x_{i+1}:

- We start with a set of initial conditions, $\mathbf{y}_0$ at x_0.
- Then we set up a grid of x values. The distance between two x-values is called the step size, and we label it by h.
- We calculate four numbers: k_1, k_2, k_3 and k_4. The first one is given as $k_1 = hf(x_i, \mathbf{y}_i)$.
- The next three numbers are $k_2 = hf(x_i + h/2, \mathbf{y}_i + k_1/2)$, $k_3 = hf(x_i + h/2, \mathbf{y}_i + k_2/2)$ and $k_4 = hf(x_i + h, \mathbf{y}_i + k3)$.
- Then we calculate y_{i+1} like this:

$$y_{i+1} = y_i + \frac{1}{6}(k_1 + k_2 + k_3 + k_4). \tag{B.12}$$

In the end, we end up with numerical values for our functions $\mathbf{y}$ at all the points x in our grid.

B.2.2 Linear interpolation

When I have solved the set of differential equations numerically according to the previous subsection, I end up with the desired quantity $y(x)$ evaluated at discrete points x_i, where the x-grid is set up before we solve the equations. Comparing with observational data, we will need to know $y(x)$ for some value of x that is between to points x_i and x_{i+1} in our grid. We then use linear interpolation to find $y(x)$. The formula is then simply

$$y(x) = \frac{y(x_{i+1}) - y(x_i)}{x_{i+1} - x_i}(x - x_i) + y(x_i). \tag{B.13}$$

This formula is simply derived based on Figure B.1 on the next page.

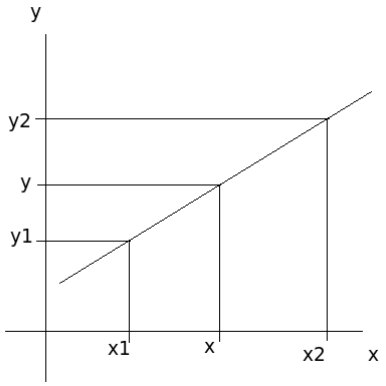

Figure B.1: Linear interpolation. We know y_1 at x_1 and y_2 at x_2, and want to find y at x between these points.

B.2.3 Numerical integration

I will need to do numerical integration in this thesis. For this I will use the trapezoidal rule, which I will explain here. We start with a function $f(x)$ that we want to integrate over the interval $[a, b]$. Then we compute the function in N mesh points x_i between a and b, in such a way that $x_0 = a$ and $x_N = b$. We also have a stepsize dx which is $x_{i+1} - x_i$ for some integer $i \in [0, N-1]$. The integral is then approximated like this:

$$\int_a^b f(x)dx = f(a) + \sum_{i=1}^{N-1} \frac{f(x_i)}{2} + f(b). \tag{B.14}$$

B.3 Statistics

As mentioned above, a big part of this thesis is about observational data. Then we also need some statistics, so we can say how good the data constrains the models. This section is based on parts of [30].

The main statistical quantity we will use is the χ^2 estimator. We have made a model where we have some parameters that we can change, and we want to find the combination of parameters that best fits our model to a data set. The data set contains N independent observations, which consists of points x_i, observations y_i and observation errors σ_i, where $i \in \{1, 2, \ldots, N\}$ labels the observations. For each set of parameters in our model, we plug in the observed points x_i and compute $\hat{y}_i$ based on the model. This is then to be compared with the observed y_i. If all the data points y_i are uncorrelated,

Table B.1: The entries are the differences from the best value of χ^2 to the given significance level, when we have m free parameters that we are fitting.

Significance level σ	2	3
1σ	2.3	3.53
2σ	5.99	7.82
3σ	9.21	11.34

we can define the χ^2 estimator like this:

$$\chi^2 = \sum_{i=1}^{N} \frac{(y_i - \hat{y}_i)^2}{\sigma_i^2}. \tag{B.15}$$

The best model is then given by the combination of parameters that gives the smallest value for χ^2.

Now, what if there are correlations between the data? Then we make a covariance matrix, C. On the diagonal, we gather the errors for each data point, and in the non-diagonal entries, we insert the correlation coefficient. So $C_{ij}, i \neq j$ is the correlation between data point i and data point j. The diagonal elements of the covariance matrix is the error of that data point squared: $C_{ii} = \sigma_i^2$. Now we make a vector $\mathbf{X}$ where each entry is the estimated quantity $\hat{y}_i(x_i)$ (based on a model) minus the corresponding observed quantity y_i: $X_i = \hat{y}_i(x_i) - y_i$. Then we get this simple expression for the χ^2 estimator:

$$\chi^2 = \mathbf{X}^T C^{-1} \mathbf{X} = \sum_i \sum_j X_i C_{ij}^{-1} X_j. \tag{B.16}$$

Now that we have the χ^2 estimator as a function of some parameters, we will draw confidence regions of χ^2 in the parameter space. These plots then shows how far away in terms of parameter combinations from the lowest value of χ^2 we must go in order to have a model that significantly differs from our data set. In the cases we will work with, we will constrain either two or three parameters, and we will use three significance levels, which is just one, two and three standard deviations σ. This will then correspond to differences from the best χ^2 value according to Table B.1.

Bibliography

[1] Øystein Elgarøy, "Ast4220: Cosmology i." `http://www.uio.no/studier/emner/matnat/astro/AST4220/h09/course-material/lectures.pdf`.

[2] Øystein Elgarøy, "The galaxy correlation function and power spectrum." `http://www.uio.no/studier/emner/matnat/astro/AST4320/h12/undervisningsmateriale/galaxyclustering.pdf`.

[3] G. Caldera-Cabral, R. Maartens, and L. A. Urena-Lopez, *Dynamics of interacting dark energy*, *AIP Conf.Proc.* **1241** (2010) 741–748, [doi:10.1063/1.3462711].

[4] http://www.wolfram.com/mathematica, May, 2014.

[5] **SNLS Collaboration** Collaboration, J. Guy *et al.*, *SALT2: Using distant supernovae to improve the use of Type Ia supernovae as distance indicators*, *Astron.Astrophys.* **466** (2007) 11–21, [arXiv:astro-ph/0701828], [doi:10.1051/0004-6361:20066930].

[6] S. Jha, A. G. Riess, and R. P. Kirshner, *Improved Distances to Type Ia Supernovae with Multicolor Light Curve Shapes: MLCS2k2*, *Astrophys.J.* (2007).

[7] R. Amanullah, C. Lidman, D. Rubin, G. Aldering, P. Astier, *et al.*, *Spectra and Light Curves of Six Type Ia Supernovae at $0.511 < z < 1.12$ and the Union2 Compilation*, *Astrophys.J.* **716** (2010) 712–738, [arXiv:1004.1711], [doi:10.1088/0004-637X/716/1/712].

[8] Øystein Elgarøy, "Perturbation theory." `http://www.uio.no/studier/emner/matnat/astro/AST4320/h12/undervisningsmateriale/perturbation.pdf`.

[9] R. Lazkoz, S. Nesseris, and L. Perivolaropoulos, *Comparison of Standard Ruler and Standard Candle constraints on Dark Energy Models*, *JCAP* **0807** (2008) 012, [arXiv:0712.1232], [doi:10.1088/1475-7516/2008/07/012].

[10] **SDSS Collaboration** Collaboration, W. J. Percival *et al.*, *Baryon Acoustic Oscillations in the Sloan Digital Sky Survey Data Release 7 Galaxy Sample*, *Mon.Not.Roy.Astron.Soc.* **401** (2010) 2148–2168, [arXiv:0907.1660], [doi:10.1111/j.1365-2966.2009.15812.x].

[11] C. Blake, E. Kazin, F. Beutler, T. Davis, D. Parkinson, *et al.*, *The WiggleZ Dark Energy Survey: mapping the distance-redshift relation with baryon acoustic oscillations*, *Mon.Not.Roy.Astron.Soc.* **418** (2011) 1707–1724, [arXiv:1108.2635], [doi:10.1111/j.1365-2966.2011.19592.x].

[12] J. C. Mather, E. Cheng, R. Shafer, C. Bennett, N. Boggess, *et al.*, *A Preliminary measurement of the Cosmic Microwave Background spectrum by the Cosmic Background Explorer (COBE) satellite*, *Astrophys.J.* **354** (1990) L37–L40, [doi:10.1086/185717].

[13] B. W. Carroll and D. A. Ostlie, *An Introduction to Modern Astrophysics*. Pearson Addison Wesley, second ed., 2007.

[14] W. Hu and N. Sugiyama, *Small scale cosmological perturbations: An analytic approach*, *Astrophys. J.* **471** (1996) 542–570, [arXiv:astro-ph/9510117], [doi:10.1086/177989].

[15] **WMAP Collaboration** Collaboration, E. Komatsu *et al.*, *Five-Year Wilkinson Microwave Anisotropy Probe (WMAP) Observations: Cosmological Interpretation*, *Astrophys.J.Suppl.* **180** (2009) 330–376, [arXiv:0803.0547], [doi:10.1088/0067-0049/180/2/330].

[16] R. Durrer, *The Cosmic Microwave Background*. Cambridge University Press, 2008.

[17] S. Dodelson, *Modern Cosmology*. Academic Press, 2003.

[18] J. Sola, *Vacuum energy and cosmological evolution*, arXiv:1402.7049.

[19] J. Sola, *Cosmological constant and vacuum energy: old and new ideas*, *J.Phys.Conf.Ser.* **453** (2013) 012015, [arXiv:1306.1527], [doi:10.1088/1742-6596/453/1/012015].

[20] Øystein Elgarøy, "Kosmologisk perturbasjonsteori: I ditt ansikts sved skal du ete ditt brød." `http://folk.uio.no/oelgaroy/forelesning_3.pdf`.

[21] Øystein Elgarøy, "Kosmologisk perturbasjonsteori: Einsteintensoren vender tilbake." `http://folk.uio.no/oelgaroy/forelesning_4.pdf`.

[22] Øystein Elgarøy, "Initialbetingelser: I begynnelsen var ϕ."

[23] C.-P. Ma and E. Bertschinger, *Cosmological perturbation theory in the synchronous and conformal Newtonian gauges*, *Astrophys.J.* **455** (1995) 7–25, [arXiv:astro-ph/9506072], [doi:10.1086/176550].

[24] P. Callin, *How to calculate the CMB spectrum*, arXiv:astro-ph/0606683.

[25] T. Clemson, K. Koyama, G.-B. Zhao, R. Maartens, and J. Valiviita, *Interacting Dark Energy – constraints and degeneracies*, *Phys.Rev.* **D85** (2012) 043007, [arXiv:1109.6234], [doi:10.1103/PhysRevD.85.043007].

[26] Øyvind Grøn and S. Hervik, *Einstein's general theory of relativity.* Springer, 2007.

[27] Øystein Elgarøy, "A short introduction to general relativity." `http://folk.uio.no/hke/AST5220/lecture_1.pdf`.

[28] E. F. Taylor and J. A. Wheeler, *Exploring Black Holes - Introduction to General Relativity.* Addison Wesley Longman, 2000.

[29] M. L. Boas, *Mathematical Methods in the Physical Sciences.* Wiley, third ed., 2006.

[30] **Particle Data Group** Collaboration, J. Beringer *et al.*, *Review of Particle Physics (RPP)*, *Phys.Rev.* **D86** (2012) 010001, [doi:10.1103/PhysRevD.86.010001].